UNIVERSITA' DEGLI STUDI DI MILANO

Dipartimento di Biotecnologie Mediche e Medicina Traslazionale

Dottorato di Ricerca in Scienze Biochimiche XXIX ciclo

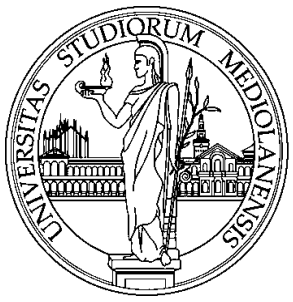

STUDY OF THE ROLE OF PLASMA MEMBRANE SPHINGOLIPIDS IN CYSTIC FIBROSIS AIRWAYS INFECTION

Docente guida: Prof. Sandro SONNINO
Tutor: Dr. Massimo AURELI
Coordinatore del Dottorato: Prof. Sandro SONNINO

Tesi di Dottorato di
Domitilla SCHIUMARINI
Matricola: R10449

Anno Accademico 2015-2016

Summary

Cystic fibrosis (CF), the most common autosomal recessive disease among Caucasians, is caused by mutations in the gene encoding the cystic fibrosis transmembrane conductance regulator (CFTR). Among the wide spectrum of clinical and phenotypic manifestations occurring in CF, lung pathology is the main cause of morbidity and mortality. Progressive airway disease, chronic non-resolving inflammation, persistent bacterial infection are already observed in the majority of young children with CF. The prolonged airway inflammatory response induces permanent damage of CF airways leading to the loss of lung function in the majority of CF patients.

In this respect, treatments with corticosteroids and ibuprofen have demonstrated potential benefits in CF patients, even though limited efficacy or the occurrence of side effects. For these reasons, the identification and the development of novel and more powerful anti-inflammatory drugs for CF airway disease remains a priority.

Despite intensive research of the past few decades, the mechanisms involved in the onset of CF lung disease are not fully understood. Increasing lines of evidence highlighted the involvement of sphingolipids (SLs) in the development of CF lung pathology. SLs are cell membrane amphiphilic components that are located mainly in the external layer of the plasma membrane (PM) where they play important roles in the modulation of fundamental cell functions. Previous studies have demonstrated an abnormal SL metabolism in CF lung disease. In particular, increased levels of ceramide derived from sphingomyelin hydrolysis are related to the pro-inflammatory state as well as the inflammation response to bacterial infection occurring in CF lung disease. In addition, a recent study provides the evidence that ceramide derived from glycosphingolipid degradation (GSL) is involved in the inflammation response to bacterial infection of CF human epithelial bronchial cells; these data demonstrated that the pharmacological inhibition of GBA2, whose enzymatic activity produces ceramide at the cell surface, is associated with a significant reduction of the inflammatory response to *P. aeruginosa* infection. Moreover, GBA2 down-regulation reduces the intrinsic pro-inflammatory state typical of CF bronchial cells.

On the bases of these findings, the first aim of my PhD project was to study the possible correlation between ceramide formed at the PM through the action of the PM glycohydrolases and IL-8 release and expression.

The obtained results suggest that in CF bronchial epithelial cells, *P. aeruginosa* infection promotes the recruitment in restricted area of PM of the all glycohydrolases necessary for the complete GSL catabolism. At this site, the presence of both enzymes and their substrates allows a rapid and local change of PM architecture; this event, together with the formation of ceramide-enriched platforms

might form a macromolecular complex involved in the activation of the inflammatory response. In this context, I found that GBA2 could play an important role in the development of the pro-inflammatory state typical of CF lung disease.

In particular, GBA2 silencing could represent a new promising therapeutic strategy to reduce both the pro-inflammatory state and the inflammatory response to bacterial infection in CF bronchial epithelial cells. On these bases, the second objective of my PhD project was to set up a new strategy for GBA2-targeted siRNA delivery in CF epithelial bronchial cells. To this purpose, in collaboration with a group of biophysicists, I developed a lipid-based carrier to promote the transfection of genetic material. We developed two kinds of vehicles; DC-Chol/DOPE mixture assembled with siRNA (Lipoplex) and a DC-Chol/DOPE mixture with a siRNA pre-condensed with protamine (Nanoparticles). Our results showed that the Nanoparticles represented the most promising system to down-regulate GBA2 activity.

Collectively, the results obtained in this study strongly support a role for GBA2 in the establishment of the pro-inflammatory state of CF. This finding provides promising bases for the use of modulators of SL metabolism as possible therapeutic strategies for CF lung inflammation.

Introduction

Cystic Fibrosis

Cystic fibrosis is the most common autosomal genetic recessive disease among Caucasians, affecting approximately 1 in 2500-4000 newborns. The main cause of CF is the mutation of gene that encodes for the cystic fibrosis transmembrane conductance regulator (CFTR).
The principal phenotype of CF is represented by the accumulation of viscous mucus at the epithelial surface of different organs as lungs, pancreas, gut and testes, which often results in inflammation and organ failure. CF patients usually die at an early age, mostly due to chronic lung infection and inflammation [O'Sullivan and Freedman, et al. 2009].
Thanks to the currently available CF therapies, the mean life of patients is increased from 5 year in the 1970s to around 35-40 years of age today [Borthwick, Botha, et al. 2011].

CFTR gene and tissue expression

The gene responsible for the cystic fibrosis disorder was identified in 1989 and is located to the long arm of chromosome 7 (7q31). The gene spans 190 Kb of genomic DNA and is composed by 27 exons [Kerem, Rommens, et al. 1989];[Riordan, Rommens, et al. 1989];[Rommens, Iannuzzi, et al. 1989].
The full-length CFTR mRNA contains 6128 nucleotides. All the CFTR transcription mechanisms start from around the same site but are also present some mechanisms of alternative splicing. The promoter region is characterized by consensus binding sites for different transcriptions factors as AP-1, SP1, GRE, CRE, C/EBP. In addition, CFTR expression is regulated by hormone in both males and females [Tsui and Dorfman, et al. 2013].
The expression of CFTR was deeply analyzed in both rodents and humans [Ellsworth, Jamison, et al. 2000]. CFTR mRNA is constitutively expressed in sweat gland and in gastrointestinal tract in early development, [Trezise, Chambers, et al. 1993] and is maintained for the all-adult life.
In particular, its expression is present in intestinal crypt cells, pancreatic duct, and acinar cells. CFTR is also expressed in mucin secretory cells, in gallbladder epithelia and in the Brunner glands. Measurable levels of CFTR were also detected in female and male reproductive tissue and organs, such as cervix, endometrium, fallopian tubes, and ovary as well as in epididymis head. Low and

intermediate levels of CFTR transcripts can also be found in kidney, thyroid and salivary gland [Stoltz, Meyerholz, et al. 2015].

The lung is a special case [Engelhardt, Zepeda, et al. 1994]. The expression patterns of CFTR in the fetus are maintained postnatally, except in the respiratory system. In fact, high levels of CFTR expression are found in the epithelium of the conducting airways in the fetal lung and this finding is in markedly contrast to the relative lack of expression detected in the adult lung. On the other hand, expression in submucosal gland is present only after birth, and not measurable in fetus, in fact in adult respiratory tissue the main site of expression of CFTR is the serous submucosal gland [McCarthy and Harris, et al. 2005, Tizzano and Buchwald, et al. 1995, Tsui and Dorfman, et al. 2013].

CFTR protein: function and structure

CFTR functions as ions channel, with specificity for chloride and bicarbonate, regulates Cl^-/HCO_3^- exchanges at the level of the apical membranes of epithelial cells in multiple organs [Anderson, Gregory, et al. 1991].

Through its role of chloride-bicarbonate exchanger, CFTR appears to influence local pH and thus ionic content and fluid on epithelial surface, events crucial for the formation of functional airway surface liquid in bronchial epithelia [Poulsen, Fischer, et al. 1994];[Weiser, Molenda, et al. 2011]. In addition, the local pH generated by CFTR activity, influences other ion channels including the epithelial sodium channel ENaC in the airways [Borowitz, et al. 2015].

Concerning the structure, CFTR is a protein composed by 1480 amino-acid residue and is a member of the ATP-binding cassette (ABC) transporter family. It has a typical ABC transporter architecture: two trans-membrane domains (TMDs) connected by four intracellular linkers, ICL1-ICL4, two nucleotide-binding domains (NBDs), a regulatory region (R), and N-/C- terminal extension (figure 1). The two trans-membrane domains are composed of six membrane-spanning α-helices and are predicted to form a pore for ions passage. NBD1 has an additional 35 residues insertion and NBD2 has 80 residues extension at its end, if compared with other ABC proteins. These additional peptides may be regulate CFTR channel interaction with other cellular molecules.

The regulatory region R is a random coil highly charged, is about 200 residues in length and is characterized by several consensus sequences (12 serines and 8 threonines) for protein kinase A (PKA) phosphorylation. The four intra-cellular loops are predicted to interact and transduce information between TMDs and NBDs [Moran, et al. 2014].

Channel activity has been described by three state for CFTR: open, closed and open-ready, the open ready conformation is poised to rapidly transitions into open state. CFTR activity is also dependent

on the presence of ATP and PKA phosphorylation of its R region, indeed phosphorylation of the R region is important for opening CFTR channel.

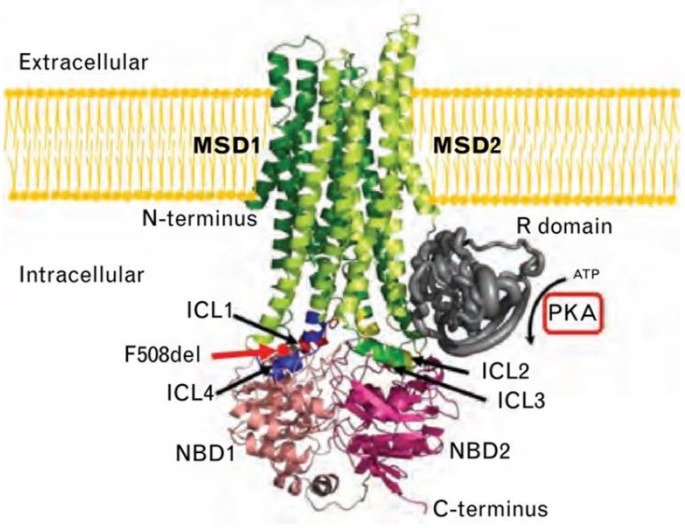

Figure 1 Theoretical domain organization of CFTR at the apical membrane *[Milla and Moss, et al. 2015]*

CFTR biogenesis

CFTR folding is a crucial point during the protein synthesis and only 30% of all immature CFTR polypeptide chains reaches the plasma membrane in mature state. In comparison, other ABC proteins are processed in a more efficient way [Cant, Pollock, et al. 2014]

The synthesis of CFTR and the first step of folding control occur in the endoplasmic reticulum (ER), by chaperons protein like Calnexin, Aha and HSP40/70/90. Both inter and intra-domain folding is required for ER exit.

The plasma membrane (PM) provides the final stages of CFTR maturation, indeed CFTR at the PM level takes part in an interactome, which probably includes members of Rab and Rho families of GTPase and cytoskeleton proteins, such as the PDZ-interacting NHERF protein [Cant, Pollock, et al. 2014].

A complete glycosylation at 4^{th} extracellular loop (residue 894 and 900), characterizes the correct and mature folded state of CFTR, even if this modification is not essential for the correct channel activity and PM localization of the protein. Some other different post-translational modifications like methylation, palmitoylation, and phosphorylation are important for correct folding, biological activity and protein stability [Cant, Pollock, et al. 2014].

Classification of CFTR mutations

Over 1000 mutations have been identified in the CFTR gene [McCharty et al 2005 Pulmonology].
Five major classes of CFTR mutations were described, according to: i) consequences on CFTR function, ii) impaired protein synthesis, iii) effects on maturation, iv) aberrant channel regulation, and v) defective channel conductance (figure 2). Classes I-III cause severe disease phenotypes whereas class IV and V/VI are generally mild-disease causing mutations [Farinha and Matos, et al. 2016]; [Cant, Pollock, et al. 2014, Fanen, Wohlhuter-Haddad, et al. 2014].

Class I mutations affect CFTR protein synthesis, resulting in the total or partial lack of protein production. Common mutations in this class are nucleotide substitutions introducing a premature stop codon (W1282X, G542X and R1162X), frame-shifting insertions or deletions, mutations in splice-junctions, a complete or partial deletion of CFTR gene or alteration that leads to changes in the exon sequence. G542X is the most frequent mutation of this class and leads to a reduced steady state level of mRNA, caused by the presence of a premature stop codon in its sequences.

Class II mutations affect the protein folding process and can be find within any CFTR domain. Even if it is translated into full-length nascent polypeptide, the misfolded protein is retained in the endoplasmic reticulum, targeted for degradation by the ubiquitin/proteasome pathway, rather than trafficked to the PM.

The most frequent CF mutation belonged to this class is the p.Phe508del. This kind of mutation causes an energetic instability of NBD1 because of the uncorrected local folding.

Class III is composed by missense mutations, which affect frequently the ATP binding domains (NBD1 and NBD2), leading to gating defects. The produced CFTR is able to reach the plasma membrane but has decreased channel opening time and decreased chloride flux, caused by resistance to activation by protein Kinase A. The most described mutation of class III is p.Gly551Asp.

Class IV mutations alter the CFTR membrane spanning domains involved in the structure of the channel. Consequently, these mutations afflict the correct channel conductance, even when the gate is open. Recently, the subclass IVb has been identified, in relation to mutations involving defects in CFTR bicarbonate conductance only.

Class V mutations are localized in the splicing-sites, leading to alteration in the proper exon recognition. As results, CFTR is fully functional at the plasma membrane but in low content, because of defective in mRNA splicing. The most frequent and well-studied is the skipping of exon 10 [Fanen, Wohlhuter-Haddad, et al. 2014].

Class VI include mutations that decrease the retention and stability of CFTR at the cell surface. Recently, class VI mutations were combined with class V, as mutations leading to a reduced amount of functional CFTR protein [Cant, Pollock, et al. 2014, Fanen,Wohlhuter-Haddad, et al. 2014, Farinha and Matos, et al. 2016].

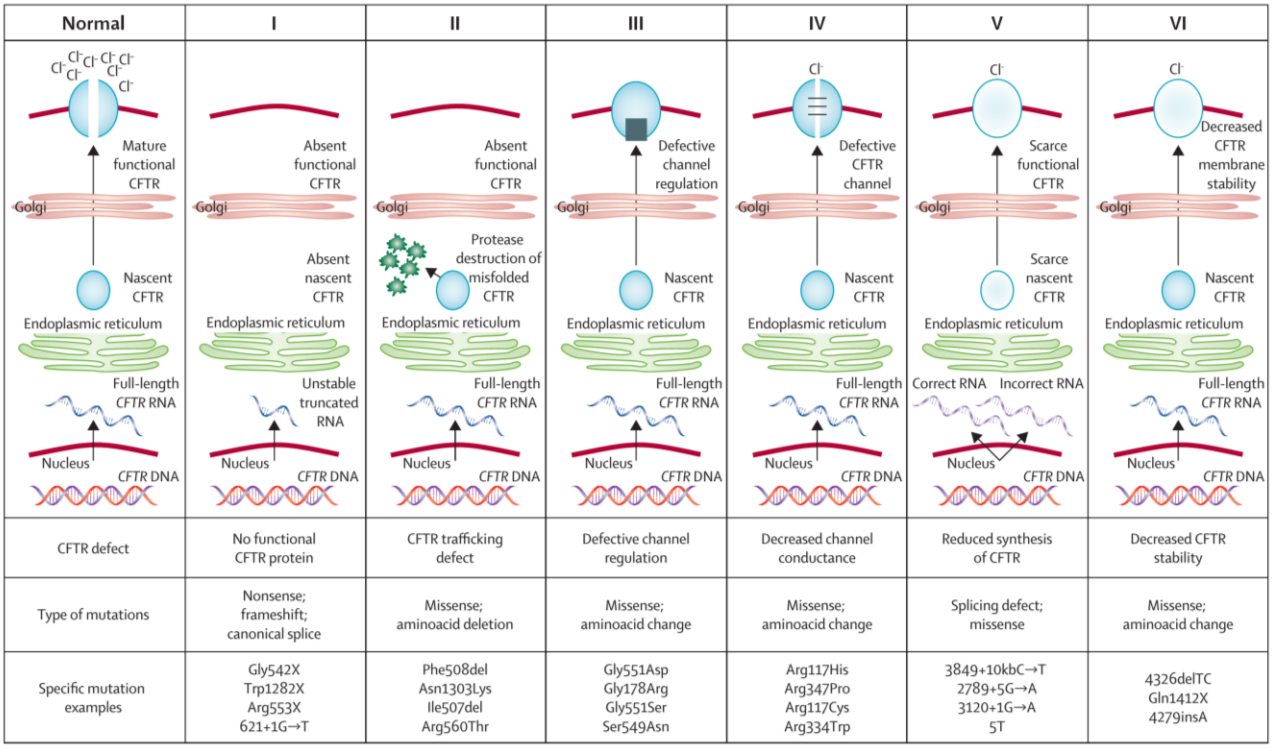

Figure 2 Classes of CFTR mutations *[Elborn, et al. 2016]*

Clinical manifestations of Cystic Fibrosis

The clinical manifestations of CF comprise a very wide spectrum of symptoms; this great variability is due, not only to the type of CFTR mutations, but also to other genetic and environmental factors, like lifestyle and therapeutic treatment.

The general clinical spectrum of CF include pancreatic, hepatic and pulmonary manifestation like pancreatic insufficiency, chronic or recurrent acute pancreatitis, biliary obstruction, sino-pulmonary manifestations as sinusitis, sputum production, airway obstruction, opportunistic pathogens in airway secretions, recurrent infections. Symptoms include also reproductive abnormalities as obstructive azoospermia, infertility and gastro-intestinal abnormalities like meconium ileus, distal intestinal obstruction syndrome and rectal prolapse [Fanen, Wohlhuter-Haddad, et al. 2014].

Since, as described above, the clinical spectrum of CF has greatly expanded, the current diagnostic practice classifies patients with classic and non-classic CF. To date, the more reliable test for CF clinical diagnose and classification is the sweat test.

The majority of patients has classic CF, this kind of patients has a sweat chloride concentration of (> 60 mmol/L) and severe multi-organ phenotype, and their organs are affected to varying degrees. Their mortality is principally due to progressive respiratory disease. From a genetic point of view, patients with classic CF have one established CF-causing mutation on each CFTR allele.

Non-classic CF individuals have a normal (<30 mmol/L) or borderline (30-60 mmol/L) sweat chloride level and generally at least milder single organ phenotype [Tizzano and Buchwald, et al. 1995].

The partition of classic and non-classic CF allows the establishment of classification of CFTR mutations into four groups, according to their clinical consequences [Castellani, Cuppens, et al. 2008].

Group A comprises mutations that cause classic CF (CF-causing), group B includes mutations that cause non-classic CF (associated with CFTR-related disorders), group C comprises mutations with not known clinical consequences and group D consists of mutations with unknown or uncertain clinical relevance. It is important to note that CFTR genotype is not a useful predictor of the severity of lung disease in the individual patient, and should not be used as an indicator of prognosis.

Cystic fibrosis lung disease and inflammation

Among all these clinical and phenotypic manifestation of CF, the main cause of morbidity and mortality in patients is progressive lung disease. CF airways are characterized by permanent structural damage and impaired lung function caused by high-intensity inflammation and inefficiency of clearing pathogens [Chmiel, Berger, et al. 2002]. The most common pathologic findings are bronchiectasis, airways obstruction and chronic infection driven by different bacteria, in particular by *Pseudomonas aeruginosa* [Chmiel and Davis, et al. 2003].

Scientist studied a large number of defects of the CF lung disease and inflammation, directly or indirectly correlated to CFTR like airway surface liquid and mucociliary clearance, the low pH of airway surface liquid and some sphingolipids abnormalities [Becker, Riethmuller, et al. 2010]; [Boucher, et al. 2007].

The airway mucus is a complex and dynamic viscous colloid that can continuously modify in response to different signals from the environment. The mucus contains different molecules as antibacterial defensins, immunoglobulin, inorganic salts, mucins and other proteins. Thanks to these components,

the airway mucus is able to explicate different functions, as to create a protective barrier against toxic products and to clear pathogens. The mucus must be sufficiently fluid to allow the elimination of particles and pathogens. The presence of CFTR influences the characteristics of the airway surface liquid and mucus layer [Perez-Vilar and Boucher, et al. 2004].

First of all the water content of airway surface liquid is regulated by CFTR, thanks to its capacity to secrete chloride ions and control sodium adsorption. The impaired regulation of sodium and chloride content in CF, caused by the absence of CFTR, leads to a defective osmotic pressure, an increased absorption of water and consequently to a dehydration of the airway surface liquid [Boucher, et al. 2007]; [Nichols and Chmiel, et al. 2015]. The most important consequence of an increase water absorption is the formation of a very viscous mucus unable to eliminate bacteria, leading to a chronic retention of pathogens and a strong inflammatory response [Cantin, Hartl, et al. 2015, Hoegger, Fischer, et al. 2014].

Some evidence suggest that CFTR is also important for the regulation of bicarbonate secretion and influences the local pH in the airway epithelium. Normal airway surface liquid has a pH of 7.0. In individual with CF, pH is lower; in particular, eight fold more acidic supporting the idea that CFTR is fundamental for the airway acid-base balance [Coakley, Grubb, et al. 2003].

Local pH is essential for the correct functionality of different proteins. In particular, characteristic proteins called mucins, principally MUC5A, MUC5B, and MUC2, which are able to attract water in the mucus [De Lisle, et al. 2009].

Mucins can be transmembrane, present on the apical part of epithelial cells, or can float as a gel. Both these kinds of mucins are localized in the periciliary space and form a protective barrier.

Some findings suggest that the correct solubilization and distribution of mucins in the surface epithelium is a pH dependent phenomenon, regulated by the action of CFTR.

In particular, mucins before secretions are highly packaged in a small granules, sequestered by electrical charge given by cations as, Calcium. Bicarbonate secreted by CFTR is able to displace cations, leading to the solubilization of mucins granules. The absence of bicarbonate causes the formation of dense layer of mucins, tightly adherent to the epithelium surface. [Cantin, Hartl, et al. 2015] [Boucher, et al. 2002, Nichols and Chmiel, et al. 2015]

In addition the low pH at the airway surface, results in the inactivation of proteins with antimicrobial properties [Pezzulo, Tang, et al. 2012].

For example, the function of pH-sensitive SPLUNC-1, that is normally able to create a strong host defense, is compromised.

Sphingolipids

Plasma membrane is composed by and extremely complex lipid composition including glycerophospholipids, cholesterol and sphingolipids [van Meer and Vaz, et al. 2005]. Glycerophospholipids are the main lipids of eukaryotic cell membranes. Sphingolipids (SLs) are minor component of the cell [Degroote, Wolthoorn, et al. 2004], and their name derives from the Greek word Sphinx, with the meaning of enigmatic. In the past, many of their functions remained unknown for a long time, but today the functions of sphingolipids have become very wide and various [Futerman and Hannun, et al. 2004].

SLs are amphipathic molecules, associated mainly with the external leaflet of the plasma membrane, characterized by a hydrophobic group inserted into the cellular lipid bilayer and a hydrophilic group protruding toward the extracellular environment [Merrill, et al. 2011].

They have a common structure which comprises a backbone called “long-chain” or “sphingoid” bases, which is represented by a 2-amino-1,3-dihydroxy-octadec-4-ene, an amino alcohol called sphingosine. Sphingosine has potentially four different chemical configuration, but only the 2S, 3R is found in nature. It is the most abundant “sphingoid” base found in mammals and is typically present linked with a long or very long- chain fatty acid, through an amide-bound. The fatty acid chain are predominantly 14 to 36 carbon atoms in length and usually saturated [Carter, Glick, et al. 1947].

The N-acylated form of sphingosine is called Ceramide (Cer), and is the hydrophobic lipid moiety of sphingolipids. Cer is the starting point for the biosynthesis of the more complex sphingolipids and glycosphingolipids (GSLs) [Merrill, et al. 2011].

The hydrophilic head group R of sphingolipids is represented by phosphocoline in the case of sphingomyelin or by an oligosaccharide chain in the case of glycosphingolipids. A particular class of glycosphingolipids has the oligosaccharide that contains a sialic acid residue, and is called Gangliosides [Merrill, et al. 2011].

In general, sphingolipids are a class of lipids essential for cell membranes structure but the past couple of decades have proved that SLs are not merely structural components of biological membranes, but also play other important roles in the cell life [Hakomori, et al. 1990].

In fact, as mentioned below, a large variety of specific SLs have been shown to modulate the cellular signaling pathway [Huwiler, Kolter, et al. 2000].

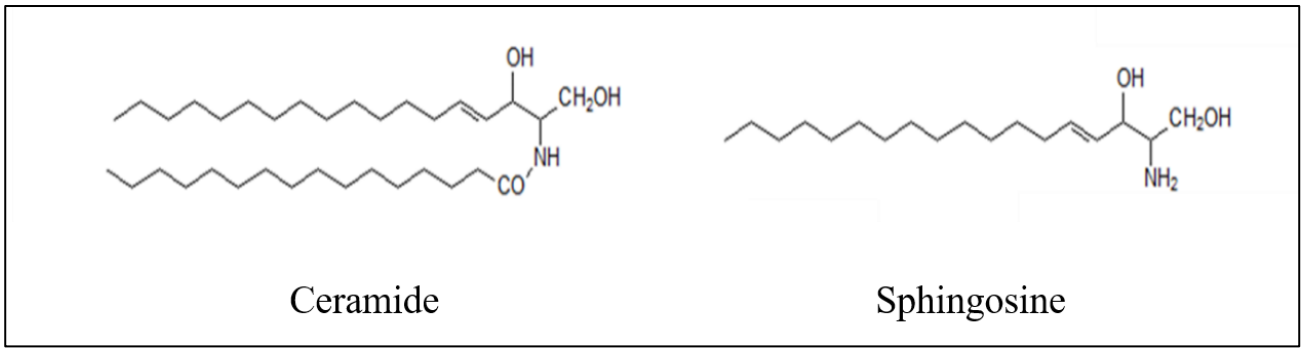

Figure 3 Chemical structure of ceramide and sphingosine.

Biosynthesis

Ceramide

The starting point of the *de novo* sphingolipids biosynthesis is the ceramide formations in the ER. The first reaction consists in the condensation of the amino acid L-serine with palmitoyl-CoA to form 3-ketosphinganine, catalyzed by the enzyme serine palmytoyl-transferase with the cofactor pyridoxal-phosphate.

Subsequently, the 3-ketosphinganine, is reduced to D-*erythro*-sphinganine by 3-ketosphinganine reductase; the N-acyltransferase called ceramide synthase (in mammalian cells are known 6 different isoforms) [Levy and Futerman, et al. 2010] leads to the formation of dihydroceramide through the acylation of sphinganine [Rother, van Echten, et al. 1992]. Notably, ceramide synthase can also directly recycle the sphingosine derived from the ceramide catabolism [Shimeno, Soeda, et al. 1998]. In the end, the major part of dihydroceramide is desaturated to ceramide thanks to the action of the enzyme dihydroceramide desaturase [Yamaji and Hanada, et al. 2015].

Sphingomyelin and Glycosphingolipids

Sphingolipids biosynthesis is a “combinatorial process” driven by different transferases, able to use a lot of different precursor and intermediates to get the final products [Kolter, Proia, et al. 2002]; [Merrill, et al. 2002]. Ceramide is transported from the ER to the Golgi apparatus where the synthesis of complex sphingolipids occurs.

Glycosyltransferases catalyze the reaction of transfer of a specific carbohydrate, from the sugar nucleotide (UDP-Glucose, UDP-Galactose) to a particular type of acceptor, as ceramide or the non-reducing end of a carbohydrate chain attached to Cer [Prinetti, Loberto, et al. 2009].

The first step of glycosylation leads to the production of Glucosylceramide (GlcCer), its formation is catalyzed by a ceramide glucosyltransferase, called GlcCer synthase [Ichikawa and Hirabayashi, et al. 1998], located at the cytosolic side of the early Golgi membrane [Jeckel, Karrenbauer, et al. 1992]. The neo-synthetized GlcCer can follow two different ways: it can reach the plasma membrane or can be translocated to the luminal side of the Golgi. At this point, GlcCer represents the common precursor of the glycosphingolipids and it is further glycosylated by different glycosyltransferase to form more complex glycosphingolipids.

The addition of a galactose residue from UDP-Gal to GlcCer, driven by a galactosyltransferase, leads to the formation of Lactosylceramide (LacCer).

One of the major branch of metabolism of LacCer is the formation of ganglio series. The ganglio series is a class of GSLs characterized by the presence of sialic acid in their oligosaccharide chain. This class is particularly abundant in the cell of the central nervous system.

The biosynthesis of the complex ganglioside occurs in the lumen of the Golgi apparatus by different glycosyltransferase. The GM3 synthase or sialyl-transferase provides to the sialylation of LacCer to form GM3. The other downstream metabolites in this pathway are formed by analogous reactions; GM3 is converted to GM2 by GM2 synthase or β-galactosamynil trasferase that transfer an N-acetylgacatosamine to GM3, and GM2 is converted to GM1 by GM1b synthase.

Neo-synthetized glycosphingolipids can reach the plasma membrane through the exocytotic vesicular traffic.

On the other hand, the neo-synthesized ceramide, in Golgi apparatus, can be used for Sphingomyelin (SM) biosynthesis [Merrill and Jones, et al. 1990]. This reaction is catalyzed by SM synthase that is able to transfer phosphorylcoline from phosphatydilcolin to the hydroxyl group in position 1 of the spingoid base of ceramide, with the release of diacylglycerol.

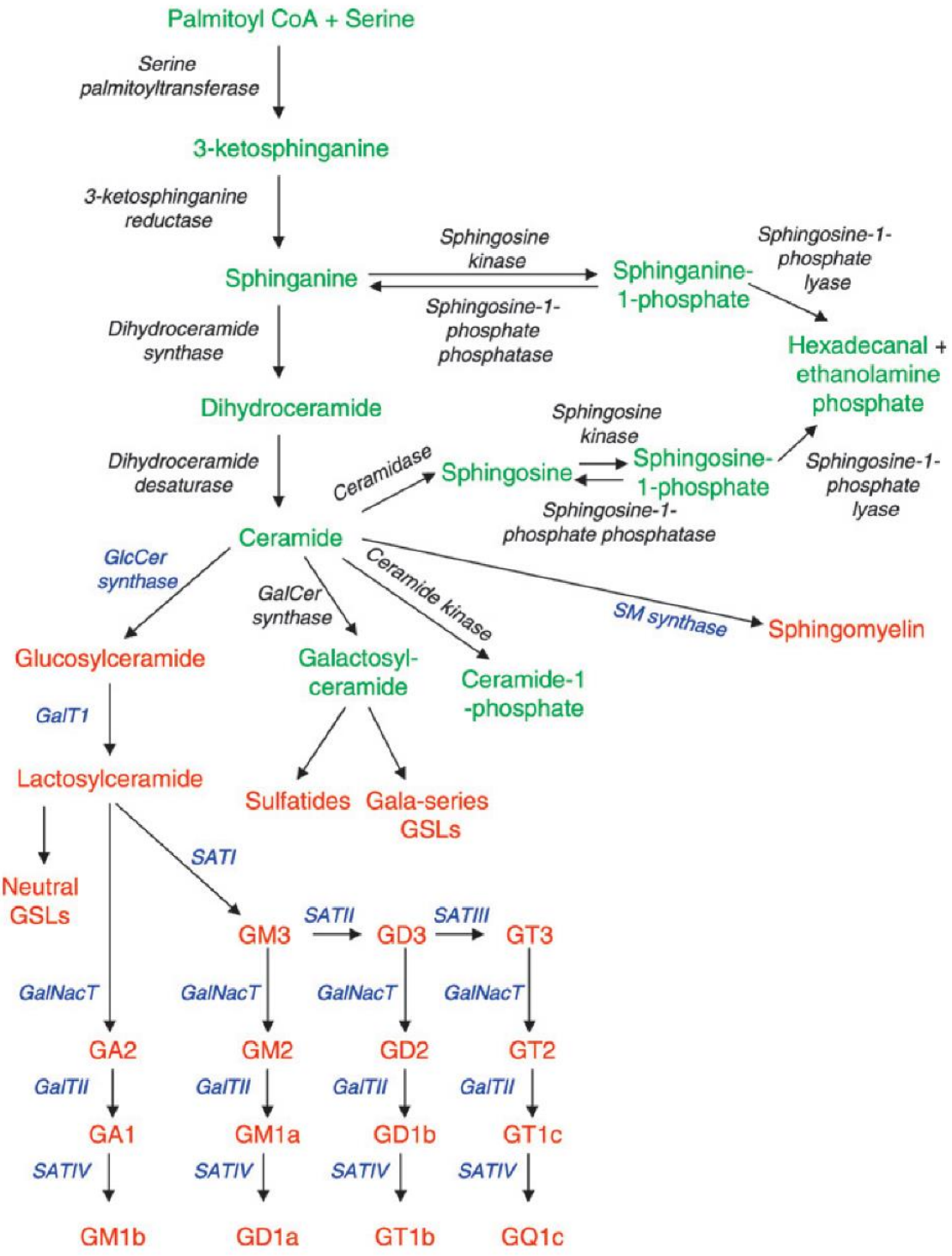

Figure 4 The metabolism of SLs in the ER and Golgi apparatus.
SLs synthesized in the ER are in greeen, and those synthetised in the Gogli apparatus are in orange [Lahiri and Futerman, et al. 2007].

Catabolism

SLs metabolic homeostasis is obtained with the balancing of biosynthesis, degradation and recycling [Gault, Obeid, et al. 2010]. The central hub of SL anabolism is the vesicular transport of neo-biosynthesized SLs from the endoplasmic reticulum and Golgi apparatus to the PM.

On the other hand, metabolic turnover and degradation of plasma membrane sphingolipids are processes occurring in the lysosomes, the acidic compartment of the cells, by the presence of specific acidic hydrolases [Bartke and Hannun, et al. 2009]. The degradation process consists in the remodeling of the hydrophilic head, driven by the lysosomal glycosidase from the non-reducing end of the glycolipid substrates. The molecules resulting from the catabolism can leave the lysosomes and further be degraded or used again to form more complex structure [Carter, Hendry, et al. 1961].

For example, during the ganglioside catabolism, GM1 is cleaved to GM2 by β-galactosidase. The resulting GM2 is than degraded to GM3 and *N*-acetyl-galactosamine through the action of β-hexosaminidase A (HexA). The β-hexosaminidases are dimeric enzymes composed by two different subunit α and β. The different possible dimerization of their subunits leads to three different isoforms of the enzymes: Hex A, Hex B and Hex S [Kytzia and Sandhoff, et al. 1985].

GM3 is a substrate of sialidase Neu1 and Neu3, which leads to the formation of LacCer and sialic acid. Sialidases are glycohydrolases, which catalyze the removal of α-glycosidically linked sialic acid. Four different isoforms have been isolated from four different genes: Neu1, Neu2, Neu3 and Neu4 [Fingerhut, van der Horst, et al. 1992]. Neu1, Neu2, Neu3 are predominantly localized in the lysosomes, cytosol and plasma membrane respectively. Neu4 is present in mitochondria and endoplasmic reticulum.

The degradation of LacCer is driven by β-galactocerebrosidase, which removes galactose obtaining GlcCer [Zschoche, Furst, et al. 1994].

The GlcCer obtained by the reaction of β-galactocerebrosidase is further degraded to ceramide by the action of β-Glucosidase. GBA1 is the first enzyme identified as β-glucosidase and is lysosomal-associated. GBA1 hydrolyze the glycosidic linkage of GlcCer, conduritol B Epoxide (CBE) inhibits this enzyme.

On the other hand, SM is converted to Cer by sphingomyelinase (SMase). The eukaryotic cells are characterized by acid sphingomyelinase (aSMase) and neutral sphingomyelinase. The acid one is principally located in lysosome environment [Spence, et al. 1993].

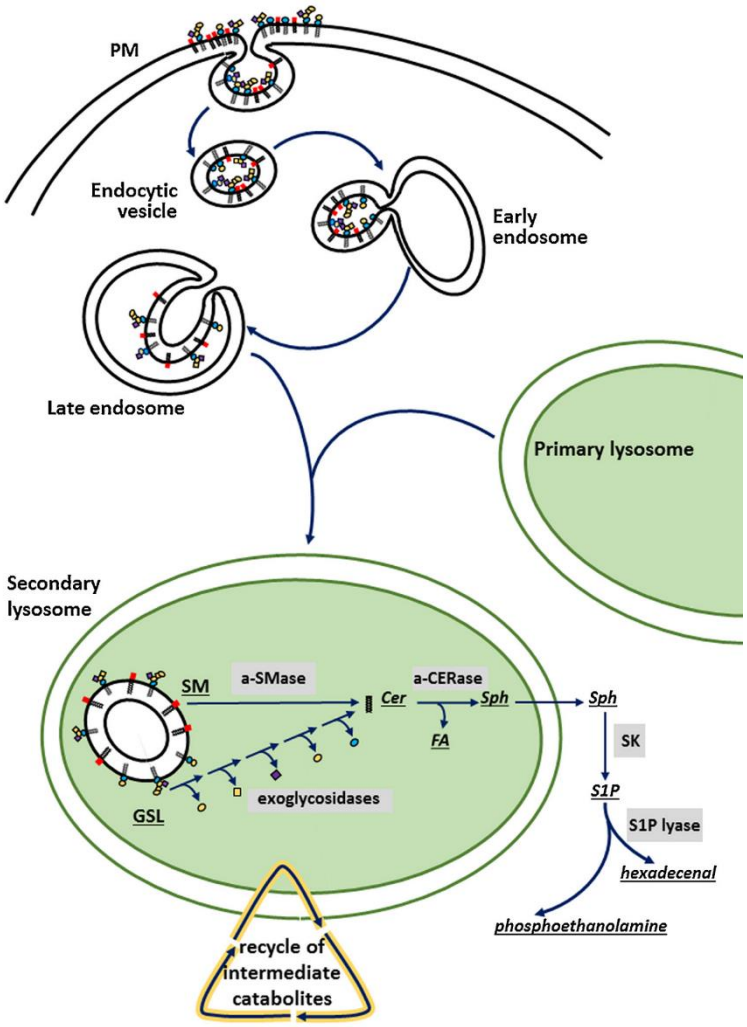

Figure 5 Sphingolipid catabolism in the endo-lysosomal compartment.
Sphingolipids catabolism starts from invaginations of plasma membrane (PM) portion leading to the formation of endocytic vesicles, which are incorporated in the primary lysosome.
In secondary lysosome, different exoglycosidases sequentially cleave off the sugar residues from the non-reducing end of glycosphingolipids (GSL) producing ceramide (Cer).
Cer can be also obtained from the sphingomyelin (SM) catabolism by the action of the acidic-sphingomyelinase (a-SMase). [Aureli, Schiumarini, et al. 2016]

Sphingolipid metabolism at the plasma membrane level

Several process are responsible for the plasma membrane sphingolipids pattern and content. The principals are neo-biosynthesis in endoplasmic reticulum and Golgi, membrane turnover with final catabolism in lysosomes and membrane shedding.

Moreover, some recent data reported that enzyme involved in the sphingolipids metabolism are able to modify the sphingolipids head group directly at the PM level [van Meer, Voelker, et al. 2008].

In fact, some of the same enzymes of the sphingolipids biosynthesis and catabolism are found to be associated with the cell surface. It has been observed that these enzymes are often available as a series

of couple that catalyze the same reaction in opposite direction, contributing to the in situ changes of SL composition. This phenomenous leads to very important biological consequences, considering

that could be instrumental to modulate cell function, with no involvement of the complex intracellular metabolic machinery.

The couple of Sialidase/Sialyl trasferase represents the first example. The PM sialidase is Neu3 that preferentially hydrolyzed the α 2-3 external ketosidc linkages, being ineffective on inner sialic acid residues. The role of Neu3 is to modify the ganglioside composition at the cell surface

Furthermore, it has been demonstrated also the presence of β-hexosaminidase A at the PM level, in combination with the β-hexosaminyl transferase.

A particular case is represented by a PM-associate sphingomyelin synthase (SMS2) because is an enzyme genetically distinct from the Golgi's one. SMS2 is present in combination with SMases. Three different SMases are available in eukaryotic cells: secreted SMase, acid SMase and neutral SMase. Only a particular isoform of neutral SMase, the nSMase2, works at the PM level.

In addition, the β-galactosidase and the β-glucosidase acts at the cell surface. In particular two different β-glucosidase have been detected; GBA1 which is the same of lysosome and a non-lysosomal β-glucosylceramidase GBA2.

GBA2, like GBA1, is involved in the degradation of GlcCer to glucose and ceramide. It is considered a key enzyme in the glycosphingolipids homeostasis. GBA2 is not localized in the lysosome but is strongly associated with the plasma membrane, with five possible transmembrane domains. The most powerful inhibitor of GBA2 is N-5-adamantane-1-yl-methoxypentyl) deoxynojirimicin (AMP-DNM), followed by miglustat [Boot, Verhoek, et al. 2007].

GBA2 is ubiquitously distributed in several tissue and cell lines, in particular is expressed in brain, heart, skeletal muscle, kidney and placenta. In minor part is detectable in spleen, liver, small intestine and lung [Aureli, Loberto, et al. 2012, Aureli, Samarani, et al. 2016].

Of particular interest in the context of Cystic Fibrosis are the enzymes involved in the catabolism of sphingolipids, leading to the formation of ceramide and in the regulation of its content at the plasma membrane level, even considering the peculiar role of ceramide in the host defense and inflammation in CF lung disease.

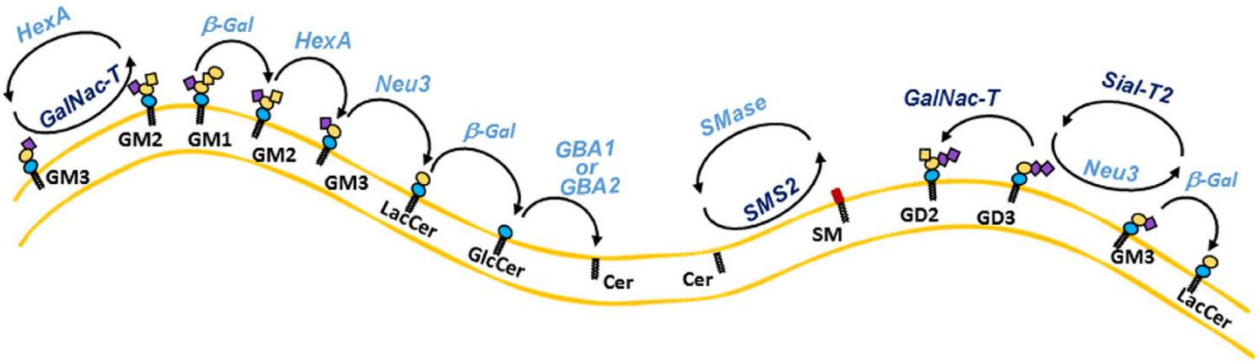

Figure 6 Schematic representation of sphingolipid metabolism occurring at the cell surface. *[Aureli, Schiumarini, et al. 2016]*

Biochemical role of sphingolipids

Several evidences in literature suggest that lipids are not only structural component of cell membrane but also fundamental actors of cell signaling and regulatory pathway [Hannun and Obeid, et al. 2008, Ohanian and Ohanian, et al. 2001].

Ceramide, ceramide-1-phosphate, sphingosine, and sphingosine-1-phosphate have been shown to be involved in the regulation of a number of cellular events such as proliferation, differentiation, motility, growth, senescence, and apoptosis [Giussani, Tringali, et al. 2014]. Ceramide and S1P have been proposed to have opposite roles in these processes. The balance between ceramide and S1P, which are metabolically interconnected, determines the entrance into one or more of these pathways. Complex GSLs are also involved in cell physiology by acting as antigens, mediators of cell adhesion, binding agents for microbial toxins and growth factors, and modulators of signal transduction [Lahiri and Futerman, et al. 2007]. In particular, SLs together with cholesterol, saturated phospholipids and a specific pool of proteins organize macromolecular complex at the cell PM called lipids rafts. The lipids rafts theory was postulated in 1980s on the bases of the spontaneous lateral segregation of sphingolipids. This definition was subsequently modified to introduce the notion that lipid rafts correspond to membrane areas stabilized by the presence of cholesterol within a liquid-ordered phase [Sonnino and Prinetti, et al. 2013].

Nowadays, different studies reported in literature, describe membrane rafts as a dynamic nanoscale domain enriched in sphingolipids, cholesterol and ceramide, which play an important role in cell signal transduction [Simons and Sampaio, et al. 2011].

The forces that control the formation and dynamics of lipid rafts are not fully understood yet, but one of the important point is that the preponderance of saturated hydrocarbon chains in cell SLs allows cholesterol to be tightly interacted [Simons and Sampaio, et al. 2011].

Lipids rafts are mainly studied exploiting their resistance to solubilization by non-ionic detergent, like Triton X-100. Detergent-resistant membrane (DRM) complexes float to low density during sucrose gradient centrifugation and are enriched in rafts proteins and lipids, providing a simple means of identifying possible rafts component [Simons and Sampaio, et al. 2011].

Using this experimental approach it has been found that lipid rafts are characterized by heterogeneous protein and lipid content with a specific segregation of lipids formed by saturated and long hydrocarbon chains. Probably, in lipid rafts, SLs modulate the functional features of several membrane proteins by lateral interactions between SLs and plasma membrane protein, and by short-range alterations of the physico-chemical properties of the protein membrane microenvironment. In fact, one of the most important property of lipid rafts is that they can include or exclude proteins to variable extents [van Meer and Lisman, et al. 2002].

Proteins with rafts affinity include glycosylphosphatidylinositol (GPI)-anchored proteins, doubly acylated proteins, such as Src-family kinases or the α-subunits of heterotrimeric G proteins, cholesterol-linked and palmitoylated protein and transmembrane proteins.

It is not yet clear why some transmembrane protein are included into lipid rafts, but some studies suggests the amino acids in the trasmembrane domains near the exoplasmic leaflet are critical as well as specific post-translational modification such as palmitoylations or myristoylations. In addition, a monomeric transmembrane protein may have a short residence time in rafts, but when the same protein is crosslinked or oligomerized, its affinity for rafts increase.

The distribution of lipid rafts over the cell surface depends on the cell type. Generally, they are more abundant at the plasma membrane level, but are also present in the biosynthetic and endocytic pathway, as Golgi apparatus and endoplasmic reticulum. For example, in polarized epithelial cells, as epithelial bronchial cells, lipid rafts accumulate in the apical plasma membrane.

A common theme is that the clustering of separate rafts exposes proteins to new membrane environments, enriched in specific enzyme, forming signaling platform, able to activate intracellular pathway like inflammatory response or apoptosis.

Moreover, if receptor activation takes place in a lipid raft, the signaling complex is protected from non-rafts enzymes such as membrane phosphatase that otherwise could affect the signaling process.

Generally, raft binding recruit proteins to a new-environment, where the phosphorylation state can be modified by local kinases and phosphatases, resulting in downstream signaling. Nervous system provides many examples of lipid rafts associated signaling. One example is represented by GDNF

signaling. The glial-cell-derived neurotrophic factor (GDNF) family of ligands is important for the development and maintenance of the nervous system. GDNF binds to a multicomponent receptor complex that is composed of GPI-linked GDNF receptors-α (GFR-α) and the trans-membrane tyrosine kinase, RET. The receptor subunit GFRα and RET are not associated with each other in the absence of ligand. However, after extracellular GDNF stimulation, RET moves into rafts, where it associates with GFRα in lipid rafts.

One subclass of lipid rafts is found in cell surface invagination called caveolae involved in the regulation of several signaling processes including that mediated by the insulin receptor.

IR is present in lipid rafts of normal adipocytes [Gustavsson, Parpal, et al. 1999] and localized in caveolae [Kabayama, Sato, et al. 2005], where the β-subunit of IR interacts with caveolin-1 through a binding motif recognizing the scaffold domain of caveolin-1 [Couet, Li, et al. 1997]. IR can form also a distinct complex with caveolin-1 and GM3 within lipid membrane domains [Kabayama, Sato, et al. 2007]. Interestingly, in 3T3-L1 adipocytes, the induction of insulin resistance by treatment with TNFα was accompanied by the upregulation of GM3 synthase, leading to an increase of cellular GM3 [Tagami, Inokuchi Ji, et al. 2002] that accumulated in detergent-resistant membranes. In insulin resistance, the association between IR and GM3 was increased, while its association with caveolin-1 was decreased, indicating that the excess amount of GM3 in lipid membrane domains leads to the displacement of IR from the complex with caveolin-1. This finding suggests that the regulation of IR/ caveolin-1 by GM3 could be responsible for the changes in insulin response in adipocytes.

Many other signaling pathways work thanks to the presence of lipid raft suggesting that these structures are involved in a great variety of cellular functions and biological events.

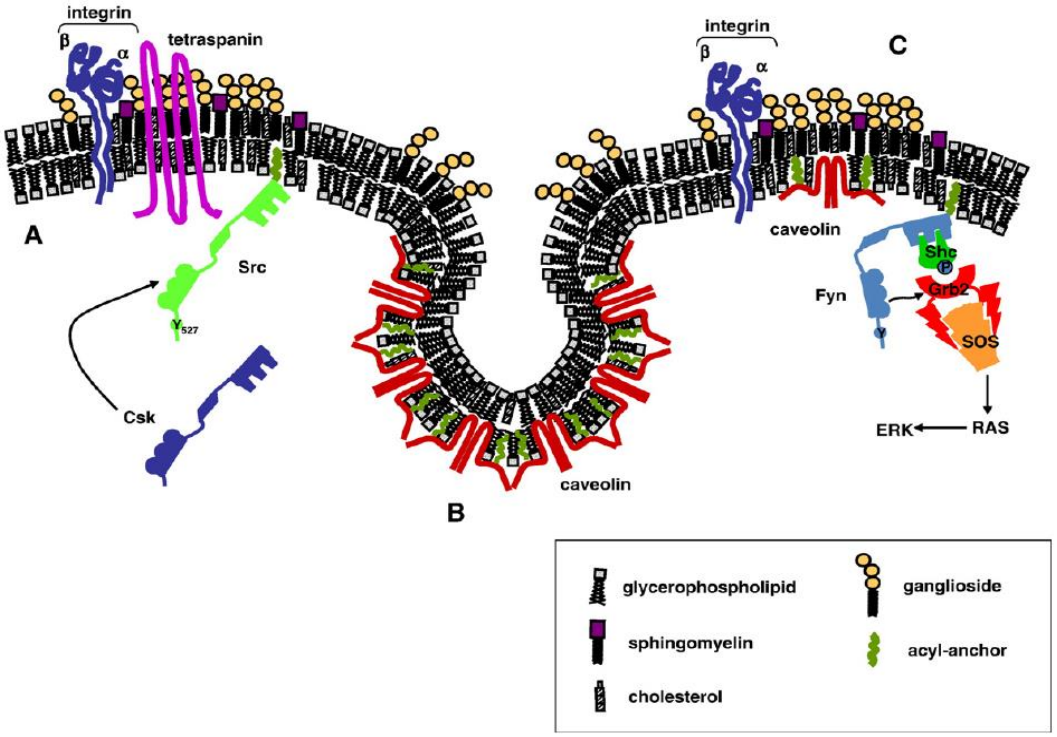

Figure 7 Membrane model containing different DRM

Sphingolipids in Cystic Fibrosis

Lung Sphingolipids

A complex pattern of SLs characterises human lung tissue. Globosides, including globotetraosylCer and globotriaosylCer, are the major class of neutral glycolipids, followed by LacCer, GlcCer and tetrahexosylCer. In addition, among sialylated GLSs, in the lung are present fourteen different types of gangliosides. The most abundant is GM3 followed by GM1, disialo GD3, and trisialosyllactosylCer GT3. [Mansson, Mo, et al. 1986]

SLs and their metabolism play an important role in lung development. For instance, the SL rheostat composed by Cer and S1P, promoting apoptosis and cell survival respectively, is required for growth of lung structure at all stages of lung development, as well as for pulmonary physiology preservation. More generally, the regulation of ceramide levels is important for lung homeostasis maintenance.

Different studies reported the involvement of Cer in pulmonary infection, driven by a wide range of pathogens including *Neisseria gonorrhoeae*, *Neisseria meningitidis*, *Staphylococcus aureus*,

Pseudomonas aeruginosa, *Listeria monocytogenes*, *Salmonella typhimurium*, *Escherichia coli*, mycobacteria, measles virus, rhinovirus, and sindbis virus [Seitz, Grassme, et al. 2015].
Cer is suitable to manage bacterial and viral infection thanks to its biophysical properties. Cer is characterized by high hydrophobicity, low amphiphilicity and is able to create small Cer-enriched membrane domain thanks to hydrophobic interaction. Indeed, is reported that, different stimuli, including bacterial infections, are responsible for the creation of Cer-enriched platforms [Teichgraber, Ulrich, et al. 2008].

Sphingolipids involvement in Cystic Fibrosis lung disease and infection

Large amount of pro-inflammatory mediators, as interleukin-8 (IL-8), IL-6 and tumour necrosis factor (TNF)-α characterize the airways of CF patients. This condition cause the recruitment of neutrophils, unable to vanquish bacteria, leading to an amplification of inflammation and perpetual infection.
Bacterial component bind different receptors, expressed on epithelial cell surface, such as Toll like receptors 2, 4 and 5. This binding activates a series of kinases that culminate in a nuclear translocation of transcription factor and expression of pro-inflammatory genes.
Concerning the involvement of SLs in CF lung infection, some studies reported that GSLs of epithelial cell surface could operate as receptor for microorganism. In particular, for *P. aeruginosa*, it has been show that some clinically strains of this bacterium are able to bind asialo-GM1 and asialo-GM2.
Conversely, the role of Cer in CF inflammation and infection is under debate. For instance, Guilbault and colleagues demonstrated that plasma of CF patients displays significantly low levels of several Cer species. In particular, they found in C57BL/6-CFTR mice an overall reduction of Cer level in lung, plasma, ileum and pancreas compared with WT mice [Guilbault, Wojewodka, et al. 2009].
Vilela and co-workers tried to elucidate the possible molecular mechanism involved in the reduction of ceramide in CF, using immortalized human respiratory tracheal epithelial cells.
CF tracheal epithelial cells are characterized by a high level of glutathione that could decrease the intracellular Cer content through the inhibition of neutral sphingomyelinase. The increased activation of the pro-inflammatory transcription factor (NF)-kB, which is responsible for the abnormally high inflammatory response in CF, seems to be due to Cer deficiency. In fact, increased Cer levels, obtained by treatment of CFTR-deficient tracheal epithelial cells with fenretinide, results in an improved ability to control *Pseudomonas aeruginosa* infection [Guilbault, De Sanctis, et al. 2008, Vilela, Lands, et al. 2006]

On the other hand, Teichgraber and colleagues reported an age dependent accumulation of Cer in the respiratory tract of uninfected mutant mice lacking CFTR. To explain these findings they suggest that, the loss of CFTR induces an alkalinisation of intracellular vesicles that strongly reduces the activity of acid ceramidase, without substantial modification of acid sphingomyelinase activity [Teichgraber, Ulrich, et al. 2008]. This accumulation of Ceramide seems to be involved in the age-dependent pulmonary inflammation and in the high susceptibility to *P.aeruginosa* infection.

In contrast to Teichgraber and colleagues, Becker reported that inhibition of the acid sphingomyelinase reduces Cer levels and leads to an amelioration of the inflammatory response to *P.aeruginosa* [Becker, Tummler, et al. 2010]. These controversial data seems to be caused by the different mouse models used.

Despite these contradictory results, Brodlie and colleagues described for the first time an increased Cer level in the lower airway epithelium of CF patients. In addition, they found an increased level of Cer in lung colonized by *P.aeruginosa* [Brodlie, McKean, et al. 2010]

At this regard, ceramide itself is important for host defenses; in particular ceramide-enriched membrane platforms seems to be essential to clear bacteria and probably are involved in the mediation and control of the infection of several pathogens, like *Pseudomonas aeruginosa.* [Uhlig and Gulbins, et al. 2008, Yang and Uhlig, et al. 2011]

These ceramide-enriched domains recruit some different receptors and signaling molecules, such as CD95, CD40 and CD14 important for the apoptosis or the activation of inflammatory response.For instance, Grassme in 2001 described how *P.aeruginosa* infection leads to the activation of ASMase and its translocation to the plasma membrane of normal epithelial cells. In this situation, ceramide, produced by SM hydrolysis, together with CD95 clusterization leads to *P. aeruginosa* internalization, induces apoptosis and regulates the cytokine response in the infected cells [Grassme, Becker, et al.]. These different studies suggests us that ceramide plays a very important role in the mechanism of host defense and inflammation in CF.

Moreover, in addition to these data, the ceramide, which comes from catabolism of complex GSLs at the PM level, seems to plays an important role in the pro-inflammatory state of CF and in the inflammation caused by the infection of *P.aeruginosa.* In particular, the inhibition of GBA2 with miglustat, suggests its involvement in the production of ceramide at the cell surface of airway epithelial cells, after the infection caused by *P. aeruginosa.* Indeed, treatment of CF epithelial bronchial cells with miglustat reduce immune response after *P. aeruginosa* infection; more specifically Loberto and colleagues reported a down-regulation of chemokines, proinflammatory cytokines and the intercellular adhesion molecule-1 [Loberto, Tebon, et al. 2014]

In addition, the silencing of GBA2 with specific siRNA leads to a strong reduction of IL-8 secretion both in presence and in absence of *P. aeruginosa* infection in CF epithelial airway cells.
All these findings open the possibility of targeting Cer metabolism as new therapeutic strategies for CF lung disease.

Relationship between CFTR and sphingolipids

Scientific literature describes CFTR as a transmembrane protein associated with lipid rats. Taking into account this characteristic, is reasonable to speculate that the stabilization of the protein or the modulation of its function is driven by SLs interaction.
For instance, Hamai et al reported a relationship between CFTR expression and SL synthesis. Mutated CFTR or decreased expression leads to an increased SL synthesis and as consequence, an increase content of SM, sphingosine and sphinganine at the PM level. In addition, it was observed that the lack of CFTR causes an alteration of PM Ceramide composition; in particular, there is an increased content of long-chain Cer species. The increased Cer production can be interpreted as a cellular response to the plasma membrane destabilization. In this context, even the SL synthesis could be a compensatory mechanism directed to increase membrane stability [Hamai, Keyserman, et al. 2009].
Another example of this process is represented by the study of Itokazu and colleagues, which described a direct correlation between PM levels of ganglioside GM1 and CFTR expression. CFTR-silenced human airway cells have a decreased content of GM1 and a depressed β-integrin signalling, resulting in a reduction of cell motility. They demonstrated that the addition of GM1 to this type ofcells, partially restores cell migration. In addition, they demonstrated that the recovery of CFTR in CFTR-silenced cells significantly increases GM1 levels. On the other hand, the pharmacological inhibition of CFTR in normal cells, decreases GM1 content [Itokazu, Pagano, et al. 2014]. These data have implications for the CF pathology, where altered SL levels in CF airway epithelial cells is probably involved in a diminished process of wound repair.
Ramu and colleagues published data related to the regulation of CFTR function by the PM micro-enviroment. They described that the inhibition of CFTR current is caused by the formation of ceramide from SM hydrolysis. The clusterization of CFTR in membrane areas rich in ceramide makes more difficult the channel activation by phosphorylation of regulatory domain [Ramu, Xu, et al. 2007].
This situation becomes worse with the presence of some pathogens, like *Pseudomonas aeruginosa*, which has a SMase activity that hydrolyses SM in situ, leading to the formation of Cer. The reduced

CFTR activity caused by *P. aerugionosa,* is accompanied also by an impaired mucociliary clearance and, as consequence, a decreased ability to clear bacteria [Stonehouse, Cota-Gomez, et al. 2002].

Ceramide produced by bacterial SMase has an effect on CFTR stabilization even influencing the regulation of a scaffolding protein ERM (ezrin/radixin/moesin). The ERM complex regulates cytoskeletal plasma membrane interaction.

In particular, Ezrin is important for the CFTR activation because acts as a PKA-anchoring protein, recruiting a PKA to the proximity of CFTR, leading to its activation. Some data reported that ceramide promotes ERM dephosphorylation and, as consequence its inactivation, through a protein phosphatases.

Although several findings clearly demonstrated that CF pulmonary disease is characterized by altered SL metabolism, unfortunately, the direct involvement of SLs in the pathogenesis of CF lung disease is still unclear.

Future progress in understanding the critical role of SLs in the pathophysiology of Cystic Fibrosis could open new perspectives for the development of alternative SL-based therapeutic strategies to reduce the inflammatory response as well as to rescue or increase the CFTR function at the cell surface.

Aim

Airway obstruction, infection and inflammation are the most severe pathophysiologic feature of CF lung disease and for this reason, are direct target of many current and candidate therapies and treatment for this pathology.

There are many therapies available to manage airway infection, inflammation and mucus alteration. For instance, the drugs suitable to treat bacterial infection are tobramycin, fluroquinolone and different inhaled antibiotic combination [Cantin, Hartl, et al. 2015]. Considering anti-inflammatory therapies, Ibuprofen and corticosteroids are the only effective anti-inflammatory drug, recommended as a beneficial therapy for patient from 7 to 18 years of age, even though limited efficacy or the occurrence of severe side effects [Hoffman and Ramsey, et al, Konstan, Schluchter, et al. 2007].

Hence, the identification and development of novel and more potent anti-inflammatory drugs for CF airway disease remains a priority. SLs metabolism seems to be a potential new target for therapeutic intervention. In particular, Ceramide seems to be involved in the process of infection and inflammation of CF. As mentioned in detail in the introduction, Becker and colleagues reported that inhalation of acid sphingomyelinase inhibitors, such as amitriptyline, trimipramine, desipramine, fluoxetine or sertraline reduce pulmonary inflammation and prevent lung infection in CF mice [Becker, Riethmuller, et al.]. On the same frame of work, Nahrlich and colleagues conducted a phase IIb randomized, double bind, placebo controlled study, to test an *in vivo* beneficial effect of amitriptyline. They reported that this drug is safe and it reduces ceramide in lung of CF patients [Nahrlich, Mainz, et al. 2013]. In addition, recent findings reported by Caretti and colleagues demonstrated that the use of myriocin, an inhibitors of the ceramide *de novo* synthesis, leads to reduce bacterial infection [Caretti, Bragonzi, et al. 2013].

On the other hand, emerging and promising data derive from the study related to in situ plasma membrane catabolism of complex glycosphingolipids and the inflammatory response to *P. aeruginosa*. The inhibition of GBA2 by iminosugars such as Miglustat shows an anti-inflammatory effect in vitro by reducing *P.aeruginosa* induced immunoreactive ceramide levels [Dechecchi, Nicolis, et al. 2011].

Taking into account the increasing interest on the SL metabolism as target of CF anti-inflammatory therapy and considering the important results correlated to the use of Miglustat, I explored the potential involvement of GBA2 in the ceramide-mediated signaling process, following *P.aeruginosa* infection of CF human epithelial bronchial cells.

The study is based on the preliminary evidence that suggests the link between GLS catabolism leading to the PM cer production, and the inflammatory response in CF, even after the infection with *Pseudomonas aeruginosa.*

More in detail, preliminary results demonstrate that both the inhibition of GBA2 activity by miglustat and the down-regulation of its expression are associated with a significant reduction of IL-8, in CF human airways epithelial cells, infected with *P. aeruginosa.* Moreover, GBA2 knockdown results in a reduction of the intrinsic pro-inflammatory state of these cells, since it was observed a reduction of IL-8 basal level in not infected cells.

However, no data are available regarding the mechanistic link between the involvement of GBA2 and the inflammation state characteristic of CF.

For this reason in this thesis work, I focused my attention mainly on the involvement of the PM glycohydrolases in the CF inflammation process, with particular interest for GBA2, which seems to play an important regulatory role. I studied the possible correlation among the ceramide production at the PM level through the action of the PM glycohydrolases, and IL-8 release and expression.

Considering all these aspects, the specific aims of my PhD project were:

1. <u>The Identification of the molecular mechanism linking the PM glycohydrolases and the inflammation response in CF lung disease:</u>

First, I characterized CF and non-CF epithelial bronchial cells in terms of glycohydrolases activity and SLs pattern. I compared the different behavior of glycohydrolases and changes in SLs composition in CF and non-CF cells after infection with *Pseudomonas aeruginosa.*

Moreover, I studied the PM microenvironment of the glycohydrolase by lipid rafts isolation, with particular interest on GBA2, after the infection of *Pseudomonas aeruginosa.* I also investigated the effect of the bacterial infection on the plasma membrane localization of the different glycohydrolases.

2. <u>Development and characterization of a Nanoparticles-based siRNA-GBA2 delivering system.</u>

The second objective of my work was based on the important findings that shows that the silencing of GBA2 leads to a reduction of the pro-inflammatory status of CF bronchial epithelial cell, as well as reduction of inflammatory response after bacterial infection. This evidence suggests the possibility to work on the down-regulation of GBA2 for the development of a new therapeutic option. With this purpose, I studied a new strategy to delivery siRNA in CF epithelial bronchial cell in order to knock down GBA2.

More in details, I first identified the best siRNA sequences giving the highest GBA2 down-regulation in term of expression and activity. Subsequently, I developed, in collaboration with a group of

physicist, a high efficient multicomponent nanoparticle, useful for the delivering of siRNA targeting GBA2.

After the nanoparticles assembly, we proceed with a physical characterization by Dynamic light scattering. Subsequently, we evaluated the transfection potential in CF bronchial epithelial cells.

Finally, we tested the toxicity of the assembled nanoparticles by a cell proliferation assay and we evaluated the expression of biochemical marker of cell damage.

Materials and Methods

Cell models

CuFi-1: CuFi-1 cells line are a generous gift of A. Klingelhuts, Pkarp and J Zbaner, University of Iowa, Iowa city. [Zabner, Karp, et al. 2003]

CuFi-1 are Cystic Fibrosis human epithelial bronchial cells characterized by the homozygous mutation ΔF508/ΔF508, growth and propagated into normal plastic flasks, pre-coated with collagen (Collagen IV from human placenta- Sigma Aldrich).

10 mg of Collagen IV was dissolved in 16,6 ml di H_2O and 33,3 µl of acetic acid, and left at 37°C under gentle shacking until the complete dissolution.

I used as culture medium; "Bronchial Epithelial Basal Medium" (BEBM) supplemented with specific factors: 5 µg/mL insulin, 0.5 ng/mL hEGF, 0.5 µg/mL hydrocortisone, 0.5 µg/mL epinephrine, 50 µg/mL amphotericin B, 10 µg/mL transferrin, 6.5 ng/mL triiodothyronin, and 0.13 mg/mL bovine pituitary extract (all supplied by Lonza; singleQuot Kit Lonza) to obtain Bronchial Epithelial growth medium (BEGM). To BEGM was added glutamine (2mM) and Penicillin/Streptomycin (100 u/ml and 100 µg/ml respectively). The cells were cultured as monolayer in a humidified atmosphere at 37°C and 5% CO_2.

NuLi-1: NuLi-1 are wild type (non-CF) human epithelial bronchial cells, cultured in the same way of CuFi-1 cells as previously described by Dechecchi and Colleagues[Dechecchi, Nicolis, et al. 2008].

Bacterial strain

For infections experiments I used heat killed *Pseudomonas aeruginosa* strain PAO-1, kindly provided by A. Prince (Columbia University, New York).

PAO-1 was grown in a trypticase soy broth (TSB) or agar (TSA) as described by Dechecchi and colleagues [Dechecchi, Nicolis, et al. 2008]. The organism was killed by heating to 65°C for 30 minutes.

Bacterial infection and evaluation of the inflammatory response in vitro

Cells were infected for 4 hours with a PAO-1 concentration of 100 CFU/cells.
The inflammatory response to PAO1-1 infection was studied at the transcriptional level by measuring IL-8 chemokine expression as described by Dechecchi and colleagues. [Dechecchi, Nicolis, et al. 2011] Briefly, 50 ng of cDNA was amplified by the Platinum SYBR Green qPCR Super MixUDG (Invitrogen, Carlsbad, CA, USA) in a 1X final concentration in a total volume of 25 µl reaction. The target genes and the respective calibrator genes were amplified in separate tubes.
Amplification conditions were: an initial denaturation/activation step of 95°C for 2 min, followed by 50 repeats of 95°C for 15 s and 60°C for 30 s. Single Tube qRT-PCR was performed according to the comparative CT method and in duplicate [Dechecchi, Nicolis, et al. 2011].

Cell sphingolipid labelling with [1-^{3}H]-sphingosine

The sphingolipids analyses was performed through a sensitive method based on the use of [1-^{3}H]-sphingosine, as isotopic labelled sphingolipids precursor. This method allows the quick and sensitive screening of sphingolipids patterns and the quantitative evaluation of sphingolipids turnover in cultured cells.
The [1-^{3}H]-sphingosine was administered as tracer in non-bioactive concentration for two hours (pulse) in order to allow the steady state metabolic labelling of all cell sphingolipids [Loberto, Prioni, et al. 2005]. Briefly, [1-^{3}H]-sphingosine dissolved in methanol was transferred into a sterile glass tube and dried under a nitrogen stream, and [1-^{3}H]-sphingosine was solubilized in an appropriate volume of pre-warmed (37° C) medium (BEGM) to obtain a concentration of 0,3 nM.
The correct solubilisation was verified by measuring the number of dpm in a aliquot of medium.
After 2 hours of incubation (pulse) the medium was removed and cell were incubated for 48 h (chase) in fresh culture medium without the radioactive sphingosine. After chase, cells were collected and were used to perform the analysis of radioactive lipid or for DRM preparation.

Biotinylation

After the treatment of cells with PAO-1 or PBS for control sample, cells were incubated with 0.25 mg/ml of sulfo-NHS-biotin in PBS, pH 7.4 (5 ml/flask) for 30 minutes at 4°C.

The sulfo-NHS-biotin in excess was quenched by washing each flask with 5 ml of glycine (100 mM) in PBS. Thanks to these experimental conditions, the biotinylation is restricted to the cells surface and the internalization of the biotin derivative does not occur [Chigorno, Valsecchi, et al. 1990] [Aureli, Prioni, et al. 2010].

Isolation of detergent resistance membrane (DRM) fractions

DRM were prepared by ultracentrifugation on discontinuous sucrose gradient of cells subjected to homogenization with 1% Triton X-100 as previously described by Aureli and colleagues. [Aureli, Prioni, et al. 2010]

Briefly, after centrifugation at 270xg for 10 minutes, cell pellet was lysed in 1.2 ml of 1% Triton X-100 in 10 mM TNEV buffer (TrisHCl 10 mM, NaCl 150 mM, EDTA 5 mM, pH 7.5) in presence of 1 mM Na_3VO_4, 1 mM PMSF, and 75 mU/ml aprotinin, and Dounce homogenized (11 strokes, tight). Cell lysate (2 mg of cell protein/ml) was centrifuged 5 min at 1300x*g* to remove nuclei and cellular debris and the post nuclear supernatant (PNS) was removed and transferred in a different tube.

1ml of PNS was mixed with 1 ml of 85% sucrose (w/v) in TNEV Buffer (TrisHCl 10 mM, NaCl 150 mM, EDTA 5mM and pH 7.5) and 1 mM Na_3VO_4, placed at the bottom of a discontinuous sucrose gradient (30% and 5%), and centrifuged for 17 hr at 200,000x*g* at 4°C.

After ultracentrifugation, eleven fractions were collected, starting from the top of the tube. The light-scattering band, corresponding to the DRM fraction, was located at the interface between 5% and 30% sucrose, corresponding to fraction 4 or 5. Equal amounts of the low-density fractions (4 and 5) were mixed to obtain the DRM fraction, whereas equal amounts of the high-density fractions (10 and 11) were mixed to obtain the HD fraction. DRM and HD fractions were used for the lipid analyses and for hydrolases assays. The entire procedure was performed at 0-4°C on ice immersion. For the lipid analyses, low-density (4 and 5) and high-density fractions (10 and 11) were dialyzed and lyophilised.

The obtained samples were subjected to lipid extraction with $CHCl_3/CH_3OH/H_2O$. The total lipid extract was analysed by thin layer chromatography (HPTLC). Aliquots of the total lipid extracts from DRM and HD fractions were subjected to a two-phase partitioning as described below.

Immunoprecipitation

In order to isolate DRM, belonging only to plasma membrane, the DRM fraction was immunoprecipitated with streptavidin-coupled magnetic beads (Thermo-Fisher), which recognize the biotinylated protein with high affinity. The magnetic beads were washed twice with PBS and the mixture of DRM and beads were stirred overnight at 4°C. The immunoprecipitated was recovered by centrifugation according to manufactures instruction. Under these conditions (domain-preserving conditions), we preserved the organization of lipid domains [Aureli, Prioni, et al. 2010].

Sphingolipid analysis

Cells or DRM and HD fractions were lyophilized and subjected to lipid extraction and sphingolipids analyses.

Total lipids from lyophilized cells were extracted with $CHCl_3/CH_3OH/H_2O$ 20:10:1 by vol, followed by a second extraction with $CHCl_3/CH_3OH$ 2:1 by vol. The total lipid extracts were subjected to a two-phase partitioning by adding 20% water to the lipid extract. The radioactivity associated with the total lipid extract, the aqueous and the organic phases were evaluated by liquid scintillations using beta-counter system.

[^{3}H]SLs of total extracts and organic phases were separated by high performance thin layer chromatography (HPTLC) using the solvent system $CHCl_3/CH_3OH/H_2O$ 110:40:6 by vol, and those of aqueous phases with $CHCl_3/CH_3OH$/0.2% aqueous $CaCl_2$, 50:42:11 by vol. [^{3}H]-SLs were identified by digital autoradiography using ^{T}Racer system (Biospace Lab) and quantified by M3vision software. The lipid identification was performed using purified radioactive standards [Scandroglio, Venkata, et al. 2008].

Generation of GBA2-GFP overexpressing epithelial bronchial cell line

To generate a CuFi-1 and NuLi-1 cell line, overexpressing GBA2 tagged with GFP, the OriGene Company cloned the cDNA into a lentiviral vector (pLenti-GBA2-GFP). A lentiviral vector containing only GFP (pLenty-GFP) was used to generate Mock cells. Viral particles were generated by transfecting 3 µg of pLenti-GBA2-GFP or pLenti-GFP vectors and 9 µg of packaging vector mix

(coding for Gag, Pol Tat, Rev and VSVG) in 293FT cells by LipofectamineTM 2000 Reagent (Invitrogen).
Supernatant media were collected 48h after transfection, filtered through a 0.4 µm membrane, and used to infect CuFi-1 and NuLi-1 cells. [The viral titers were determined by transducing the 293FT cells with 10 fold serial dilutions of the lentiviruses supernatant (10-2-10-6 dilutions) or not transduced].

At 48 h after transduction, cells were plated under puromycin selection (5 µg/mL). After 10 days of selection, the cells were stained with crystal violet and were counted. CuFi-1 and NuLi-1 cells were infected with 1 ml of each lentivirus stock. After 1 day, medium was replaced with fresh medium containing the specific antibiotic to select the positive clones. To obtain the constitutive clones the transduced cells were selected with 5 µg/ml of puromycin and after 3 weeks of selection, colonies were separated and expanded.
Clones obtained were analyzed morphologically for the GBA2 tagged with GFP or GFP expression by confocal microscopy using cells fixed with paraformaldehyde (2% in PBS) for 20 min.

Enzymatic activity associated with cell plasma membrane

The assay, used during my experiments, allows the detection of the plasma membrane associated activity directly on living cells, using fluorigenic substrates. This method is based on the observation that the fluorigenic substrates commonly used for the in vitro assay of glycohydrolase activities are not taken up by living cells [Aureli, Loberto, et al. 2011].
In fact, under the appropriate experimental conditions, it is not possible to observe any fluorescence associated with cells. Moreover, the artificial substrates did not undergo to spontaneous hydrolysis or to hydrolysis driven by secreted enzymes. Thus, their hydrolysis under these experimental conditions is due exclusively to the PM-associated enzymatic activities [Aureli, Masilamani, et al. 2009].
PM associated activities of β-Galactosidase (β-Gal), β-Glucosidase GBA1, β-Glucosidase GBA2, β-Hexosaminidase (β-Hex) and sphingomyelinase (SMase) activities were determined on living cells, plated in 96-well microplate at density of 20000 cells/well, by a high throughput assay.
For GBA1 and GBA2 assays, cells were pre-incubated for 30 minutes at room temperature with 5 nM AMP-dNM [adamantane-pentyl-dNM; N-(5-adamantane-1-yl-methoxy-pentyl) deoxynojirimycin] and 1 mM CBE (Sigma) in DMEM-F12, respectively [Overkleeft, Renkema, et al. 1998].

β- Gal, β-Hex and β-Glucosidase activities were assayed using the artificial substrates 4-134 methylumbelliferyl-β-D-galactopyranoside (MUB-Gal), MUG and 4-methylumbelliferyl-β-D-glucopyranoside (MUB-Glc) solubilized in DMEM-F12 without phenol red at pH 6 at the final concentrations of 250 µM, 2 mM and 6 mM respectively. SMase activity was assayed using the artificial substrates 6-hexadecanoylamino-4-methylumbelliferyl-phosphoryl-choline (H-MUB-PC) solubilized in the same DMEM-F12 at the final concentration of 100 µM. At different time points aliquots of medium (10 µl) were analyzed by fluorimeter in a microplate reader (Victor, Perkin Elmer) (MUB: λex: 355 nm /λem: 460nm; H-MUB: λex: 405 nm /λem: 460nm) after adding 190 µl of 0.25 M glycine (containing 0,3% Triton X-100 for SMase assay), pH 10.7.

Standards free MUB and H-MUB were used to establish the calibration curves in order to quantify the substrates hydrolysis.

The enzymatic activity was expressed as pmol of products on mg protein per hour.

Enzymatic activity associated with cell lysate or sucrose gradient fractions

The enzymatic activities of β-Glucosidase GBA1 and GBA2, β-Galactosidase, β-Hexosaminidase, and SMase in the total cell lysates were determined using fluorigenic substrates as described by Aureli and colleagues, with few modifications [Aureli, Gritti, et al. 2012, Gatti, Lombardo, et al. 1985]

Briefly, cells were washed twice with PBS, were harvested and suspended in water in the presence of a protease inhibitor cocktail (Sigma-Aldrich). Total cell protein were evaluated by DC protein assay (Biorad) according to manufacturer instruction.

Equal amount of cell proteins were transferred into a 96-well microplate and the assay was performed three-fold in replicate. MUB-Glc was solubilized in McIlvaine buffer (pH 6) at the concentration of 24 mM. MUB-Gal, MUG and H-MUB-PC was solubilized in McIlvaine buffer (pH 5.2) at the concentration of 250 µM, 2 mM and 100 µM respectively.

For GBA1 and GBA2 assays, cells were pre-incubated for 30 minutes at room temperature with 5 nM AMP-dNM [adamantane-pentyl-dNM; N-(5-adamantane-1-yl-methoxy-pentyl) deoxynojirimycin] and 1 mM CBE (Sigma).

The reaction mixtures were incubated at 37°C under gentle shaking. After transferring 10 µl of the reaction mixtures to a 96 black well microplate and adding 190 µl of glycine (0.25M, pH 10.7), the obtained fluorescence was detected at different time points by a Victor microplate reader (Perkin Elmer)

Standards free MUB and H-MUB were used to establish the calibration curves in order to quantify the substrates hydrolysis.

The enzymatic activity was expressed as pmol of product on mg protein per hour.
The enzymatic activity associate with the sucrose gradient fractions were expressed as pmol of product on volume of fraction per hour.

Western blot analyses

Proteins from cell homogenates or gradient fraction sample were separated by SDS-PAGE gels and transferred onto PVDF membrane by electroblotting. Gel was made at 10% of acrilammide. After blocking with 5% skim milk in TBS-T buffer, membranes were incubated overnight at 4°C with primary antibodies. Caspase 8, NF-kB, P-FADD, RIP, Caspase-3, p62 (Cell Signaling), calnexin (BD), LC3b (Sigma) were used at the final dilution of 1:1000. GAPDH (Sigma) was used at the dilution of 1:7000.
After washing, the reaction with secondary antibodies (horseradish peroxidase-conjugated antibodies) was performed and enhanced chemiluminescencce detection (Pierce) was conducted as described in the manufacture instruction. GAPDH and calnexin were used as control.
For immunoprecipitation samples, I used HRP-conjugated streptavidin in order to visualize the biotinylated proteins. The data acquisition was performed using a Mini HD9 (UviTec, Cambridge) and analyzed by Nine Alliance mini HD9 software.

GBA2 silencing

To perform silencing experiments of GBA2 gene, I selected six different siRNA sequences, purchased form Quiagen, targeting different positions within GBA2 mRNA.
CuFi-1 cells were transiently transfected with siRNA anti-GBA2 or scrambled duplexes, complexed with cationic liposomes Lipofectamine 2000.
The silencing efficiency was evaluated by enzymatic activity and mRNA expression at different time points.

Cationic liposomes

The binary mixture DC-Chol/DOPE, at a molar ratio Φ = (neutral lipid/total lipid) = 0.5 were prepared by mixing appropriate amounts of the lipids dissolved in chloroform. The solvent was removed under

gentle stream of nitrogen and then kept under vacuum for 1 hour to ensure complete solvent removal. The lipid film were hydrated with water at the concentration of 20 mg/ml. Lipid mixture was then treated until clarity in an ultrasonic bath and stored at room temperature for 1 day, to attain liposome stability.

Cationic lipoplexes

23 bp DNA was used as a mimic of 23 bp siRNA in order to build nanovectors with the same structural feature as those of the cell delivered vectors, but in large amount to perform X-ray characterization. DNA was solubilized in ultrapure water (5mg/ml). DNA fragments of 23 base pairs were used.
Self-assembled DC-Chol/DOPE-DNA lipoplexes were prepared at the weight ratio ρ = cationic lipid/DNA = 5, by proper drop-addition of the DNA solution to CL dispersion and incubated at room temperature for 20 minutes. The solution did not show any microscopic precipitation.

Nanoparticle system

A 23 bp DNA, as mimic of 23 bp siRNA, was pre-complexed with protamine by dissolving protamine sulfate in Milli-Q water (2.5 mg/ml), then added dropwise to an equal volume of DNA solutions under gentle shaking, with a weight ratio (protamine/DNA) Rw = 0.5. At this ratio protamine/DNA complexes are negatively charged thus suitable to interact with cationic liposome. The protamine/DNA solution was then mixed with the cationic liposomes at weight ratio ρ = cationic lipid/DNA = 5. Self-assembled DC-Chol/DOPE-protamine/DNA NP were kept at room temperature for 20 minutes in order to stabilize it. The solution did not show any macroscopic precipitation.

NP for in vitro delivery of siRNA

Liposomes for nanovector preparation were prepared at 0.1mg/ml DC-Chol concentration and at lipid molar ratio Φ = (neutral lipid/total lipid) = 0.5, as above. For each transfection-solution, 50 µl protamine/siRNA solution containing 100pmol of siRNA were prepared in weight ratio Rw=0.5. After 20 minutes equilibration time, protamine/siRNA solution was properly drop-added to the liposome solution fulfilling the weight ratio ρ = cationic lipid/siRNA = 5 [Zhang, Li, et al. 2010].

Dynamic light scattering

Dynamic Laser Light Scattering measurements were carried out on a home designed apparatus. Sample were properly diluted, with filtered water (polycarbonate membranes, 0.2 μm pore size) inorder to avoid multiple scattering. The correlation functions of the scattered intensity were measured at T = 25°C. Data were collected at 90 ° scattering angle, and analyzed with Cumulants Method giving the particle average size and polydispersity index. The weigh-average size distribution was obtained with the CONTIN analysis.

Statistical analysis

All the experiments were performed in triplicate and statistical significance was determined by Student-Neumann-Keuls post hoc test (comparison between two groups) and for more than two groups by one-way or two-way ANOVA (followed by Turkey or Dunnett Neueman-Keuls on Bonferroni post test), with $p < 0.05$ as significant.

Results

Effect of bacterial infection on the plasma membrane composition of CF epithelial bronchial cells

Sphingolipids characterization and evaluation of hydrolases activity of CF and non-CF epithelial bronchial cell lines

In order to study the involvement of ceramide pathway in the intrinsic pro-inflammatory state of CF and to investigate the role of ceramide during bacterial infection, I chose the commonly used CF (CuFi-1) and non-CF (NuLi-1), cell models of human epithelial bronchial cells.

CuFi-1 and NuLi-1 cell lines derive from the same bronchial district and they were cultured in the same conditions.

First, I analyzed the SLs composition of these cell lines by feeding the cells with the radioactive precursor [1-^{3}H]-sphingosine in conditions that allow the metabolic labeling of the cellular sphingolipids at the steady state. Subsequently I separated the single [^{3}H]-lipids contained in the total lipid extract through high performance thin layer chromatography (HPTLC).

The digital autoradiography of HPTLC (figure 8), shows a similar SL pattern between CuFi-1 and NuLi-1 cells even with some differences. In particular, CuFi-1 cells are characterized by a major content of Cer and GlcCer, whereas the level of SM and ganglioside GM3 are lower, if compared to NuLi-1 cells.

Interestingly, the data related to the Cer content agree with the data found in the lungs of CF patients. In fact, Brodlie and colleagues described for the first time an increased Cer level in the lower airway epithelium of CF patients [Brodlie M, McKean MC, et al. 2010]. These findings and the data reported in literature, support the use of CuFi-1 and NuLi-1 cells to study the SL involvement in the pathophysiology of CF.

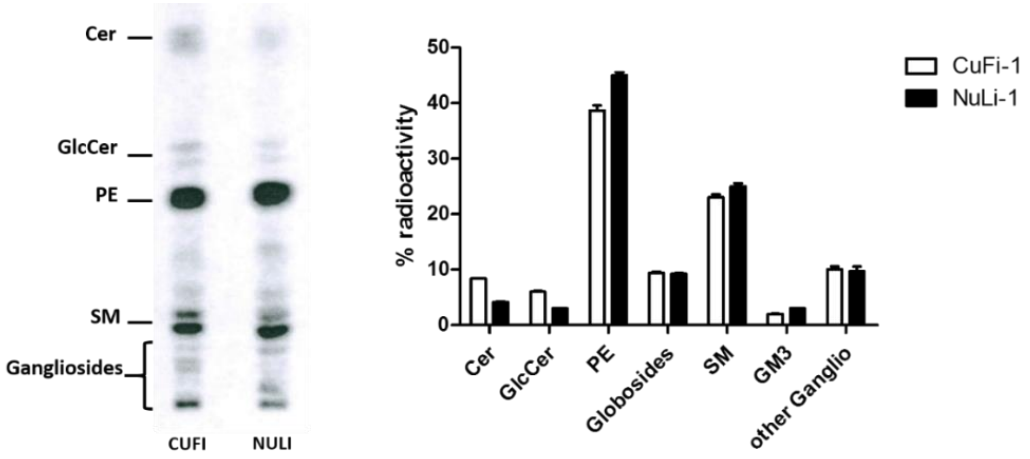

Figure 8 Sphingolipid composition of CuFi-1 and NuLi-1 cell lines.
Left: Autoradiography of HPTLC of radioactive sphingolipids obtained from total lipid extract of CuFi-1 and NuLi-1 cells. Each sample was loaded at parity of radioactivity.
Right: Semi-quantitative graph of sphingolipids species. The sphingolipids are represented as percentage of radioactivity.
Cer: ceramide; GlcCer: glucosylceramide; PE: phosphatidylethanolamine; SM: sphingomyelin

In addition, the shift from complex sphingolipids, such as GM3 and SM, to GlcCer and Cer suggests a major activation of the SL catabolic pathway in CuFi-1 cells.

Since the two main cellular district involved in the SLs catabolism are lysosomes and the cell plasma membrane, first I measured the enzymatic activity of the main SL hydrolases associated with lysosome. As shown in figure 9, I found that, for all the tested hydrolases, NuLi-1 cells show higher activity if compared to CuFi-1 cells. More in detail, the activity of β-glucosidase GBA1, β-galactosidase (β-gal) and sphingomyelinase (SMase) is double in NuLi-1 in respect of CuFi-1. Whereas the activity of GBA2 is only 20% higher in NuLi-1, compared to CuFi-1 cells.

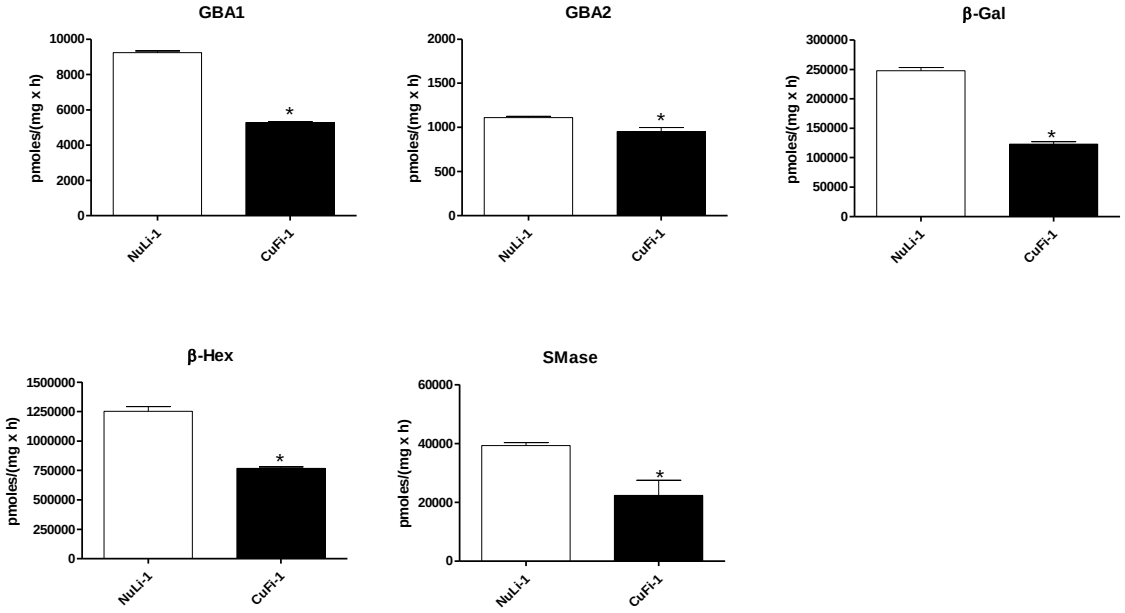

Figure 9 Hydrolases activity associate with total cell lysate of CuFi-1 and NuLi-1 cells.
The measurement of the hydrolases activity was conducted on cell lysate using an in vitro assay based on artificial fluorigenic substrates. The enzymatic activity is expressed as pmoles of products on mg of proteins per hour.
GBA1: β-Glucosidase 1; GBA2: β-Glucosidase 2; β-Gal: β-Galactosidase; β-Hex: β-Hexosaminidase; SMase: Sphingomyelinase
**p<0.05 vs NuLi-1*

Subsequently, I measured the enzymatic activity of hydrolases associated with the cell plasma membrane. Interestingly I obtained opposite results with respect to the total cell associate hydrolases. In fact, the pathological CuFi-1 cells are characterized by a double activity of the PM hydrolases if compared to the healthy NuLi-1 cells (figure 10). In particular, GBA2 is more than two times higher with respect to NuLi-1 cells.

These data suggest that the high level of ceramide of CuFi-1 cells, could be due to the increased hydrolysis of SLs, triggered directly at the cell plasma membrane level, by the in-situ action of the resident glycohydrolases.

These data agree with some data previously reported by Loberto and colleagues [Loberto, Tebon et al. 2014] on the production of Cer at the cell surface, which is involved in the activation of the inflammatory response after bacterial infection.

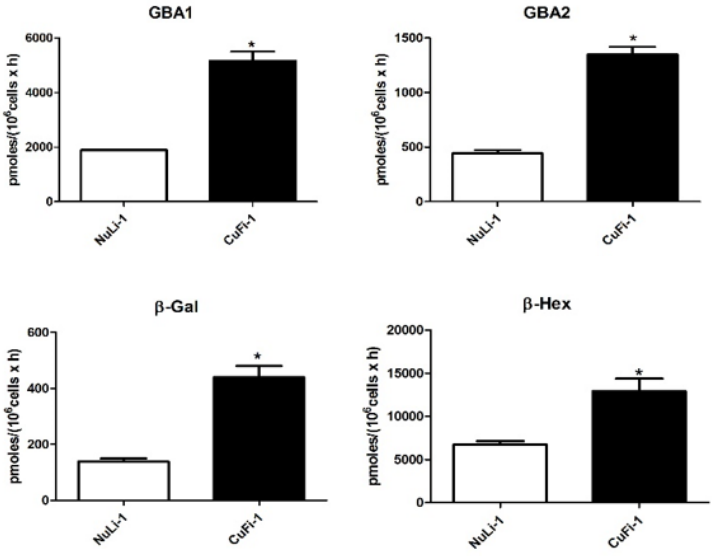

Figure 10 Hydrolases activity associate with the cell plasma membrane of CuFi-1 and NuLi-1 cell line.
The measurement of the plasma membrane hydrolases activity was conducted on living cells, using artificial fluorigenic substrates. The enzymatic activity is expressed as pmoles of products, on 10^6 cells per hour.
GBA1: β-Glucosidase1 GBA2: β-Glucosidase 2 β-Gal: β-Galactosidase β-Hex: β-Hexosaminidase
**p<0.05 vs NuLi-1*

Effect of *Pseudomonas aeruginosa* infection on the sphingolipids composition of CuFi-1 and NuLi-1 cell lines

Several lines of evidence suggest that ceramide accumulation correlates with the age-depended hyper-susceptibility of CF patients to bacterial infection. One of the main debatable aspect is related to the direct involvement of infection in the production of ceramide. In order to shed light on this aspect, I investigated the effect of *Pseudomonas aeruginosa*, the most severe pathogens in CF, to part of the molecular mechanisms involved in the modulation of ceramide level in CuFi-1 and NuLi-1 cell lines. In these experiments, cellular SLs were metabolically labelled at the steady state using [1-^{3}H]-sphingosine and the two cell lines were infected with heat killed PAO-1 for 4 hours. I found that the two cell lines were characterized by the same incorporation of radioactive sphingosine. I separated the lipids contained in the total lipid extract by HPTLC and the radioactive lipids were visualized by digital autoradiography.

The obtained results (figure 11) show that the content of Cer and GlcCer in infected CuFi-1 cells is significantly increased if compared with not infected cells. On the other hand, in NuLi-1 cells, PAO-1 infection causes only a slight increase of Cer.

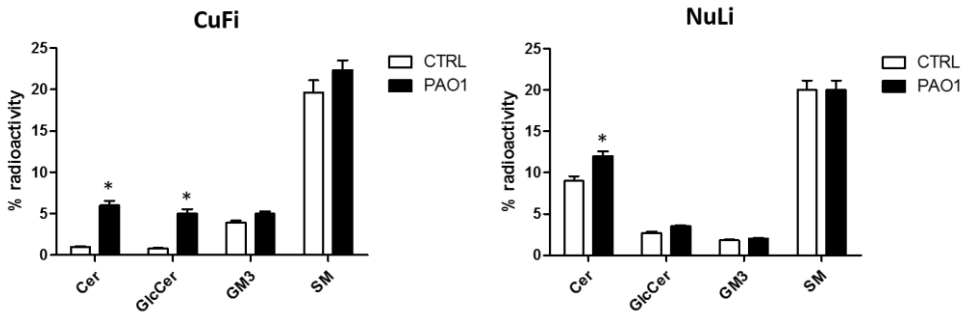

Figure 11 Effect of Pseudomonas aeruginosa infection on the sphingolipid composition of CuFi-1 and NuLi-1 cell line; GlcCer: glucosylceramide; SM: sphingomyelin.
Semi quantitative graph of sphingolipids species of CuFi-1 and NuLi-1 cells, infected or not with PAO-1. The sphingolipids are represented as percentage of radioactivity.
Cer: ceramide; GlcCer: glucosylceramide; SM: sphingomyelin
PAO-1: Pseudomonas aeruginosa CTRL: Not infected cells
**p<0.05 vs CTRL*

Effect of *Pseudomonas aeruginosa* infection on hydrolases activity.

The previously results show that *Pseudomonas aeruginosa* is able to cause significant changes in the SL composition. It has been recently demonstrated that the inhibition of GBA2 in CF human bronchial epithelial cells results in an important reduction in the inflammatory response to PAO-1 infection. Taken together these data suggest that PAO-1 infection is responsible for the activation of the SL catabolic pathway.

Based on this evidence, I investigated the effect of PAO-1 infection on the enzymatic activity of SMase and of the main glycohydrolases involved in the regulation of ceramide content as GBA1, GBA2, β-galactosidase and β-hexosaminidase, in CuFi-1 and NuLi-1 cells.

First, I infected the CuFi-1 and NuLi-1 cells with heat killed PAO-1 for 4h; after the infection, I measured the hydrolases activity associated with the total cell lysate.

Interestingly, I observed a slight increase, only for the intracellular SMase activity of infected NuLi-1 cells but I did not find any significant difference in the activity of the total cell hydrolases of CuFi-1 and NuLi-1, between infected and not infected cells (figure 12 and figure 13).

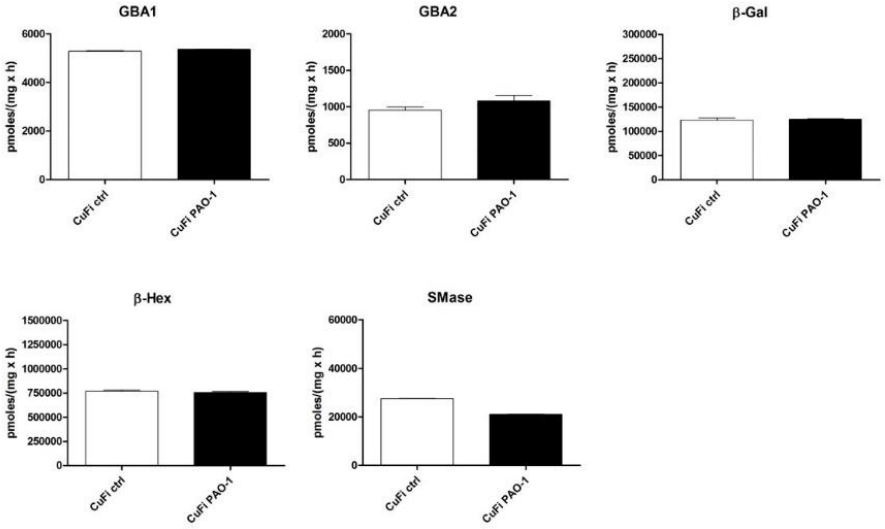

Figure 12 Effect of Pseudomonas aeruginosa infection on the activity of total cell hydrolases of CuFi-1 cells.
The measurement of the hydrolases activity was conducted on cell lysate using an in vitro assay and artificial fluorigenic substrates. Before the assay, the cells were treated for 4 hours with PAO-1. The same cells, not infected with PAO-1, were used as control.
The enzymatic activity is expressed as pmoles of products, on mg of proteins, per hour.
GBA1: β-Glucosidase 1; GBA2: β-Glucosidase 2; β-Gal: β-Galactosidase; β-Hex: β-Hexosaminidase; SMase: Sphingomyelinase
PAO-1: Pseudomonas aeruginosa; Ctrl: Not infected cells

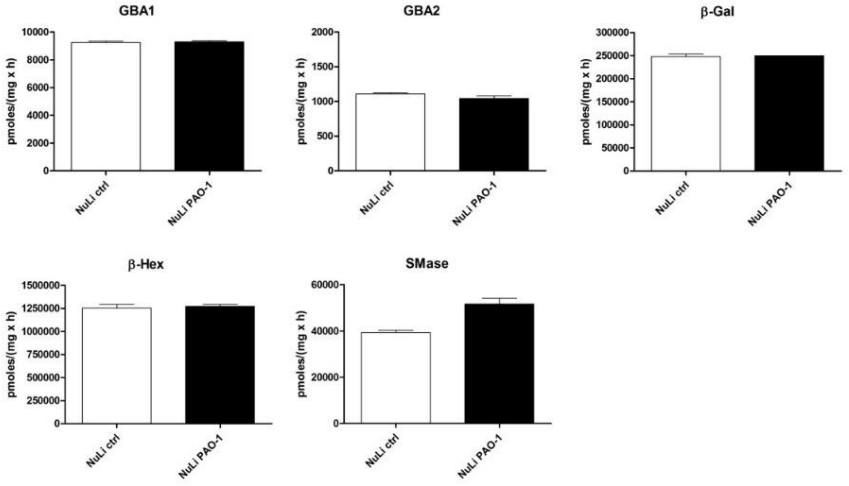

Figure 13 Effect of Pseudomonas aeruginosa infection on the activity of total cell hydrolases of NuLi-1 cells.
The measurement of the hydrolases activity was conducted on cell lysate using an in vitro assay and artificial fluorigenic substrates. Before the assay, cell were treated for 4 hours with PAO-1. The same cells, not infected with PAO-1, were used as control
The enzymatic activity is expressed as pmoles of products on mg of proteins per hour.
GBA1: β-Glucosidase; GBA2: β-Glucosidase 2; β-Gal: β-Galactosidase; β-Hex: β-Hexosaminidase
PAO-1: Pseudomonas aeruginosa; Ctrl: Control

Subsequently, I measured the activity of GBA1, GBA2, β-Gal and β-Hex associated with the cell surface of CuFi-1 and NuLi-1 cells subjected or not to PAO-1 infections.

Even in the hydrolases activity associated with the PM, I did not observe any significant difference between infected and not infected cells, for both CuFi-1 and NuLi-1 cell line for the exception of an increase in β-Gal activity in infected NuLi-1 cells (Figure 14 and 15).

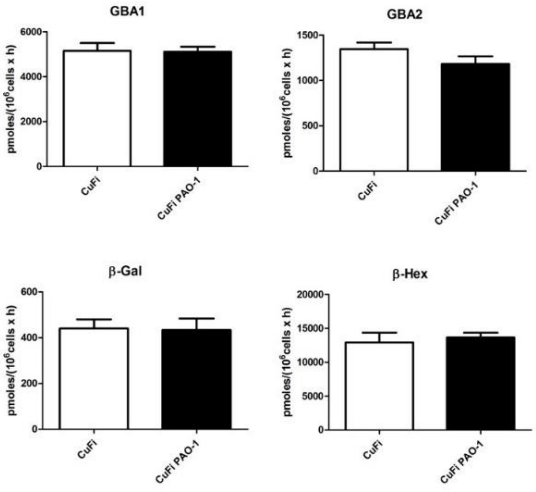

Figure 14 Effect of Pseudomonas aeruginosa infection on PM hydrolases of CuFi-1 cells. *The measurement of the plasma membrane hydrolases activity was conducted on living cells, using artificial fluorigenic substrates. Before the assay, cell were treated for 4 hours with PAO-1. The same cells, not infected with PAO-1, were used as control*
The enzymatic activity is expressed as pmoles of products on 10^6 per hour.
GBA1: β-Glucosidase 1; GBA2: β-Glucosidase 2; β-Gal: β-Galactosidase; β-Hex: β-Hexosaminidase
PAO-1: Pseudomonas aeruginosa; Ctrl: not infected
**p<0.05 vs CuFi-1*

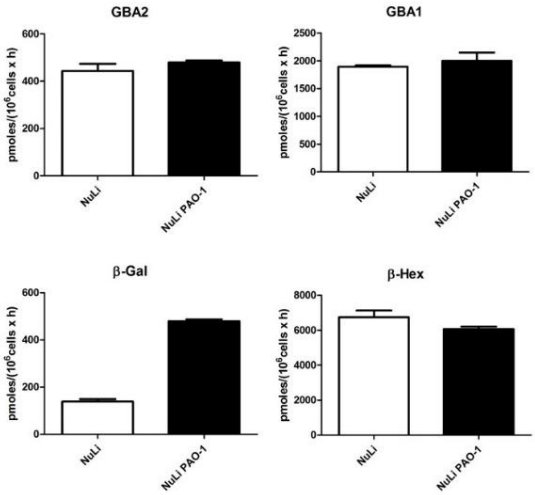

Figure 15 Effect of Pseudomonas aeruginosa infection on PM hydrolases of NuLi-1 cells. *The measurement of the plasma membrane hydrolases activity was conducted on living cells, using artificial fluorigenic substrates. Before the assay, cell were treated for 4 hours with PAO-1. The same cells, not infected with PAO-1, were used as control.*
The enzymatic activity is expressed as pmoles of products on 10^6 per hour.
GBA1: β-Glucosidase 1; GBA2: β-Glucosidase 2; β-Gal: β-Galactosidase; β-Hex: β-Hexosaminidase
PAO-1: Pseudomonas aeruginosa; Ctrl: not infected
**p<0.05 vs NuLi-1*

The high-throughput cell live enzymatic assay, used to measure the hydrolases activity associated to the plasma membrane, allows determining the enzymatic activity associated with the entire cell surface, without the possibility to focus on a particular plasma membrane area.

It is known that sphingolipids within plasma membrane segregate and form specific membrane domain called lipid rafts that are involved in the activation and regulation of different intra-cellular pathways.

In order to study the involvement of this particular membrane domain, I labeled cell SLs at the steady state with [1-^{3}H]-sphingosine and then I infected both CuFi-1 and NuLi-1 cell lines with PAO-1 for 4 hours. Finally, I isolated the lipid rafts from infected and not infected cells, as detergent resistant membrane (DRM) following the procedure described in details in “material and method”.

In order to isolate the DRM fraction, I loaded on a discontinuous sucrose gradient the same amount in term of volume and protein of cells, lysed with 1% Triton X-100. After ultra-centrifugation, I collected eleven fraction and I measured the radioactivity associated to each of them.

As expected, I found an enrichment in the radioactivity in low-density fraction 4 and 5 suggesting a sphingolipid enrichment. The remaining radioactivity was associated with the high-density (HD) fraction. The HD fraction represents all the cell membrane part, solubilized through the action of the detergent Triton X-100.

Interestingly in both CuFi-1 and NuLi-1 cells, PAO-1 infection causes a 20 % increase of the radioactivity associated with the DRM (figure 16).

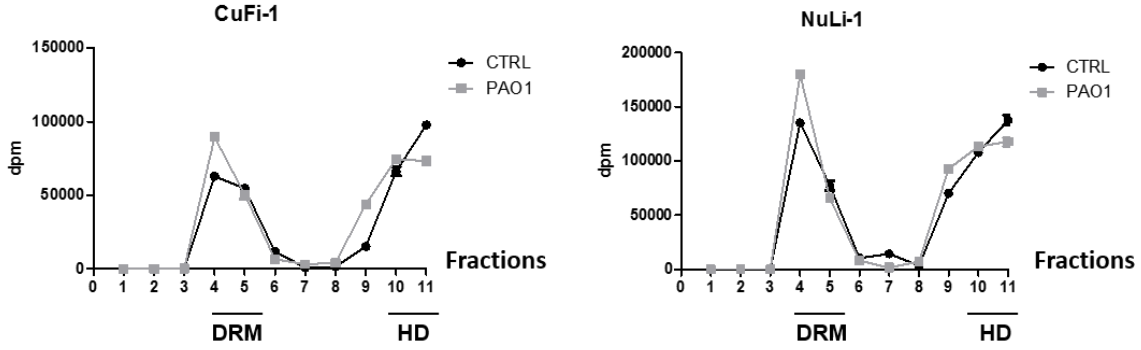

Figure 16 Radioactive sphingolipids distribution
Radioactive sphingolipid distribution among gradient fractions obtained from CuFi-1 and NuLi-1 cells infected or not with Pseudomonas aeruginosa (PAO-1).
DRM: detergent resistant membrane fractions HD: high-density fractions CTRL: not infected cells.

Furthermore, I analyzed the sphingolipid composition of DRM and HD of CuFi-1 and NuLi-1 cells, infected or not with PAO-1. Total lipid extract obtained from DRM and HD fraction were subjected to a two phase partitioning obtaining an organic and aqueous phase.

Subsequently I analyzed the sphingolipid pattern associated to both organic and aqueous phase. Interestingly, I found an intriguing difference in the composition of DRM-associate ganglioside between CuFi-1 and NuLi-1 cell line. In particular, the main ganglioside of CuFi-1 cells is GM3, whereas in NuLi-1 cells is GM1.

In the DRM fraction of CuFi-1 cells infected with PAO, I found an increase of ceramide, SM and GM1 content. Whereas, HD fractions of CuFi-1 infected cells are characterized by a reduced content of SM and GM3 and by an increase in ceramide level again (figure 17).

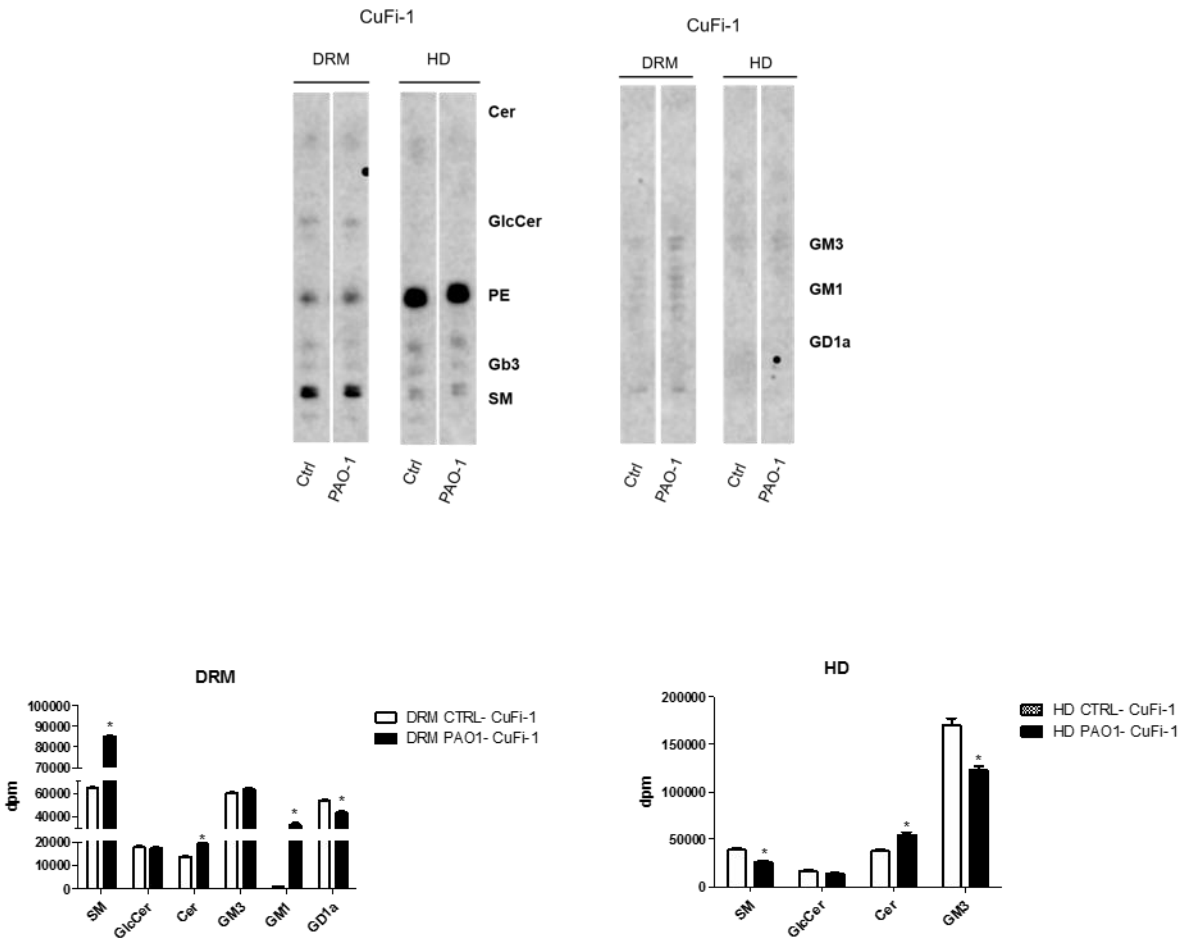

Figure 17 Sphingolipids pattern of DRM and HD fractions obtained from CuFi-1 cells, treated or not with Pseudomonas aeruginosa
Up: Autoradiography of HTLC of radioactive lipids contained in the organic phase (left) and aqueous phase (right) obtained from detergent resistance membrane (DRM) and high-density (HD) fractions of CuFi-1 cells, infected or not with PAO-1.
Each sample was loaded at parity of radioactivity.
Down: Semi quantitative graph of sphingolipids species. The sphingolipids are represented as dpm associate with the DRM or HD fraction.
Cer: ceramide; GlcCer: glucosylceramide; PE: phosphatidylethanolamine; SM: sphingomyelin. GM3, GM1, GD1a: ganglioside
PAO-1: Pseudomonas aeruginosa; Ctrl: not infected cells
**p<0.05 vs DRM/HD ctrl*

On the other hand, the DRM of NuLi-1 cells infected with PAO-1 show a reduction of ganglioside GD1a, followed by an increase in SM, GM3 and GM1 content, compared to control cells. I did not observe a significant increase of ceramide in DRM of infected NuLi-1 cells compared to control. In HD fraction, I did not found any significant differences in the sphingolipid pattern between control and infected cells, except for a slight increase in GM3 content (figure 18).

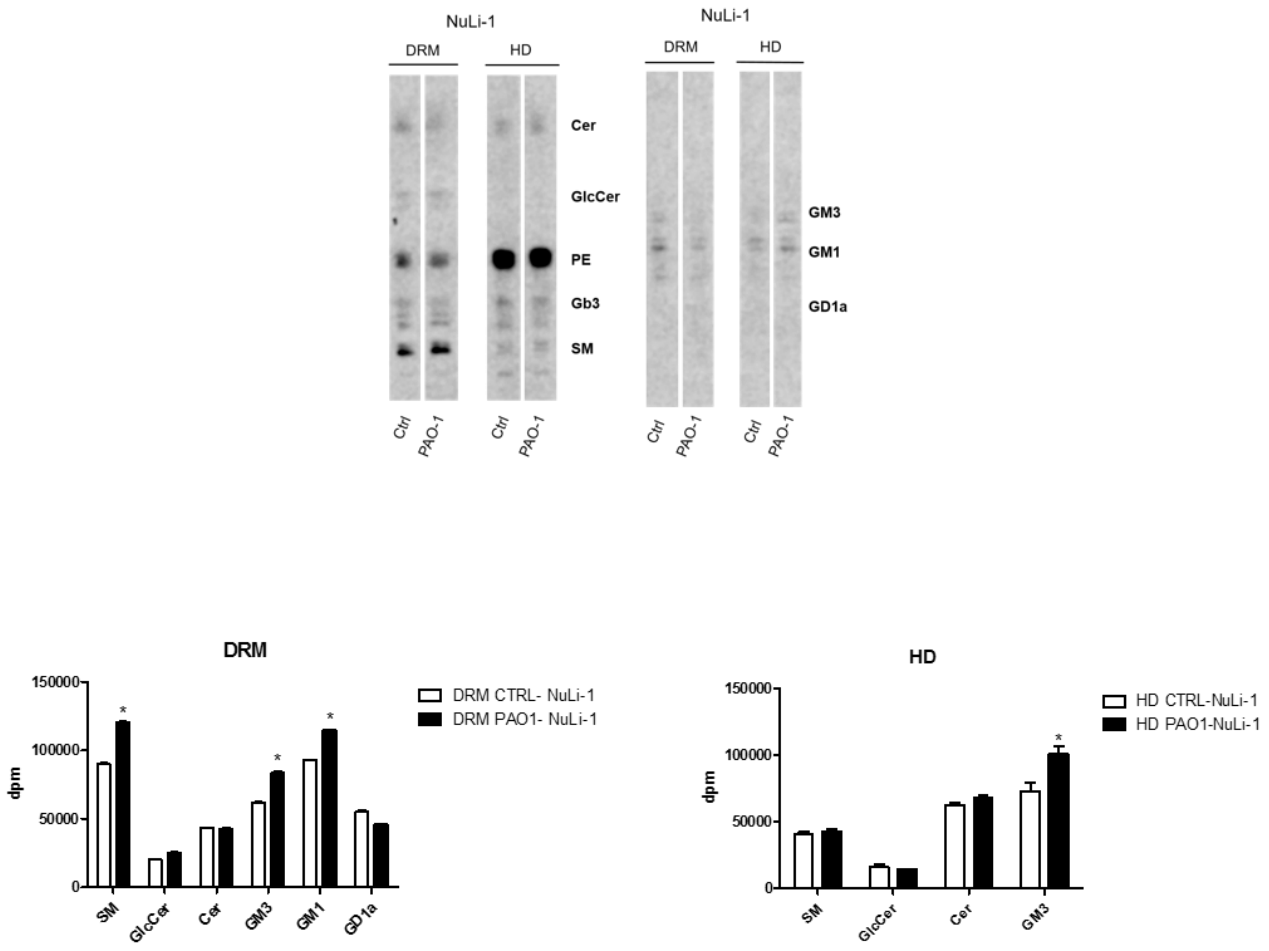

Figure 18 Sphingolipids pattern of DRM and HD fractions obtained from NuLi-1 cells, treated or not with Pseudomonas aeruginosa
Up: Autoradiography of HTLC of radioactive lipids contained in the organic phase (left) and aqueous phase (right) obtained from detergent resistance membrane (DRM) and high-density (HD) fractions of NuLi-1 cells, infected or not with PAO-1.
Each sample was loaded at parity of radioactivity.
Down: Semi quantitative graph of sphingolipids species. The sphingolipids are represented as dpm associate with the DRM or HD fraction.
Cer: ceramide; GlcCer: glucosylceramide; PE: phosphatidylethanolamine; SM: sphingomyelin; GM3, GM1, GD1a: ganglioside
PAO-1: Pseudomonas aeruginosa Ctrl: not infected cells
**p<0.05 vs DRM/HD ctrl*

In addition, I found that in CuFi-1 cells, the modification of sphingolipid DRM composition is also associated with changes in the protein composition of DRM present at cell surface level (figure 19). In fact, the protein pattern obtained by immunoprecipitation of the biotinylated proteins associated with the cell surface is different between infected and not infected cells.

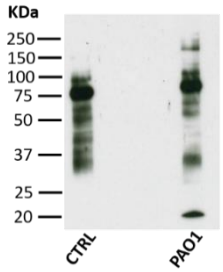

Figure 19 Effect of Pseudomonas aeruginosa infection on protein composition of the external leaflet of DRM of CuFi-1 cells
Immunoblotting images of protein pattern obtained by immunoprecipitation of the biotinylated proteins associate with the cells surface of CuFi-1 cells infected or not with PAO-1.
PAO-1: Pseudomonas aeruginosa; Ctrl: not infected cells

These data suggest that PAO1 infection causes a reorganization of the lipids rafts both in term of protein and lipid composition.

Furthermore, I investigated the effect of PAO-1 infection on the hydrolases associated with the DRM fraction obtained from CuFi-1 and NuLi-1 cells.

In CuFi-1 cells, I was able to measure the activity of GBA1, β-Gal, β-Hex and SMase. Unfortunately, I could not measure the activity of GBA2 that is inhibited by the presence of the Triton X-100.

The obtained results show that I found a significant increase in all the DRM associated activities upon infection with PAO-1 (figure 20). In particular, the data I obtained demonstrate that GBA1 and SMase activities have doubled, and β-Gal and β-Hex increased more than three fold.

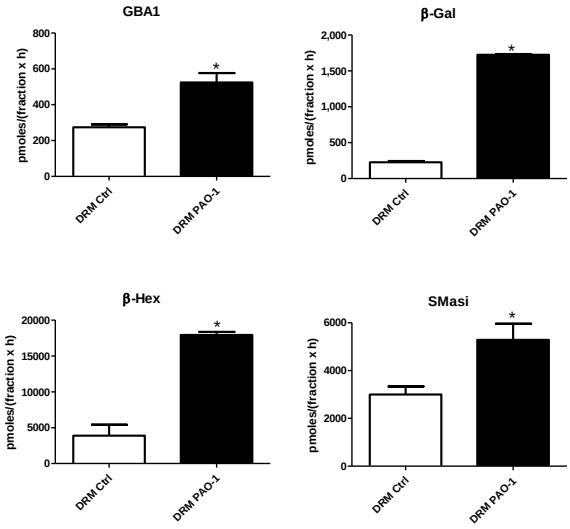

Figure 20 Hydrolases activity associate with DRM fractions from CuFi-1 cells, infected or not with PAO-1.
The measurement of the hydrolases activity was conducted on DRM fraction, using an in vitro assay based on artificial fluorigenic substrates. The enzymatic activity was evaluated on the same volume of DRM fraction.
The enzymatic activity is expressed as pmoles of products, on total volume of fraction, per hour.
GBA1: β-Glucosidase 1; β-Gal: β-Galactosidase; β-Hex: β-Hexosaminidase; SMase: Sphingomyelinase
DRM: detergent resistance membrane fraction; PAO-1: Pseudomonas aeruginosa; Ctrl: not infected cells
**p<0.05 vs DRM Ctrl*

I measured the same hydrolases activity in HD fraction, but as shows by the graphs in figure 21, I did not find any significant difference in term of enzymatic activity between infected and not infected cells. I performed the same analyses on DRM and HD fractions of NuLi-1 cells.

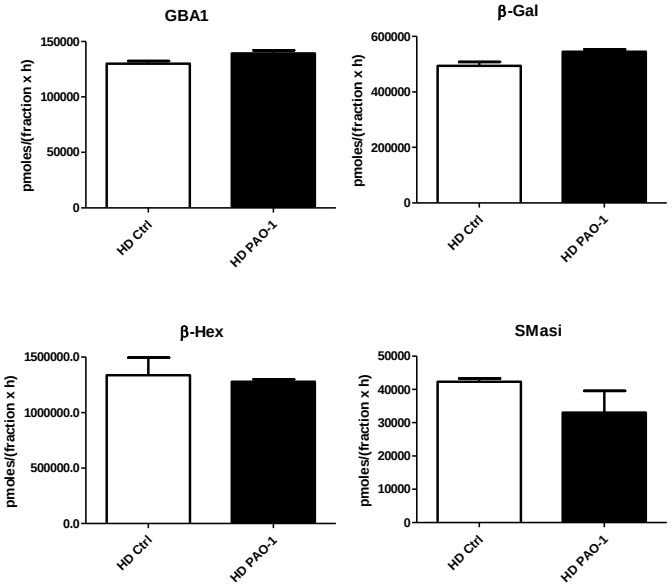

Figure 21 Hydrolases activity associate with HD fractions from CuFi-1 cells infected or not with PAO-1.
The measurement of the hydrolases activity was conducted on HD fraction, using an in vitro assay based on artificial fluorigenic substrates. The enzymatic activity was evaluated on the same volume of HD fraction
The enzymatic activity is expressed as pmoles of products on volume of fraction per hour.
GBA1: β-Glucosidase1 β-Gal: β-Galactosidase β-Hex: β-Hexosaminidase SMase: Sphingomyelinase
HD: high density fraction PAO-1: Pseudomonas aeruginosa Ctrl: not infected cells
**p<0.05 vs DRM Ctrl*

Interestingly, the data I obtained demonstrate a decrease of all DRM associated activities in DRM derived from cells subjected to PAO-1 infection (figure 22), an opposite effect in respect to CuFi-1 cells.

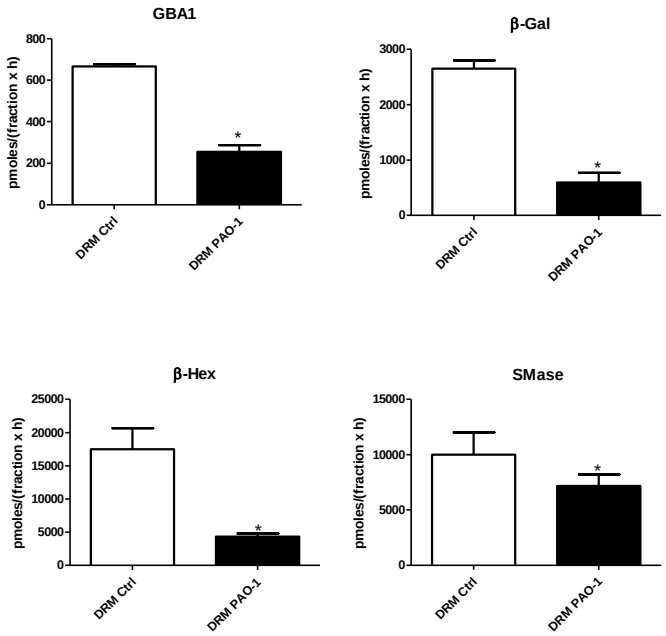

Figure 22 Hydrolases activity associate with DRM fraction from NuLI-1 cells, infected or not with PAO-1.
The measurement of the hydrolases activity was conducted on DRM fraction, using an in vitro assay based on artificial fluorigenic substrates. The enzymatic activity was evaluated on the same volume of DRM fraction.
The enzymatic activity is expressed as pmoles of products on volume of fraction per hour.
GBA1: β-Glucosidase 1; β-Gal: β-Galactosidase; β-Hex: β-Hexosaminidase; SMase: Sphingomyelinase
DRM: detergent resistant membrane fraction; PAO-1: Pseudomonas aeruginosa; Ctrl: Control
**p<0.05 vs DRM Ctrl*

As CuFi-1 cells, even in this case, I did not find any significant differences in the hydrolases activity associated with HD fraction, between infected and not infected cells (figure 23).

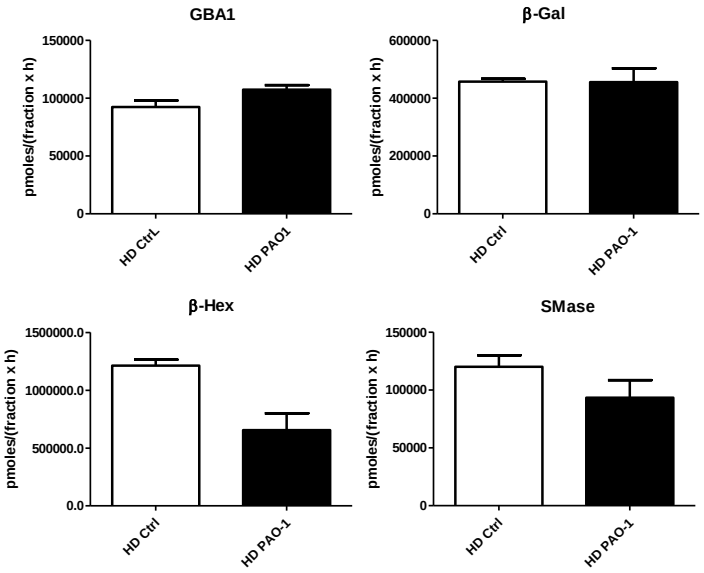

Figure 23 Hydrolases activity associate with HD fraction from NuLi-1 cells, infected or not with PAO-1.
The measurement of the hydrolases activity was conducted on HD fraction, using an in vitro assay based on artificial fluorigenic substrates. The enzymatic activity was evaluated on the same volume of HD fraction.
The enzymatic activity is expressed as pmoles of products on volume of fraction per hour.
GBA1: β-Glucosidase 1; β-Gal: β-Galactosidase; β-Hex: β-Hexosaminidase; SMase: Sphingomyelinase
HD: high-density fraction; PAO-1: Pseudomonas aeruginosa; CTRL: not infected cells

These data clearly show that PAO-1 infection causes important changes in the DRM structure.

The information obtained from CuFi-1 cells suggest that PAO-1 infection leads to the activation of SL catabolic pathway, which culminates in the production of ceramide, followed by changes also in the protein composition.

Concerning NuLi-1 cells, the behavior of the hydrolases observed after PAO-1 infection is quiet difficult to understand. For sure, the glycohydrolases involved in glycosphingolipids catabolism have a role in the creation of a good arrangement of cell surface, suitable to manage the bacterial infection. However, we are not able to explain in detail, the meaning of this molecular mechanism.

PAO1 infection alter the signaling pathway mediated by CD95

To figure out the possible molecular mechanism linking the cell surface modification after bacterial infection, with the activation of inflammatory response, and in particular, the release of IL-8, I investigated the possible activation of CD95 pathway, including the regulatory protein phospho-FADD, RIP, NF-kB and Caspase 8.

Clustering of activated receptors in ceramide-enriched membrane domains was demonstrated in literature for several receptors including CD95, DR5, or CD40 [Schutze, Tchiko, et al 2008].

To investigate this pathway, I infected the CuFi-1 cells with PAO-1 for 4 h, and then I conducted a western blot analysis on the obtained lysates.

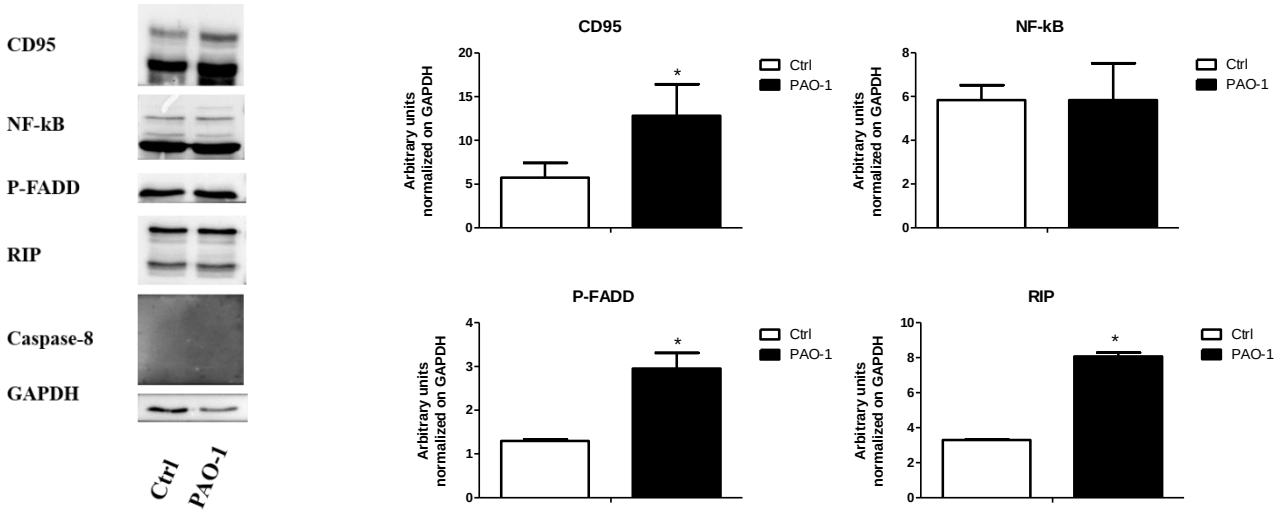

Figure 24 Effect of Pseudomonas aeruginosa (PAO-1) infection on the activation of CD95 pathway in CuFi-1 cells
Left: Immunoblotting analyses, obtained from CuFi-1 cells infected or not with PAO-1.
Right: quantitative analyses of protein, expressed in arbitrary units compared to GAPDH.
PAO-1: Pseudomonas aeruginosa; CTRL: not infected cells
**p<0.05 vs CTRL*

The obtained data suggest the probable involvement of this pathway as possible link between the modification occurring at the cell surface after PAO-1 infection and the release of IL-8. In fact, as reported in figure 24, I found that all the principal regulatory protein of the pro-inflammatory pathway are activated, including the mediator phospo-FADD. In addition, the presence of RIP suggests that the extrinsic apoptotic pathway is not activated, further confirmed by the absence of Caspase-8.

CF and non-CF epithelial bronchial cells stable-overexpressing GBA2

Characterization of CuFi-1 and NuLi-1 cell overexpressing GBA2

Evidence in literature [Loberto, Tebon, et al. 2014] on the correlation between GBA2 silencing and the reduction of the IL-8 mRNA expression in CuFi-1 cells, both infected or not with *P.aeruginosa*, suggests that GBA2 could have an important role in the activation of the inflammatory response in CF. However, the details of molecular mechanism involving GBA2 are still unknown.

Some technical limits make difficult to study GBA2. In fact, as reported above, the use of detergent Triton X-100 for the DRM isolation inhibits the GBA2 activity. In addition, an efficient antibody against GBA2 is not commercially available.

In order to overtake these limits, I decided to stably-overexpress GBA2 linked with GFP in both NuLi-1 and CuFi-1 cells.

As control cells, I generated a Mock cells line by the overexpression of the only GFP. After three weeks, several clones were selected and I morphologically analyzed it by confocal microscopy, to detect the GFP-tagged GBA2 (figure 25).

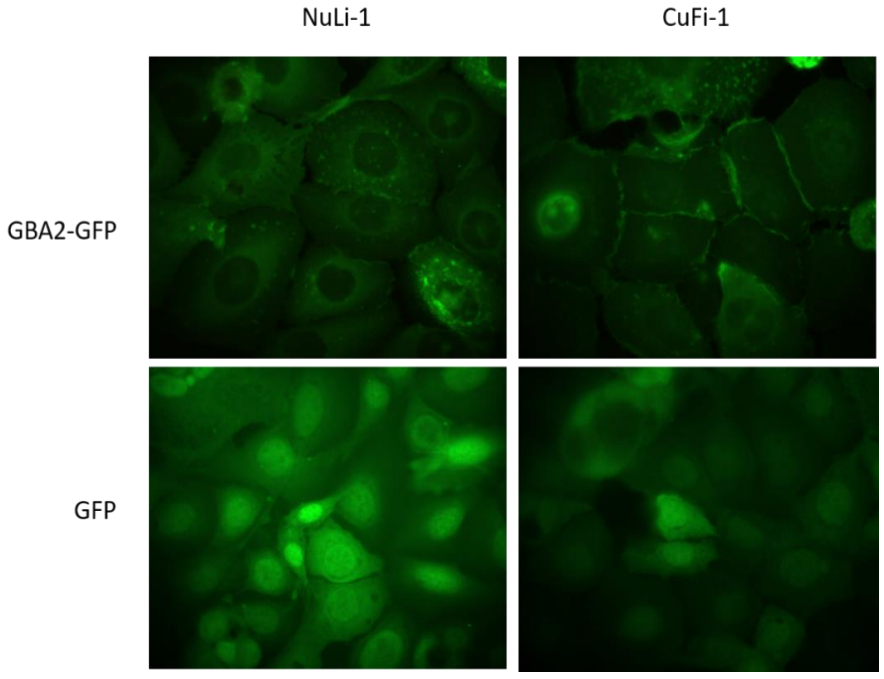

Figure 25 Confocal images of CuFi-1 and NuLi-1 overexpressing GFP (Mock), CuFi-1 and NuLi-1 overexpressing GBA2-tagged GFP (GBA2-GFP)

As shown in figure 25 I was able to obtain clones stably overexpressing GBA2 at the PM level for both cell lines.

I started to measure the activity of GBA2 in CuFi-1 mock (GFP) and in GBA2 overexpressing cells (GBA2-GFP) either intracellularly or directly at the cell plasma membrane.

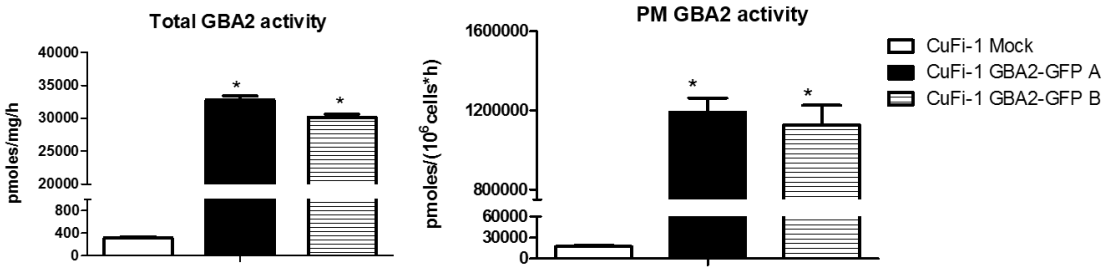

Figure 26 Total and plasma membrane enzymatic activity of GBA2 measured in CuFi-1 overexpressing GFP and in CuFi-1 overexpressing GBA2 tagged-GFP.
The measurement of the total GBA2 enzymatic activity was conducted on cell lysate using an in vitro assay based on artificial fluorigenic substrates.
The enzymatic activity is expressed as pmoles of products on mg of proteins per hour.
The measurement of the plasma membrane enzymatic activity of GBA2 was conducted on living cells, using artificial fluorigenic substrates. The enzymatic activity is expressed as pmoles of products on 10^6 cells per hour.
GBA2: β-Glucosidase 2;
CuFi-1 Mock: CuFi-1 overexpressing GFP; CuFi-1 GBA2-GFP A/ B: CuFi-1 overexpressing GBA2 tagged with GFP
**p<0.05 vs Mock*

As shown in figure 26 CuFi-1 GBA2-GFP cells are characterized by 80-fold increase in the total GBA2 activity and by an increase of 40 fold increase at the cell surface.

Several evidences in literature reports that the cells react to the alteration of the activity of one of the enzymes involved in the SL metabolism by modifications in the activity of other enzymes involved in the same catabolic pathway [Aureli, Bassi, et al. 2012]**.** For this reason I measured in mock and CuFi-1 GBA2-GFP the activity of the main cell hydrolases.

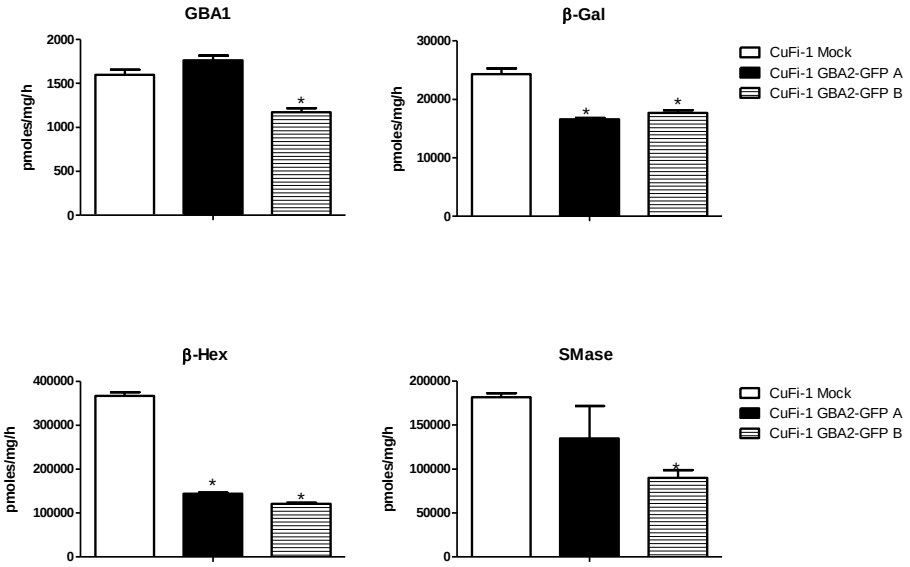

Figure 27 Total cell associated hydrolases activity of CuFi-1 overexpressing GFP and overexpressing GBA2-tagged GFP.
The measurement of the hydrolases activity was conducted on cell lysate using an in vitro assay based on artificial fluorigenic substrates. The enzymatic activity is expressed as pmoles of products, on mg of proteins, per hour.
GBA1: β-Glucosidase1; β-Gal: β-Galactosidase; β-Hex: β-Hexosaminidase; SMase: Sphingomyelinase GBA2:
CuFi-1 Mock: CuFi-1 overexpressing GFP; CuFi-1 GBA2-GFP A/ B: CuFi-1 overexpressing GBA2 tagged with GFP
**p<0.05 vs Mock*

The results obtained show that the overexpression of GBA2 in CuFi-1 cells causes a reduction of β-Hex of more than double and a reduction of SMase activity from ~180000 pmoles/mg/h to less than 100000 pmole/mg/h in the total cell lysate (figure 27). Furthermore, I evaluated in both mock and GBA2 overexpressing CuFi-1 cells the activity of the β-glucocerebrosidase GBA1, β-galactosidase and β-hexosaminidase directly at the plasma membrane of living cells. As shown in figure 28 I found an important increase of β-gal compared to mock cells.

In addition, GBA1 is more than doubled, especially in the second clone (CuFi-1 GBA2-GFP B), whereas β-Hex remains constant.

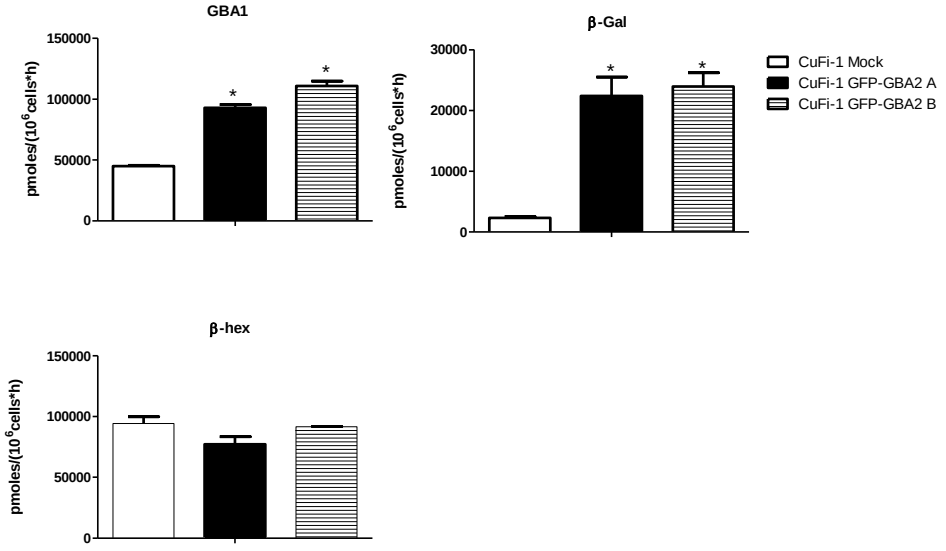

Figure 28 Plasma membrane hydrolases activity in CuFi-1 overexpressing GFP and CuFi-1 overexpressing GBA2-tagged GFP.
The measurement of the plasma membrane hydrolases activity was conducted on living cells, using artificial fluorigenic substrates. The enzymatic activity is expressed as pmoles of products, on 10^6 cells, per hour.
.GBA1: β-Glucosidase; β-Gal: β-Galactosidase; β-Hex: β-Hexosaminidase
CuFi-1 Mock: CuFi-1 overexpressing GFP; CuFi-1 GBA2-GFP A/ B: CuFi-1 overexpressing GBA2 tagged with GFP
**p<0.05 vs Mock*

I characterized also the NuLi-1 cells overexpressing GBA2-GFP. As show in figure 29 overexpressing cells show 100-fold increase in GBA2 activity in total cell lysate in comparison to Mock cells. Whereas, at the cell surface the overexpression causes an increase of GBA2 activity of about 30-fold.

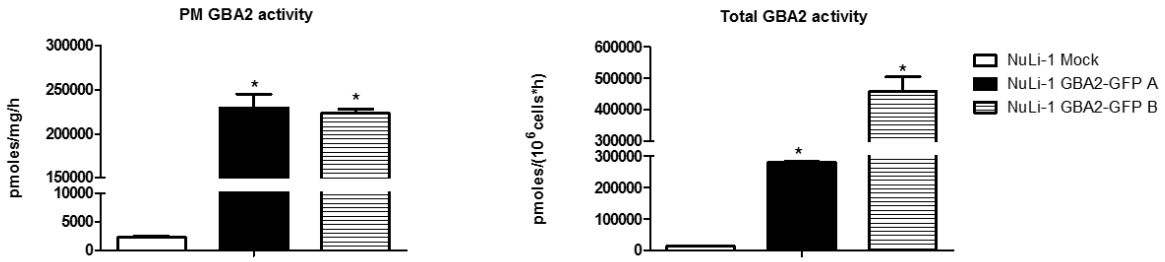

Figure 29 Total and plasma membrane enzymatic activity of GBA2 measured in NuLi-1 overexpressing GFP and in NuLi-1 overexpressing GBA2-tagged GFP.
The measurement of the total GBA2 enzymatic activity was conducted on cell lysate using an in vitro assay and artificial fluorigenic substrates. The enzymatic activity is expressed as pmoles of products on mg of proteins per hour.
The measurement of the plasma membrane enzymatic activity of GBA2 was conducted on living cells, using artificial fluorigenic substrates. The enzymatic activity is expressed as pmoles of products on 10^6 cells per hour.
GBA2: β-Glucosidase 2; NuLi-1 Mock: NuLi-1 overexpressing GFP; NuLi-1 GBA2-GFP A/ B: NuLi-1 overexpressing GBA2 tagged with GFP
**p<0.05 vs Mock*

Even in this case I measured the activity of the GBA2- correlated hydrolases both intracellularly and at the plasma membrane. As shown in figure 30 I found no changes in the intracellular activity of β-glucocerebrosidase GBA1, β-galactosidase and β-hexosaminidase between mock and overexpressing GBA2 NuLi-1 cells for the exception of slight decrease of GBA1 and SMase activity in one of the generated monoclonal cell line.

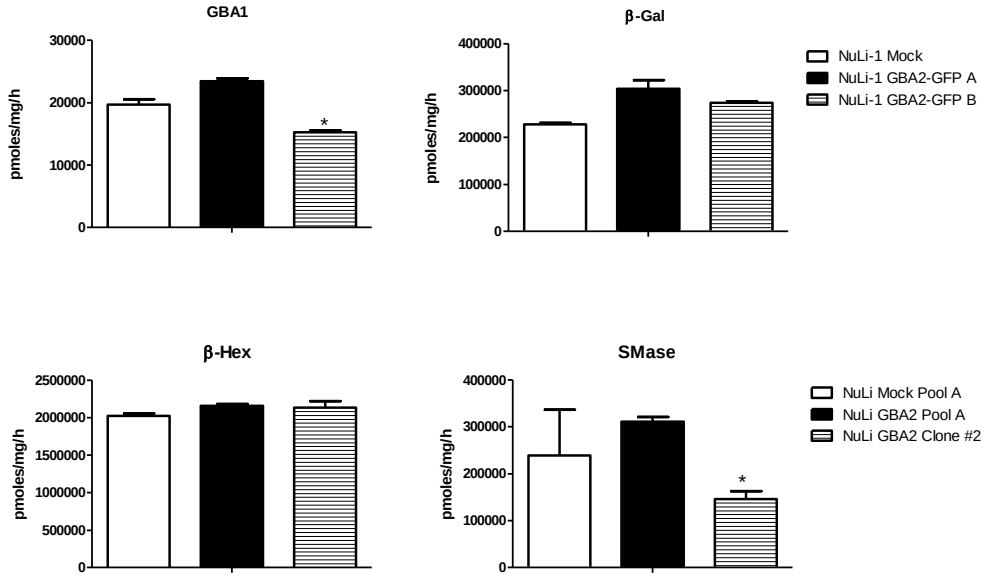

Figure 30 Total cell associated hydrolases activity in NuLi-1 overexpressing GFP (Mock) and NuLi-1 overexpressing GBA2-tagged GFP.
The measurement of the hydrolases activity was conducted on cell lysate using an in vitro assay based on artificial fluorigenic substrates. The enzymatic activity is expressed as pmoles of products, on mg of proteins, per hour.
GBA1: β-Glucosidase1; β-Gal: β-Galactosidase; β-Hex: β-Hexosaminidase; SMase: Sphingomyelinase
NuLi-1 Mock: NuLi-1 overexpressing GFP; NuLi-1 GBA2-GFP A/ B: NuLi-1 overexpressing GBA2 tagged with GFP
**p<0.05 vs Mock*

Concerning the activities associated with plasma membrane, I found a slight increase in β-glucocerebrosidase and β-galactosidase whereas β- hexosaminidase activity is reduced (figure 31).
I analyzed the effect of GBA2 overexpression on the SLs pattern of both CuFi-1 and NuLi-1 cells overexpressing GBA2 by a metabolic labeling at the steady state using the radioactive precursor [1-^{3}H]-sphingosine.
As expected, I found that both CuFi-1 and NuLi-1 cells overexpressing GBA2, are characterized by a decrease of GlcCer, associated to an increase of Cer and SM (figure 32).

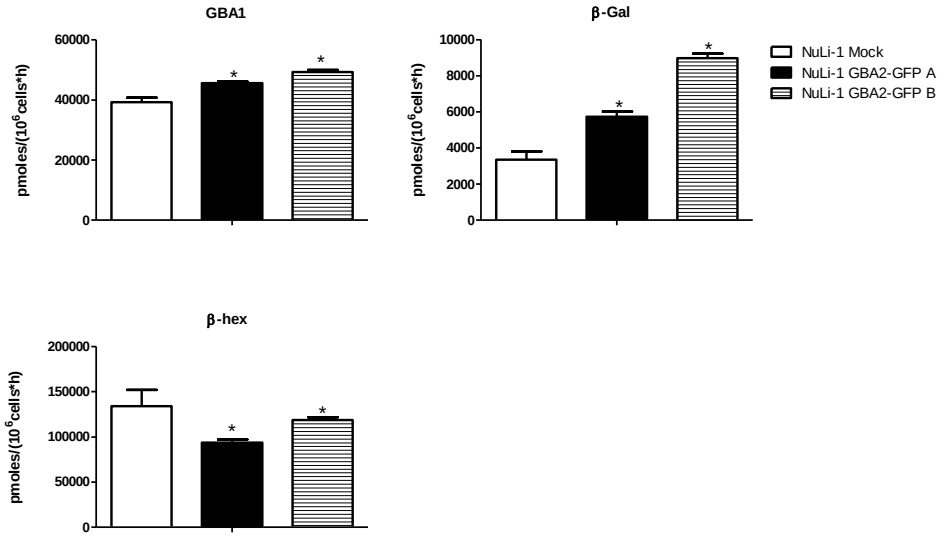

Figure 31 Plasma membrane hydrolases activity in NuLi-1 overexpressing GFP and CuFi-1 overexpressing GBA2-tagged GFP.
The measurement of the plasma membrane hydrolases activity was conducted on living cells, using artificial fluorigenic substrates. The enzymatic activity is expressed as pmoles of products on 10^6 cells per hour. NuLi-1 GBA2 GFP: NuLi-1 cell overexpressing GBA2 tagged with GFP.
GBA1: β-Glucosidase; β-Gal: β-Galactosidase; β-Hex: β-Hexosaminidase
NuLi-1 Mock: NuLi-1 overexpressing GFP; NuLi-1 GBA2-GFP A/ B: NuLi-1 overexpressing GBA2 tagged with GFP
**p<0.05 vs Mock*

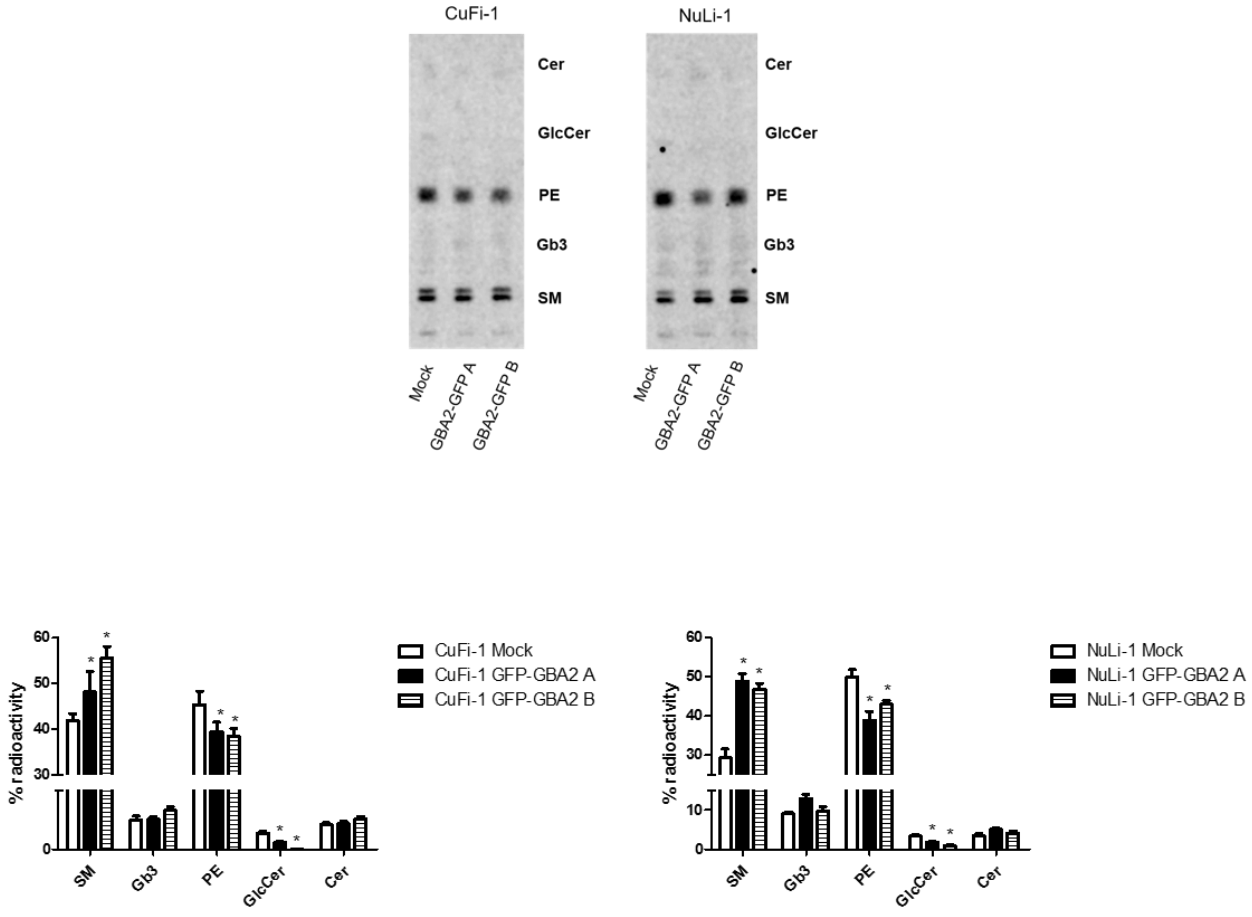

Figure 32 Radioactive sphingolipids composition of CuFi-1 and NuLi-1 cell line overexpressing GBA2 compared to mock cells
Up: Autoradiography of HTLC of radioactive lipids contained in the organic phase obtained from CuFi-1 (left) and NuLi-1 (right) overexpressing GBA2 or overexpressing GFP. Each sample was loaded at parity of radioactivity.
Down: Semi quantitative graph of sphingolipids species. The sphingolipids are represented as percentage of radioactivity.
Cer: ceramide; GlcCer: glucosylceramide; PE: phosphatidylethanolamine; SM: sphingomyelin
Mock: overexpressing GFP; GBA2-GFP A/ B: overexpressing GBA2
**p<0.05 vs CuFi-1/NuLi-1 Mock cells*

Interestingly, these data suggest that part of the ceramide produced by action of GBA2, is probably converted to SM as suggested by Sorli and colleagues [Sorli S.C et al. 2013]. This process could explain the high level of SM observed in the overexpressing cells.

Pro-inflammatory state of CuFi-1 cells overexpressing GBA2

Since it has been demonstrated that the silencing of GBA2 cause a strong reduction of IL-8 in the pro-inflammatory state of CF, I wondered which effect could have the overexpression of GBA2 on the basal inflammatory state compared to CuFi-1 cells.

To address this issue, I measured the IL-8 mRNA expression in GBA2 overexpressing CuFi-1 cells and I compared the obtained result to CuFi-1 cells.

As shown in figure 33, GBA2 overexpressing cells are characterized by a significant increase of IL-8 mRNA, and this data further support the role of GBA2 in the pro-inflammatory state of CF lung disease

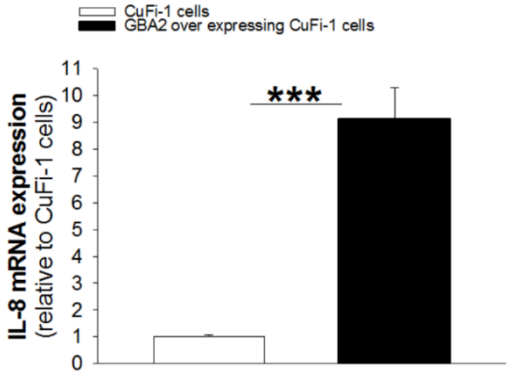

Figure 33 Pro-inflammatory state of CuFi-1 cells overexpressing GBA2 compared with CuFi-1 cells
*mRNA expression of IL-8 of CuFi-1 cells compared with CuFi-1 cells *p<0.05 vs CuFi-1 cells*

Since I did not observe any significant differences between NuLi-1 cells and NuLi-1 overexpressing GBA2, in the basal IL-8 mRNA expression, I focused my attention manly on CuFi-1 cells.

Behavior of lipid raft in CuFi-1 cell overexpressing GBA2

GBA2 overexpression in CuFi-1 cells is responsible for changes in the plasma membrane composition of both sphingolipids and enzymes involved in their catabolism, which correlates with an increased basal production of pro-inflammatory IL-8.

I decided to investigate if the potential perturbation of plasma membrane caused by the overexpression of GBA2 was able to lead to a different behavior of lipid rafts in these cells.

Interestingly, figure 34 show that GBA2 overexpressing cells are characterized by an increased radioactivity associated to the DRM, compared to CuFi-1 cells.

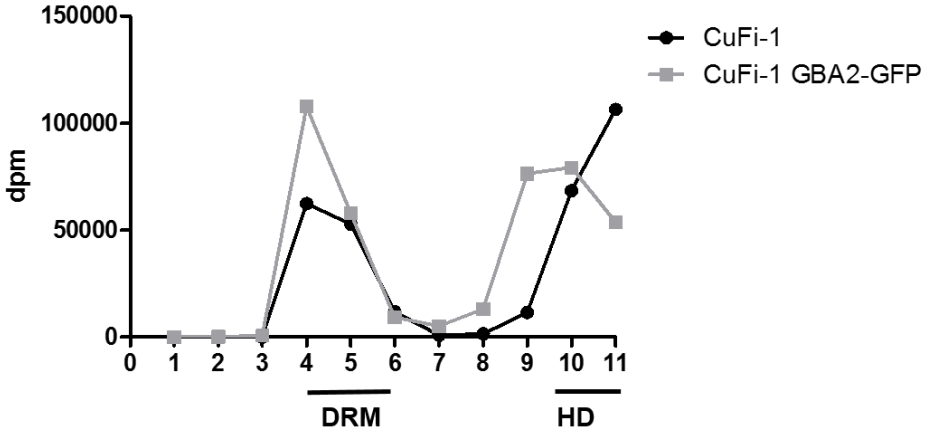

Figure 34 Radioactive sphingolipid distribution.
Radioactive sphingolipid distribution among gradient fractions obtained from CuFi-1 overexpressing GBA2 compared with radioactive sphingolipid distribution among gradient fractions obtained from CuFi-1 cells.
DRM: detergent resistant membrane fractions; HD: high-density fractions; CuFi-1 GBA2- GFP: CuFi-1 overexpressing GBA2 tagged with GFP

Subsequently I compared the sphingolipid composition of DRM of CuFi-1 to DRM of CuFi-1 GBA2 overexpressing cells.

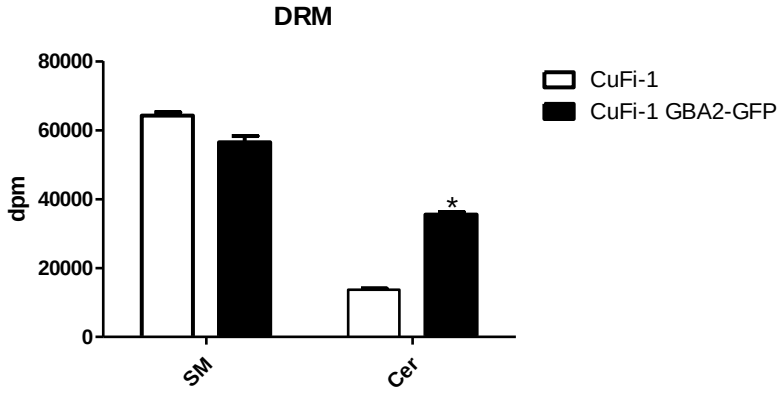

Figure 35 Comparison between lipids obtained from detergent resistance membrane of CuFi-1 and CuFi-1 cells overexpressing GBA2.
Semi quantitative graph of sphingolipids species. The sphingolipids are represented as dpm associate with the DRM fraction.
Cer: ceramide; SM: sphingomyelin.
CuFi-1 GBA2-GFP: CuFi-1 overexpressing GBA2 tagged with GFP; DRM: detergent resistant membrane
**p<0.05 vs CuFi-1*

As shown in figure 35, I found that GBA2 overexpression causes a strong increase of Cer content in the DRM without affecting the SM level.

Subsequently, I measured the enzymatic activity of GBA1, β-galactosidase and β-hexosaminidase, associated with the DRM of CuFi-1 cells overexpressing GBA2 and I compared it with the hydrolases of DRM of CuFi-1 cells.

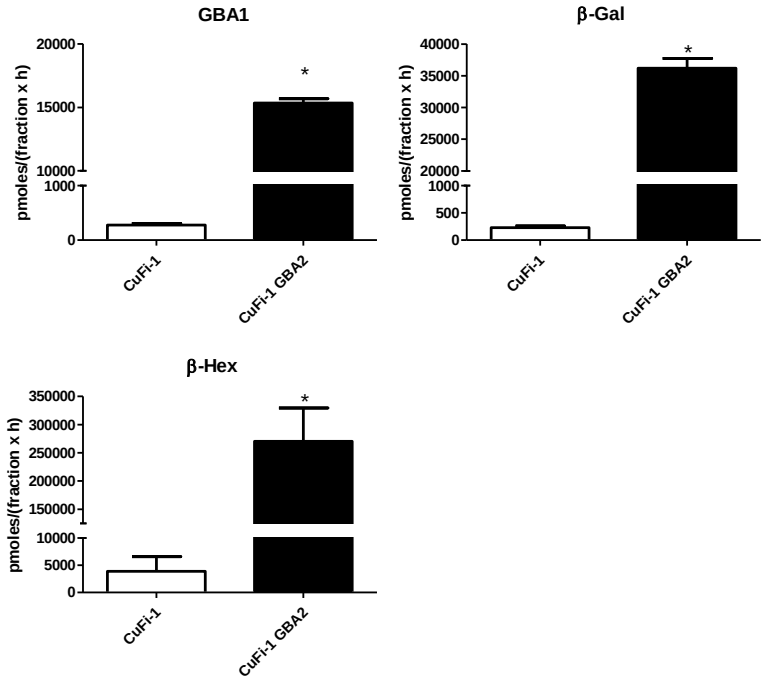

Figure 36 Hydrolases activity associate with DRM fraction from CuFi-1 cells overexpressing GBA2 compared with CuFi-1 cells
The measurement of the hydrolases activity was conducted on DRM fraction, using an in vitro assay based onartificial fluorigenic substrates. The enzymatic activity was evaluated on the same volume of DRM fraction
The enzymatic activity is expressed as pmoles of products, on volume of fraction, per hour.
GBA1: β-Glucosidase 1; β-Gal: β-Galactosidase; β-Hex: β-Hexosaminidase
DRM: detergent resistance membrane fraction; CuFi-1 GBA2: Cufi-1 overexpressing GBA2
**p<0.05 vs CuFi-1*

Interestingly, the graphs of enzymatic activities show that GBA2 overexpression leads to a strong increase of activity of the all hydrolases, at the level of DRM fraction (figure 36).

These data further support the role of GBA2 in the regulation of the pro-inflammatory state of CuFi-1 cells.

Behavior of lipid raft in GBA2 overexpressing CuFi-1 cells subjected to PAO-1 infection

Given that the interesting results obtained by the analyses of DRM obtained from GBA2 overexpressing Cells, I decided to investigate the effect of PAO-1 infection in this kind of cells.
I infected the cells with PAO-1 for 4 hour, as control I used the same cell not infected and then, I proceeded with the isolation of the DRM.

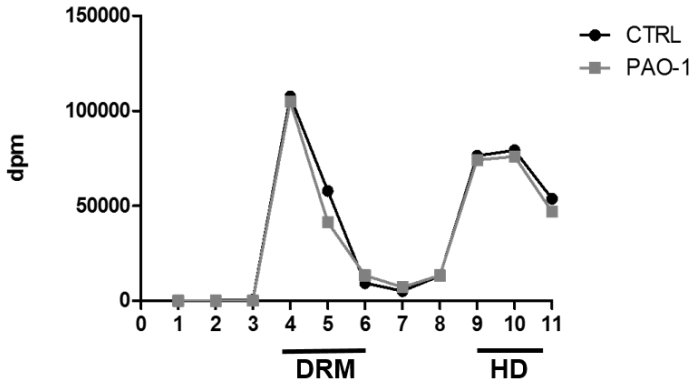

Figure 37 Radioactive sphingolipid distribution
Radioactive sphingolipid distribution among gradient fractions obtained from CuFi-1 overexpressing GBA2 infected or not with Pseudomonas aeruginosa
DRM: detergent resistant membrane fractions; HD: high-density fractions; CTRL: not infected cells PAO-1: Pseudomonas aeruginosa

As done with the DRM isolation of CuFi-1 and NuLi-1 cells, I collected eleven fractions and I measured the radioactivity associated with each of them.
As expected, I found an enrichment in the radioactivity in low-density fraction 4 and 5 that correspond to DRM fraction (figure 37). The remaining radioactivity was associated to the high-density (HD) fraction.
Interestingly in these GBA2 overexpressing cells, PAO-1 infection causes only a small increase in the radioactivity associated with the DRM (figure 37).
Subsequently I analyzed the sphingolipid composition of DRM and HD of GBA2 overexpressing CuFi-1 cells, infected or not with PAO-1 (figure 38).
Unexpectedly, I found that PAO-1 infection causes a decrease of SM and Cer in the DRM, if compared to the uninfected cells.

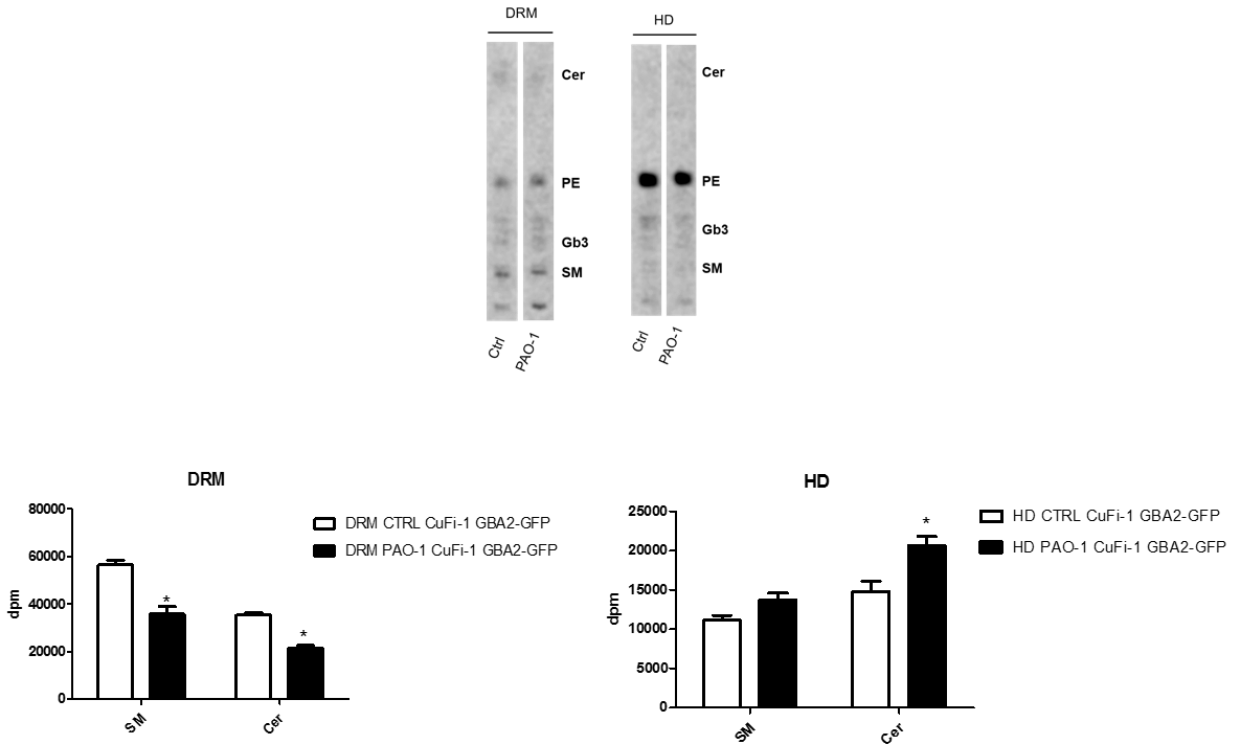

Figure 38 Lipid pattern of high-density fraction of CuFi-1 cells overexpressing GBA2, infected or not with Pseudomonas aeruginosa.
Up: Autoradiography of HTLC of radioactive lipids contained in the organic phase obtained from CuFi-1 overexpressing GBA2 treated or not with Pseudomonas aeruginosa. Each sample was loaded at parity of radioactivity.
Down: Semi quantitative graph of sphingolipids species. The sphingolipids are represented as dpm associate with the DRM (left) and HD (right) fraction.
Cer: ceramide; SM: sphingomyelin
PAO-1: Pseudomonas aeruginosa Ctrl: Not infected cells; DRM: detergent resistant membrane fraction; HD: high-density fraction CuFi-1 GBA2-GFP; CuFi-1 overexpressing GBA2
**p<0.05 vs Ctrl*

Whereas, in HD of infected cells I found a slight increase of Ceramide with respect to not infected cells, and I did not find any significant difference in the level of SM between control and infected cells. Subsequently, I measured the enzymatic activity of GBA1, β-Galactosidase and β-Hexosaminidase.

Interestingly, the graphs of enzymatic activity (figure 39) show that PAO-1 infection, in these cells, leads to a strong decrease of activity of some hydrolases such as β-Gal and β-Hex in the DRM fraction. In HD fraction, I did not find any significant difference between control and infected cells in all the enzymatic activities analyzed (figure 40).

These data suggest that probably this kind of cells does not need to response to PAO-1 infection with a recruitment of all the hydrolases at the level of DRM. In fact, they have already a great amount of GBA2 able to produce Ceramide as a response to bacterial infection.

This speculation further support the role of GBA2 in the inflammatory response to *P. aeruginosa* infection in CF epithelial bronchial cell.

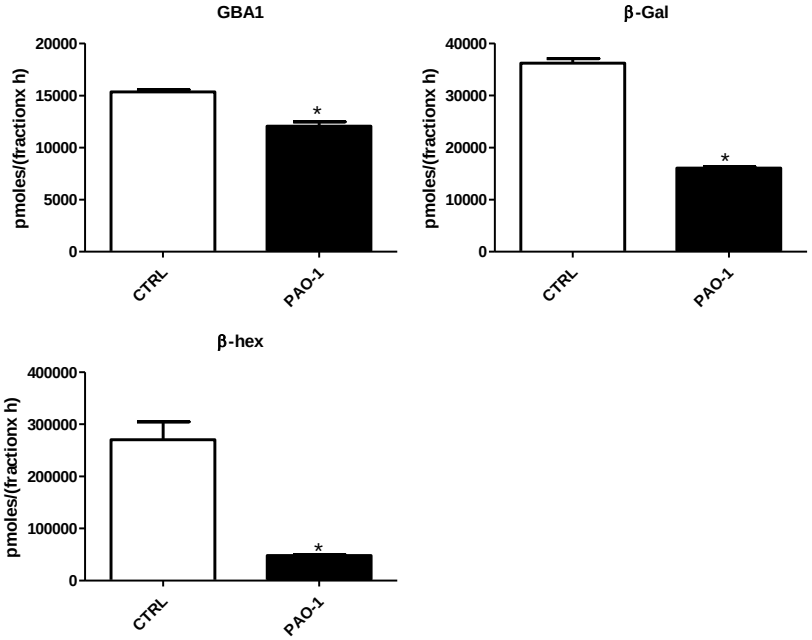

Figure 39 Hydrolases activity associate with detergent resistant membrane fraction from CuFi-1 cells overexpressing GBA2, infected or not with Pseudomonas aeruginosa.
The measurement of the hydrolases activity was conducted on DRM fraction, using an in vitro assay and artificial fluorigenic substrates, To normalize the data I did not consider the same amount of protein per sample, for each tested hydrolases, but I consider the same volume of DRM fraction. The enzymatic activity are expressed as pmoles of products on volume of fraction per hour.
B Glc Tot: Total β-Glucosidase; GBA2 β-Glucosidase 2; β-Gal: β-Galactosidase; β-Hex: β-Hexosaminidase
DRM: detergent resistance membrane fraction; PAO-1: Pseudomonas aeruginosa; CTRL: Control
**p<0.05 vs CTRL*

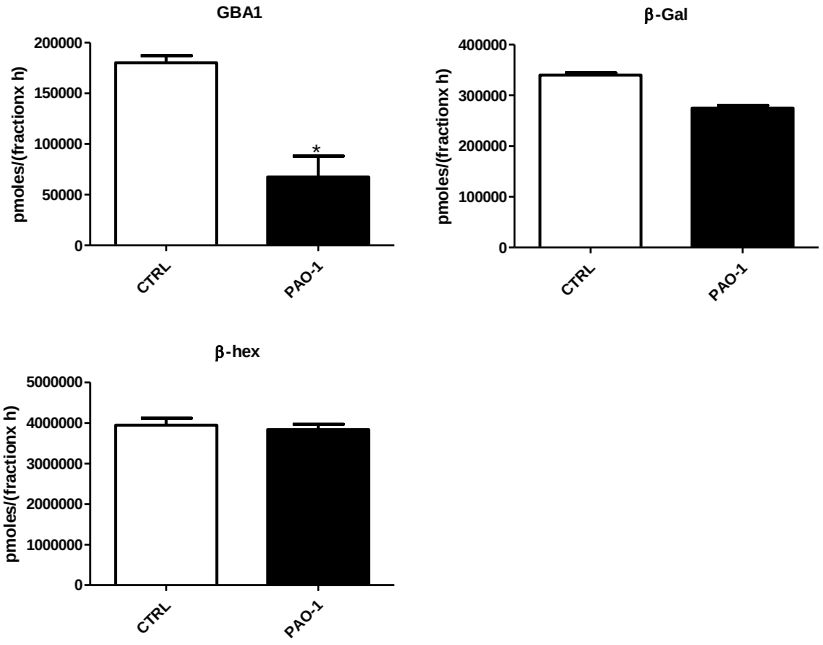

Figure 40 Hydrolases activity associate with high-density fraction from CuFi-1 cells overexpressing GBA2 infected of nor with PAO-1.
The measurement of the hydrolases activity was conducted on HD fraction, using an in vitro assay and artificial fluorigenic substrates, To normalize the data I did not consider the same amount of protein per sample, for each tested hydrolases, but I consider the same volume of HD fraction. The enzymatic activity are expressed as pmoles of products on volume of fraction per hour.
B Glc Tot: Total β-Glucosidase; GBA2 β-Glucosidase 2; β-Gal: β-Galactosidase; β-Hex: β-Hexosaminidase
HD: High-density fraction; PAO-1: Pseudomonas aeruginosa; CTRL: Control
**p<0.05 vs CTRL*

Development of a nanoparticle-based siRNA-GBA2 delivering system

Identification of the best siRNA sequences to down-regulate GBA2 and to obtain the highest anti-inflammatory effect

This PhD project is based on some preliminary results, reported by Loberto and colleagues [Loberto, Tebon, et al. 2014], demonstrating that the GBA2 silencing results in a reduction of IL-8 mRNA level in CF bronchial cells. The anti-inflammatory effect was observed not only after the infection with *P.aeruginosa* but also in absence of bacterium. This evidence suggests the possibility to use specific siRNA sequences to down-regulate GBA2, as a new therapeutic option to reduce the intrinsic pro-inflammatory state of CF tissue and the inflammatory response to *P. aeruginosa* infection.
To this aim, I tested six difference siRNA sequences, which target different part of GBA2 mRNA sequence (figure 41).

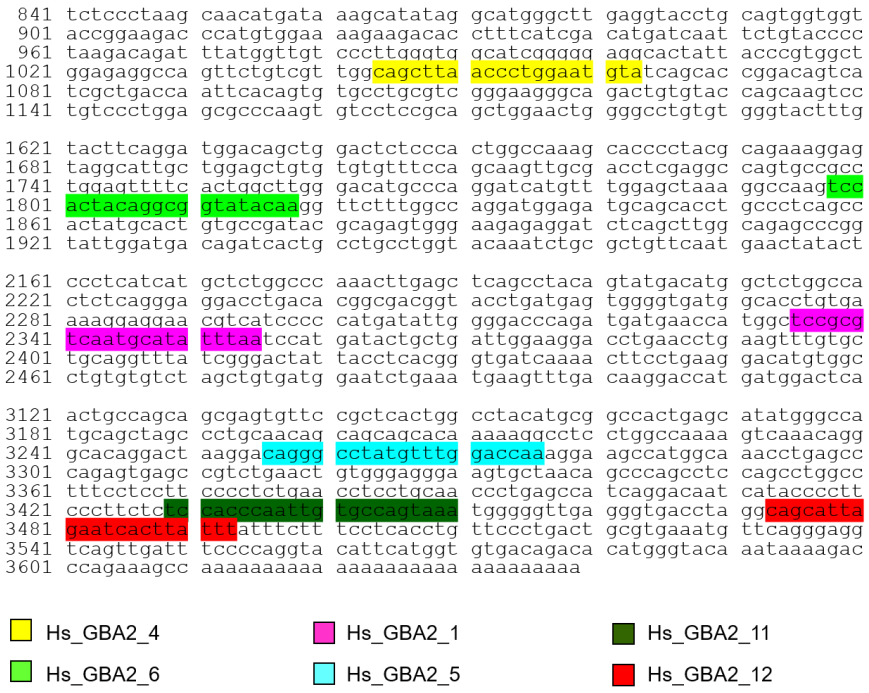

Figure 41 Six different siRNA sequences, targeting different part of human GBA2 mRNA sequence

I tested the silencing efficiency of these six different sequences in CuFi-1 cells, and then I tested the silencing efficiency of the all-possible combination of each.
As first read out system, I measured the GBA2 activity in cell transfected with single siRNA or with a combination of them using Lipofectamine 20000 as transfectant reagent.

As results, I found that the combination of the two siRNAs, targeting the catalytic site of the enzyme (Hs_GBA2_1 and Hs_GBA2_5) was the best to silence GBA2; in fact, the GBA2 activity was more than 70% decreased (figure 42).

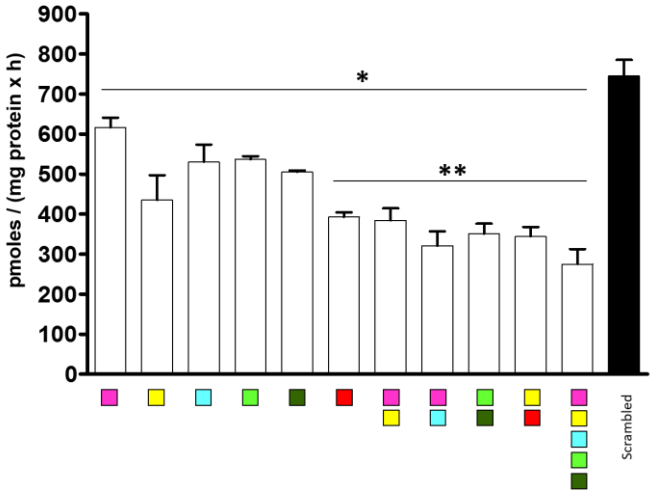

Figure 42 Effect of the GBA2-siRNA alone or in different combination, on the GBA2 activity in CuFi-1 cells.
The measurement of the total GBA2 enzymatic activity was conducted on cell lysate using an in vitro assay and artificial fluorigenic substrates. The enzymatic activity are expressed as pmoles of products on mg of proteins per hour. The colors code is referred to the legend reported in the figure 35
**p<0.003 vs scramble, ** p< 0.005 vs other group*

I confirmed the efficacy of this combination, through the measurement of the expression level of GBA2 mRNA (figure 43).

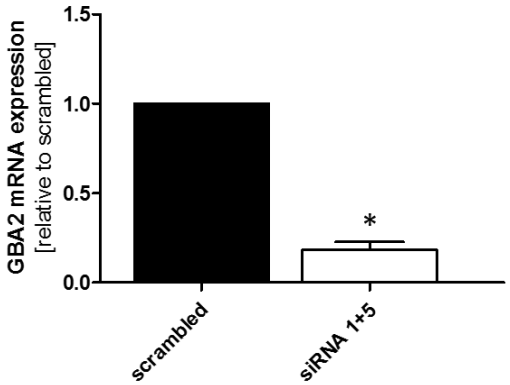

Figure 43 Effect of the combination of Hs_GBA2_1 and Hs GBA2_5 on the GBA2 mRNA expression in CuFi-1 cells.
** p<0.001 vs scrambled*

After the identification of the best combination of siRNAs, I studied the effect of GBA2 silencing on the inflammatory response to bacterial infection.
To this purpose, I administered the combination of the two siRNA to CuFi-1 cells, and then, I infected the cells with *Pseudomonas aeruginosa*. As control, I used the same silenced cells not infected.

I determined the IL-8 chemokine expression, trough qRT-PCR. As shows in figure 44, I found a significant low level of IL-8 in GBA2 transfected cells and I observed a further decrease after bacterial infection.

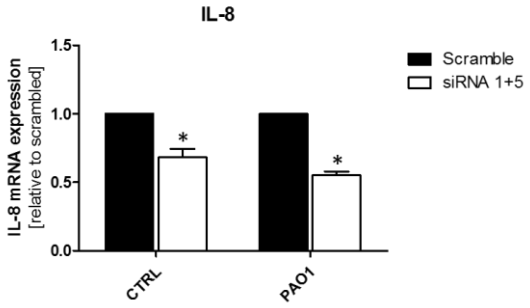

Figure 44 Effect of GBA2-siRNA 1 and 5 combined treatment in the intrinsic pro-inflammatory state and in inflammatory response to Pseudomonas aeruginosa in CuFi-1 cells.
**p<0.0001 vs scramble*

These results suggest the possibility to control the inflammatory response in CF through the specific targeting of GBA2.

Nanoparticles development for si-RNA-GBA2 delivering

Since siRNA are very unstable oligonucleotides, especially in the cytosolic and extracellular environment, I tried to stabilize the nucleic acid by its condensation with protamine. For this reason, I started to investigate the effect of the protamine-siRNA condensation on the silencing capability of siRNA.

As shown in figure 45, protamine alone does not exert any effect on GBA2 activity; moreover, the same efficiency in GBA2 silencing was obtained when the two selected siRNAs (1 and 5) were administered complexed with protamine.

These results indicate that these experimental conditions fully assure siRNA integrity and availability.

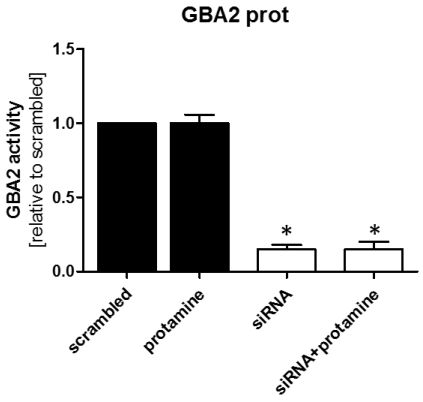

Figure 45 Influences of Protamine on the silencing efficiency of GBA2-siRNA 1 and 5
The measurement of the total GBA2 enzymatic activity was conducted on cell lysate using an in vitro assay and artificial fluorigenic substrates. The enzymatic activity is expressed as pmoles of products, on mg of proteins, per hour.
Protamine does not influence the silencing properties of GBA2-siRNA 1 and 5.
**p> 0.005 vs scrambles*

As reported above, I used Lipofectamine2000 as vector to administrate siRNA. Since Lipofectamine is a commercial mixture of cationic lipids, used only for research purpose, I decided in collaboration with a group of physicist, to change the vector adapting a lipoplex. Lipoplex is normally used for the systemic delivery of plasmids, but we tried to use it to deliver siRNA.

The delivery of genetic material is an important field in development. Lipids and DNA/RNA spontaneously aggregate in solution and form structures similar to those of the bare lipids, being DNA/RNA embedded in their aqueous moieties. For in vitro transfection models, the delivery efficiency has been correlated to both the lipid composition and the structural features of the lipid/nucleic acid complexes.

Among lipid-based nanovectors, an interesting class of core-shell nanoparticles has been shown to promote transfection efficiency in different experiments. They are obtained by precondensing the DNA with a fusogenic protein, namely protamine, before lipid interaction.

We applied a selected class of cationic lipid based nanovectors for the delivery of siRNA against GBA2 in vitro. The selected lipid composition consists of a DC-Chol/DOPE mixture that have been already studied for the systemic delivery of plasmid DNA and siRNA. We prepared DC-Chol/DOPE-siRNA lipoplexes (CL) and DC-Chol/DOPE-protamine/siRNA nanoparticles (NP). CL and NP allow studying the effectiveness of siRNA protection by protamine pre-condensation in relation to the delivery and the transfection efficiency in vitro.

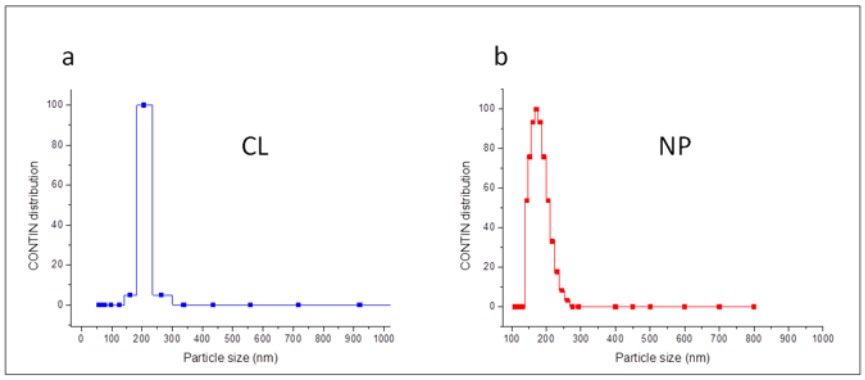

Figure 46 Characterization of lipid based nanoparticle with Dynamic light scattering
Particle size distribution of a) CL lipoplexes and b) NP nanoparticles obtained by DLS at 25°C applying CONTIN analysis

First, we performed the biophysical characterization of these nanoparticles. CL size distribution obtained by Dynamic Light Scattering (DLS) shows a well-defined population with low polydispersity and average hydrodynamic diameter D_H = 206 nm (figure 46). Particles are positively charged with a Z-potential of 24±2 mV.

After the biophysical characterization, I proceeded with the evaluation of the transfection power. I performed a set of preliminary experiments involved in the functional characterization of these two different "siRNA delivery system" in comparison with lipofectamine.

In the first part of the experiments, I used a siRNA, linked with a green fluorophore, and I performed time course experiments of 5, 24 and 48 hours. Our aims were to study the cell delivery of the siRNA, the localization within the cells and the time stability in CuFi-1 cells line.

As shown in figure 47, both lipoplexes and nanoparticles are able to enter into the cells faster with respect to the lipofectamine, as suggested by the increased fluorescence after 5 hours from the administration.

In addition, during the time course, the cell organization seems to be different and, for the NP at 48 hours, is possible to observe that part of fluorescence signal is within the nucleus.

In term of quantity, the fluorescence associated with lipoplexes (CL) and NP are higher in comparison to lipofectamine, for all the time points tested.

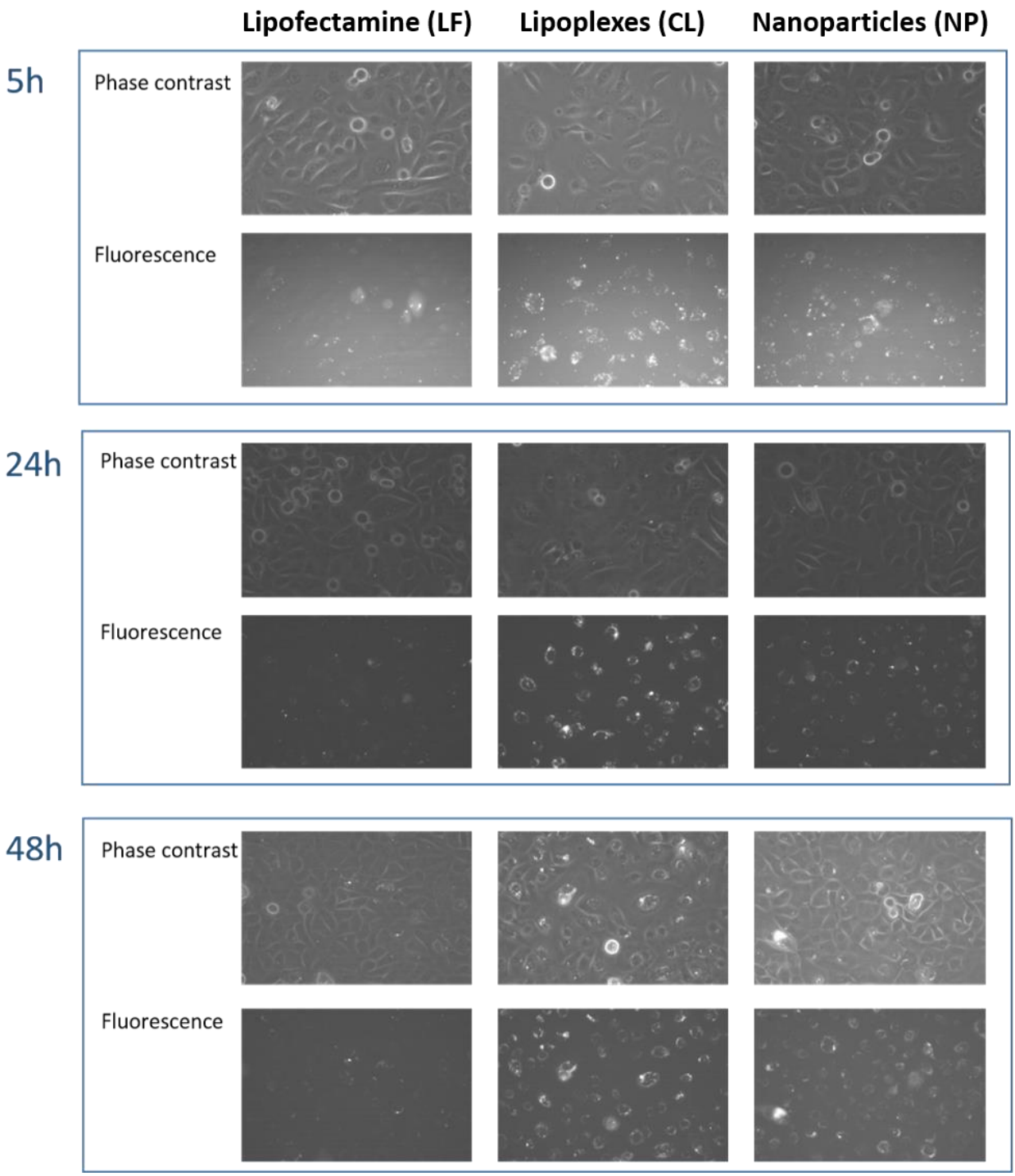

Figure 47 Images of CuFi-1 cells treated with different lipid based nanoparticle and fluorescent siRNA
Representative images, obtained with phase contrast microscopy and fluorescence microscopy, of cellular behavior of fluorescent siRNA delivered in CuFi-1 cells using lipoplexes (CL), nanoparticles (NP) and commercial lipofectamine 2000 (LF) as control.

Subsequently, I performed a time course experiments to measure the GBA2 activity after 24h (figure 48), 48h (figure 49) and 6 days (figure 50) from the transfection in order to evaluate the capability of different delivery systems to silence GBA2 and their influence on the stability of siRNA into the cells.

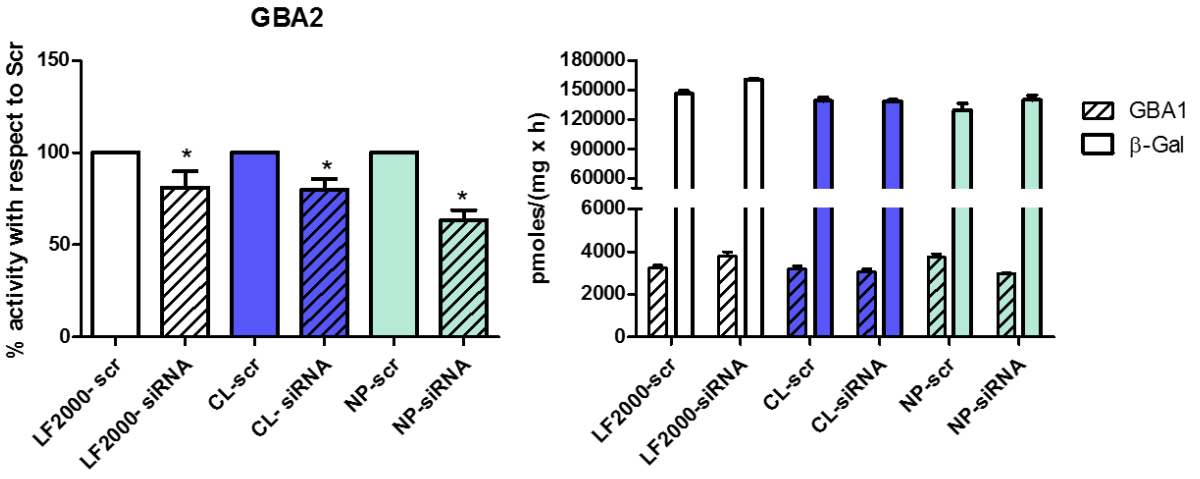

Figure 48 Evaluation of GBA2, GBA1 and β-gal activity after 24 h from transfection
Left: GBA2 activity in CuFi-1, treated with siRNA-GBA2 and siRNA scrambled loaded on lipofectamine, lipoplexes and nanoparticle after 24 h from transfection. The measurement of the total GBA2 enzymatic activity was conducted on cell lysate using an in vitro assay based on artificial substrates.
Right: GBA1 and β galactosidase activity measured on the same cells. The enzymatic activity of cells, treated with siRNA, was expressed as percentage with respect to activity obtained from cells trated with scrambled.
LF 2000: Lipofectamine 2000; CL: Lipoplexes; NP: nanoparticles; siRNA: siRNA against GBA2; Scr: Scrambled

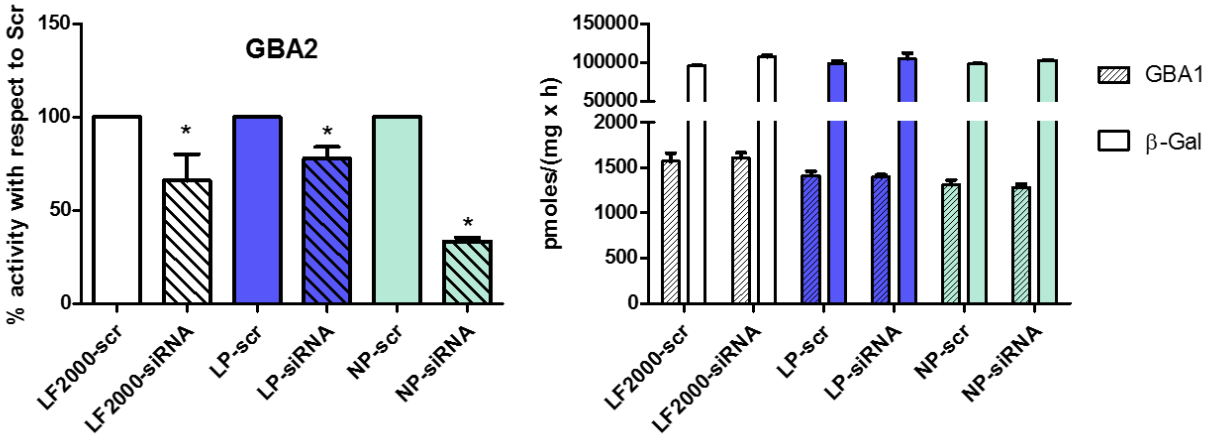

Figure 49 Evaluation of GBA2, GBA1 and β-gal activity after 48 h from transfection
Left: GBA2 activity in CuFi-1, treated with siRNA-GBA2 and siRNA scrambled loaded on lipofectamine, lipoplexes and nanoparticle after 48 h from transfection. The measurement of the total GBA2 enzymatic activity was conducted on cell lysate using an in vitro assay based on artificial substrates.
Right: GBA1 and β galactosidase activity measured on the same cells. The enzymatic activity of cells, treated with siRNA, was expressed as percentage with respect to activity obtained from cells trated with scrambled.
LF 2000: Lipofectamine 2000; CL: Lipoplexes; NP: nanoparticles; siRNA: siRNA against GBA2; Scr: Scrambled

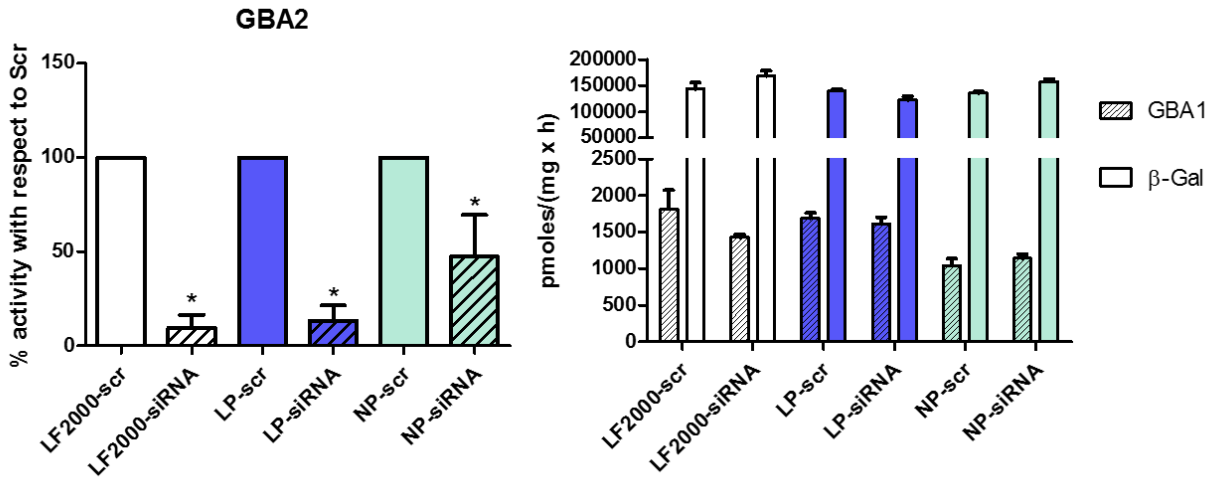

Figura 50 Evaluation of GBA2, GBA1 and β-gal activity after 6 days from transfection
Left: GBA2 activity in CuFi-1, treated with siRNA-GBA2 and siRNA scrambled loaded on lipofectamine, lipoplexes and nanoparticle after 6 days from transfection. The measurement of the total GBA2 enzymatic activity was conducted on cell lysate using an in vitro assay based on artificial substrates.
Right: GBA1 and β galactosidase activity measured on the same cells. The enzymatic activity of cells, treated with siRNA, was expressed as percentage with respect to activity obtained from cells trated with scrambled.
LF 2000: Lipofectamine 2000; CL: Lipoplexes; NP: nanoparticles; siRNA: siRNA against GBA2; Scr: Scrambled

At 24 h and 48 h, in CuFi-1 treated with the delivery system lipoplexes I observed a reduction of 20/ 30% in the GBA2 activity. Concerning the nanoparticle system, I observed a reduction of 40/50%. After 6 days, all the delivery system tested cause a strong reduction in GBA2 activity.

In order to control any possible off-target effect I measured also the enzymatic activity of GBA1 and β-Gal for all the time points. The results demonstrate that β-Gal are maintained constant during all the time course, we observed only a slight decrease of the activity of GBA1 after 6 days in cells treated with NP.

After these experiments, I evaluated the toxicity of the different delivery system tested, analyzing the expression of cell damage biochemical markers such as LC3II and p62 for autophagy and caspase 3 for apoptosis. I found that at 48 h, cells treated with CL are characterized by the activation of macroautophagy as indicated by the high level of LC3II and p62 (figure 51).

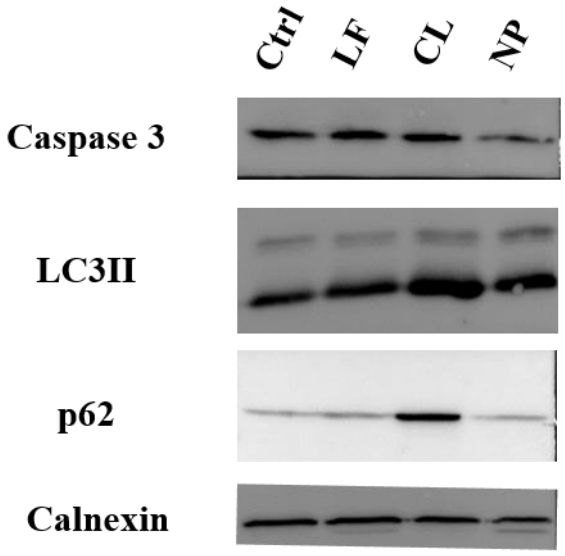

Figure 51 Immunoblotting analyses of CuFi-1 cells treated with siRNA anti-GBA2 loaded with lipofectamine, lipoplexes and nanoparticle.
Immunoblotting analyses of the biochemical markers of cell damage: LC3II and p62 for autophagy and caspase 3 for apoptosis performed on CuFi-1 cells subjected to the treatment with siRNA-GBA2 loaded on lipofectamine, lipoplexes or nanoparticles
LF: lipofectamine, CL: lipoplexes; NP: nanoparticles

Discussion

Several studies in different CF models strongly support the relationship among sphingolipids, inflammation response and susceptibility to bacterial infection. A peculiar role seems to be played by ceramide; in fact, it has been demonstrated an increase in PM ceramide levels in CF bronchi that seems to be correlated with the pro-inflammatory status typical of CF lung disease [Brodlie, McKean, et al, Teichgraber, Ulrich, et al. 2008]. Several criticism emerge from the literature regarding the origin of the ceramide accumulated in CF bronchi.

In fact, as well known, several metabolic pathways contribute to the ceramide production. Beside the main catabolic pathway occurring in lysosomes, the *de novo* biosynthesis and the hydrolysis of the sphingolipids triggered directly at the plasma membrane, by the action of the PM associated-hydrolases, could play an important role [Aureli, Loberto, et al. 2011].

Interestingly, it has been demonstrated in bronchial epithelial cells that part of ceramide is produced in response to *Pseudomonas aeruginosa* infection through the SM catabolism at the plasma membrane driven by the acid-sphingomyelinases [Grassme, Jendrossek, et al. 2003]. On the other hand, of particular relevance, bioactive ceramide could be produced by the action of PM-glycohydrolases through GSL degradation at the cell surface, as demonstrated in human fibroblast [Sonnino and Prinetti, et al. 2010] and in cancer cells [Gobbi, Re, et al. 2010]. Nevertheless, limited information are available on the involvement of these enzymes in the Cystic Fibrosis lung disease.

Recent data demonstrated that the pharmacological inhibition of GBA2, a key enzyme in the production of ceramide at the cell surface, as well as the down regulation of GBA2 expression, is associated with a significant reduction of the inflammatory response to *P. aeruginosa* infection. Moreover, the knocking-down of GBA2 is reported to cause a reduction of the intrinsic pro-inflammatory state of CF epithelial bronchial cells [Loberto, Tebon, et al. 2014].

Considering all these aspects, the specific aims of my PhD project were, i) the Identification of the molecular mechanism linking the PM glycohydrolases with the inflammation response in CF lung disease and ii) the development of a nanoparticles-based siRNA-GBA2 delivering system.

Involvement of PM hydrolases in the inflammation response in CF lung disease

Based on the previous data published in the literature I investigated the role of the PM-glycohydrolases, in the molecular mechanisms involved in the regulation of the inflammatory response in Cystic Fibrosis lung disease.

The first challenge was to choose the appropriate cellular models suitable to mimic the characteristic condition of the airway of CF patients, especially in term of sphingolipid profile.

Among the different cellular models available, CuFi-1 and NuLi-1 cell lines represent the most promising. CuFi-1 are immortalized bronchial epithelial cells deriving from a CF patients homozygous for F508del. NuLi-1 are cells of the same origin, deriving from a healthy subject. Interestingly, both cell lines are characterized by a SLs composition that recalls the features found in the lung tissue of CF patient.

In particular, I found an important difference in the composition of gangliosides between CuFi-1 and NuLi-1 cells. In fact, the main ganglioside of CuFi-1 cells is GM3, whereas in NuLi-1 cells is GM1. The composition found in CuFi-1 and NuLi-1 cells is related to the characteristics found in lung tissue. Indeed, in adult human lung, fourteen gangliosides with different carbohydrate moieties have been identified and the most abundant are monosialogangliosides GM3 and GM1 [Mansson, Mo, et al. 1986]. In addition, the difference between CF and non-CF cell lines in term of ganglioside composition, remind to some evidence reported by Itokazu and colleagues [Itokazu, Pagano, et al. 2014]. They described a direct correlation between ganglioside GM1 levels at the PM and CFTR expression and they demonstrated that the lack of CFTR is responsible for the reduction of the cellular level of GM1.

In addition, as found in CF lung tissue [Brodlie, McKean, et al.], CuFi-1 cells are characterized by a high content of ceramide.

Interestingly, I observed that CuFi-1 cells are characterized by higher activity of the PM-associated glycohydrolases when compared to NuLi-1, suggesting that part of the ceramide could be directly produced at the cell surface.

In fact, ceramide is an important factor in pulmonary host defense, in addition to the classical cytokines and chemokines, released by the respiratory epithelium. Different findings have demonstrated the involvement of Cer in pulmonary infections caused by a variety of bacterial and viral pathogens, including *Pseudomonas aeruginosa* [Seitz, Grassme, et al. 2015].

The main open question to be addressed is correlated to the relationship between ceramide and infection/inflammation. In particular, from the literature it is not clear if the plasma membrane

ceramide accumulation is an intrinsic feature of CF bronchial epithelial cells or if the ceramide is produced in response to bacterial infection.

In order to study the effect of the bacterial infection on the SL pattern, I infected both CuFi-1 and Nuli-1 cells with PAO-1 and then I analyzed the SL composition. In CuFi-1 cells, I observed a significant increase in ceramide and GlcCer content; whereas in NuLi-1 cells the effect of PAO-1 results only in a slight increase in ceramide content without affecting other cellular sphingolipids.

As well known, the study of sphingolipids, in particular the study of ceramide remains a critical issue for several reason especially for the lack of specific antibodies or probes.

For these reason, we think that the study of SLs composition and pattern within various cellular process must be followed by the measurement of the related metabolic pathway.

Consequently, after the SLs analysis, I proceed with the measurement of the main glycohydrolases involved in the GLSs catabolism, since Grassme and colleagues [Grassme, Jendrossek, et al. 2003] excluded the activation of the de-novo ceramide biosynthesis in response to PAO-1 infection. Surprisingly, I found that the bacterial infection was not able to cause significant modification on all the hydrolases activities tested, associated with PM and in total cell lysate.

Since I found an enrichment of ceramide content after bacterial infection, I expected to observe some modification in the activity of the hydrolases involved in the GLS catabolism, leading to ceramide formation. On the other hand, the methodology used to measure the enzymatic activities associated with PM allow evaluating the activities associate to the entire cell surface, without the possibility to focus on specific membrane areas.

Starting from these consideration, I begun to taking into account a possible role of lipid rafts in the process of bacterial infection and in the mechanism of activation of inflammatory response.

On this frame, some evidences in literature reported that Cer-enriched membrane domains recruit and activate receptors and signalling molecules involved in different inflammatory pathways [Grassme, Jendrossek, et al. 2003]. In addition, it has been shown that Cer-enriched platforms are formed in cells, after the application of many different stimuli, including bacterial infections [Seitz, Grassme, et al. 2015]. However, several questions remain to be addressed especially in CF bronchial epithelial cells.

To this purpose, I prepared the lipids rafts as detergent resistant membrane fraction, from both CuFi-1 and NuLi-1 cells subjected or not to PAO-1 infection. The first evidence that I obtained was a clear effect of the bacterial infection on the DRM organization. In fact, the DRM of infected cells was characterized by increased SL-radioactivity with respect to uninfected cells.

Focusing on CuFi-1 cells, in term of SL composition, I found an enrichment in ceramide, sphingomyelin and GM1 in the DRM fraction of infected cells, whereas the complex ganglioside

GD1a decreased. The shift from complex to simple sphingolipids suggest the local activation of the catabolic machinery. As expected, I found that *P.aeruginosa* infection leads to an increase of the all glycohydrolase activity tested in the DRM fraction.

On the contrary, in NuLi-1 cells, I observed an enrichment in sphingomyelin, GM1 and GM3 with no effect on the ceramide content in the DRM fraction of infected cells. Interestingly, I found that all the glycohydrolases activity associated with the DRM fraction of infected cells decreased compared to not infected cells.

Taken together these results lead to speculate that in CF cells, the bacterial infection causes an important rearrangement of the PM structure and composition. In particular, the bacterial infection leads to a recruitment of the glycohydrolases in specific membrane domains, enriched in their substrates. The concomitant presence of the glycohydrolases and their substrate causes changes in the SL composition that together with the ceramide formation organizes specific platform involved in the activation of the inflammatory response.

It is quite difficult to speculate between the different behavior of DRM-associated glycohydrolases in response to *P. aeruginosa* infection in CuFi-1 and NuLi-1 cells. The obtained experimental evidences suggest that the glycohydrolases involved in the glycosphingolipids catabolism have an important role in the establishment of a membrane environment suitable to manage the bacterial infection.

To this purpose, it is important to highlight that the mechanism of bacterial infection management are deeply different between CF and non-CF cells and could allow us giving an initial interpretation to our intricate results. For instance, although it is generally thought that *P. aeruginosa* is an extracellular pathogen, a number of different groups have found that this bacterium can be internalized in different cell types, including airways epithelial cells [Fleiszig, Zaidi, et al. 1996]; [Evans, Frank, et al. 1998];[Plotkowski, de Bentzmann, et al. 1999].

In addition, Pier and co-workers, suggested that CFTR is a cell surface receptor for non-mucoid smooth strains of *P. aeruginosa*. [Pier, Grout, et al. 1996]. They demonstrated that this strain can bind via LPS to a specific segment of the CFTR, leading to internalization into bronchial epithelial cells. Taken together, all these studies suggest that CFTR is involved in the bacterial internalization.

Based on these evidences it is reasonable to think that in NuLi-1 cells CFTR, together with the hydrolases and sphingolipids, organizes a membrane domain that in response to the bacterial infection leads to its internalization. Conversely, in CuFi-1 cells, the ceramide-enriched domain could be involved in the activation of the inflammatory response.

Since the aberrant inflammatory response is one of the main factor responsible for the onset of CF lung disease, I further investigated the role of SLs and SL catabolism in the inflammation and host

defense in CF epithelial bronchial cells. In particular, I focused my attention on the study of the possible molecular mechanism linking the cell membrane micro-domains to the activation of the inflammatory response.

One of the best candidate is represented by the integral membrane receptor CD95. In particular, CD95 is able to induce both pro-apoptotic and anti-apoptotic signals by its segregation in ceramide-enriched domain.

During the early phase of activation, CD95 recruits phospho-FADD and pro-caspase-8. The aggregation of these molecules is able to translocate into lipid rafts domain crating a dimer. At this stage, CD95 has the potential to activate non-apoptotic pathway by inducing the activation of the mitogen activated protein kinase (MAPK) and the transcription nuclear factor kB (NF-kB) [Grassmé, Jekle, et al. 2001].

In the late phase of CD95 pathway, after its triggering, CD95 is internalized in a clatrhrin-dependent manner into endosomal compartment. During endosomal trafficking, high levels of death-inducing signaling complex (DISC) and caspase-8 are recruited, resulting in a strong caspase-8 activation and as consequences, the propagation of apoptotic signaling.[Schutze, Tchikov, et al. 2008] However, the internalization of CD95 is dependent by the presence of the scaffolding protein EZRIN in its phosphorylated state. However, after PAO1 infection in CuFi-1 cells I observed an increase in the DRM ceramide content, which is an inhibitor of EZRIN phosphorylation [Adada, Canals, et al. 2014]. In this scenario, CD95 is not internalized and remains at the cell surface where activates the pro-inflammatory pathway promoting the nuclear translocation of the transcription factor NF-kB [Grassmé, Jekle, et al. 2001] **[**Bezzerri, Borgatti, et al. 2008]**.** The preliminary results obtained, support the involvement of this pathway, since I observed an increase of all the principal regulatory protein of the pro-inflammatory pathway like phospo-FADD, RIP and NF-kB.

Involvement of GBA2 in the inflammation response in CF lung disease

Among the hydrolases associated with the cell surface, GBA2 represents an important player in the regulation of the sphingolipid homeostasis directly at the plasma membrane. In addition, recent evidences support its direct role in the regulation of the inflammatory response in CF bronchial epithelial cells subjected to bacterial infection. Unfortunately, the experimental approach used for the DRM isolation does not allow studying the involvement of GBA2 because of the use of detergent, necessary for DRM isolation, inhibits its activity. In addition, the lack of specific antibodies does not permit its detection neither in the gradient fraction nor at the cell surface. For this reason, in order to study the GBA2 contribute in the inflammation response, I decided to change strategy, overexpressing

GBA2 tagged with GFP at the C-terminal in both CuFi-1 and NuLi-1 cells. As expected, I obtained monoclonal cell lines stably overexpressing GBA2 at the cell surface, as demonstrated by confocal microscopy analyses and enzymatic activity assays on living cells.

Interestingly, the subcellular localization of the overexpressed enzymes in the two different cell lines recall the endogenous GBA2. GBA2 enzymatic activity on PM is major in CuFi-1 with respect to NuLi-1 cells, conversely the enzymatic activity associate with cell lysate is major in NuLi-1 in respect to CuFi-1. Similarly, overexpressed GBA2 is preponderant on PM of CuFi-1 compared with NuLi-1. On the other hand, intracellularly the behavior is opposite, and I found a major activity in NuLi-1 in respect to CuFi-1 cells. These considerations suggest that the overexpressing cells preserve the original characteristics of CuFi-1 and NuLi-1 cells and represent a good model to study GBA2 involvement during infection and inflammatory response. GBA2 overexpressing cells are characterized by a different SLs profile if compared with Mock control cells. In particular, both CuFi-1 and NuLi-1 cells overexpressing GBA2 show a decrease of GlcCer, followed by an increase of Cer and SM.

It is possible to explain the relationship between the GlcCer reduction and the Cer increase, considering that GBA2 catalyzes the degradation of GlcCer into Ceramide. On the other hand, the high content of ceramide is probably associated to an increased synthesis of SM as suggested by Sorli and colleagues [Sorli, Colie, et al. 2013]. This could explain the high level of SM observed in the overexpressing cells.

The evidence reported by Loberto and colleagues [Loberto, Tebon, et al. 2014] demonstrating the reduction of pro-inflammatory response of CF bronchial epithelial cells after GBA2 knock-down, prompted us to evaluated the inflammatory state of CuFi-1 cells overexpressing GBA2 compared to CuFi-1 cells. Interestingly, I observed an increase in the basal level of IL-8 mRNA in the GBA2 overexpressing cells with respect to CuFi-1 cells. These results further support the role of GBA2 in the activation of the inflammatory response in CF; in fact, any effect was observed in NuLi-1 cells.

From the data obtained by PAO-1 infection in CF bronchial epithelial cells, clearly emerge a role of lipids rafts in the regulation of the IL-8 expression and secretion.

As mentioned above, GBA2 overexpression induce changes in the sphingolipid profile causing an increase in the ceramide content which is followed by an augmented production of IL-8. On the basis on this analogy, I decided to investigate the effect of GBA2 overexpression on the lipids rafts of CuFi-1 cells. Interestingly I found that DRM deriving from overexpressing cells is characterized by increased content of ceramide and by increased activity of the main glycohydrolases, involved in the glycosphingolipids catabolism. Interestingly, these data let us to speculate that the overexpression of GBA2 mimics the PAO-1 infection. In addition, GBA2 overexpressing cells do not react to the PAO-

1 infection since show decreased DRM-associated glycohydrolases activity as well as decreased ceramide and SM content. In this context, GBA2 overexpression seems to by-pass the effect of PAO-1 infection at the cell plasma membrane level. Of course, this is a speculation that need additional studies to be validated.

Development and characterization of Nanoparticles-based siRNA-GBA2 delivering system

Among all glycohydrolases, the obtained data, suggest that GBA2 could cover an important role in the creation of the pro-inflammatory state characteristic of Cystic Fibrosis lung disease as well as in the inflammatory response to bacterial infection.

In particular, its silencing could represent a new promising therapeutic strategy to reduce the pro-inflammatory state of CF bronchial epithelial cells and to reduce the inflammatory response after bacterial infection. For these reasons, the second objective of my work was to set up a new strategy to delivery siRNA in CF epithelial bronchial cell in order to knock down GBA2.

Certainly, GBA2 plays a crucial role in the extra-lysosomal GlcCer catabolism, producing ceramide that can be then rapidly converted into sphingomyelin and seems to play a crucial role in the motor-neuronal development in fetus [Boot, Verhoek, et al. 2007] [Martin, Schule, et al. 2013, Sorli, Colie, et al. 2013]. However, the inhibition of GBA2 as possible therapeutic strategy to reduce CF inflammation could be considered only postnatally and this scenario could present very limited side effect.

Moreover, GBA2 activation causes the phosphorylation of eukaryotic initiation factor 2α (eIF2α), and this event is associated to an increased expression of ATF4 family of transcription factors. Interestingly, phosphorylation of eIF2α has been observed in model of acute infection with *Clostridium difficile,* as part of the mucosal inflammatory response. It can ben speculated that GBA2 activation by *Pseudomonas aeruginosa* leads to increased expression of the transcription factors that regulates the pro-inflammatory genes in CF bronchial cells. As proof of concept, its pharmacologic inhibition with Miglustat and its knocking-down through siRNA leads to a decrease of IL-8 release after bacterial infection. The decrease of IL-8 was observed even in absence of bacterial infection correlating GBA2 also with the pro-inflammatory state of CF.

On the bases of these evidence, GBA2 represents a possible molecular target to reduce the inflammation caused by pathogens, but also to manage the typical pro-inflammatory state of CF lung disease.

Even if the pharmacological treatment with Miglustat, drug normally used to manage the Gaucher disease, leads to important results, this therapy in Gaucher patients has some limits related to serious adverse effect. The most severe is represents by diarrhea, which in particular case could leads to death. In addition, no effect in the reduction of the pro-inflammatory state in CF was observed upon miglustat treatments.

For this reason, a new challenge is represented by the development of an innovative approach to modulate the function of GBA2.

At this regard, the other goal of my thesis project was to produce high efficient Nanoparticles, with a specific designed multicomponent composition, aimed to obtain a better transfection efficacy of siRNA anti-GBA2 and lower toxicity compared with the already available lipid-based systems.

I first identified the best siRNA sequences in order to silence the activity of GBA2 achieving 70% down regulation in CuFi-1 cells.

The delivery of genetic material is an important field in continuous development. Lipids and DNA/RNA spontaneously aggregate in solution and form structures similar to those of the bare lipids, being DNA/RNA embedded in their aqueous moieties.

For these reasons, lipid-based nanoparticles represent a good solution to promote the transfection of genetic material. For in vitro transfection models, the delivery efficiency has been correlated to both the lipid composition and the structural features of the lipid/nucleic acid complexes. Thanks to a collaboration with the biophysics group belonging to my department I selected a lipid composition consisting of a DC-Chol/DOPE mixture that have been already studied for the systemic delivery of plasmid DNA and siRNA.

However, another important point to take into account for the development of nanoparticles for the delivery of siRNA, is represented by the fact that RNA is a very unstable molecules, sensible to degradation.

Among lipid-based nanovectors, an interesting class of core-shell nanoparticles have been shown to promote transfection efficiency in different experiments. They are obtained by pre-condensing the siRNA with a protein, namely protamine, before lipid interaction, in order to protect the siRNA in the intracellular environment.

Taking into account all these considerations, the silencing experiments were performed using a DC-Chol/DOPE-siRNA lipoplexes (CL) composed only by siRNA and lipids, and DC-Chol/DOPE-protamine/siRNA nanoparticles (NP), consisted in the interaction between RNA covered by protamine and lipids.

As control, I used a commercial mixture of cationic lipids, the Lipofectamine2000, normally applied as vector to administrate siRNA only for research purpose.

The first part of the experiments was performed using a florigenic siRNA in order to study its localization and stability within CuFi-1 cells. The data obtained from these experiments demonstrated that CL an NP carry siRNA in a more efficient way into CuFi-1 cells, compared to Lipofectamine 2000.

The second part of the experiment was performed to establish the capability of different delivery system to silence GBA2 and their influence on the stability of siRNA into the cells.

At all the time point considered, NP shows the best down-regulation of GBA2 activity.

Another important aspect is represented by the toxicity of the different delivery system used. The analysis of the cell-damage biochemical markers LC3II, p62 for autophagy and caspase 3 for apoptosis reveled that at 48 h, only cells treated with CL are characterized by the activation of macro autophagy. The development of NP represents an important field to study new focused delivery system, with therapeutic purpose, to diminish and manage collateral and adverse effect.

Additional investigation are needed to study more in detail the efficiency and the toxicity of this delivery system.

Conclusion

In summary, we proposed that *Pseudomonas aeruginosa* infection in Cystic Fibrosis cells, promotes the recruitment at the PM level of the several glycohydrolases involved in the GSLs catabolism, creating a platform enriched in ceramide, involved in the activation of inflammatory response.

In addition, we assumed that GBA2 could cover an important role in this context as well as in the establishment of pro-inflammatory state of CF. More important, these results further support the use of modulators of SL metabolism as possible therapeutic strategies for CF lung inflammation, concept that is becoming increasingly important in the research field of Cystic Fibrosis.

Bibliography

Adada, M., et al., *Sphingolipid regulation of ezrin, radixin, and moesin proteins family: implications for cell dynamics.* Biochim Biophys Acta, 2014. **1841**(5): p. 727-37.

Anderson, M.P., et al., *Demonstration that CFTR is a chloride channel by alteration of its anion selectivity.* Science, 1991. **253**(5016): p. 202-5.

Aureli, M., et al., *Cell surface associated glycohydrolases in normal and Gaucher disease fibroblasts.* J Inherit Metab Dis, 2012. **35**(6): p. 1081-1091.

Aureli, M., et al., *Plasma membrane-associated glycohydrolases along differentiation of murine neural stem cells.* Neurochem Res, 2012. **37**(6): p. 1344-54.

Aureli, M., et al., *Plasma membrane-associated glycohydrolases activation by extracellular acidification due to proton exchangers.* Neurochem Res, 2012. **37**(6): p. 1296-307.

Aureli, M., et al., *Remodeling of sphingolipids by plasma membrane associated enzymes.* Neurochem Res, 2011. **36**(9): p. 1636-44.

Aureli, M., et al., *Cell surface sphingolipid glycohydrolases in neuronal differentiation and aging in culture.* J Neurochem, 2011. **116**(5): p. 891-9.

Aureli, M., et al., *Activity of plasma membrane beta-galactosidase and beta-glucosidase.* FEBS Lett, 2009. **583**(15): p. 2469-73.

Aureli, M., et al., *Photoactivable sphingosine as a tool to study membrane microenvironments in cultured cells.* J Lipid Res, 2010. **51**(4): p. 798-808.

Aureli, M., et al., *Erratum to: Current and Novel Aspects on the Non-lysosomal beta-Glucosylceramidase GBA2.* Neurochem Res, 2016. **41**(1-2): p. 221.

Aureli, M., et al., *Unravelling the role of sphingolipids in cystic fibrosis lung disease.* Chem Phys Lipids, 2016. **200**: p. 94-103.

Bartke, N. and Y.A. Hannun, *Bioactive sphingolipids: metabolism and function.* J Lipid Res, 2009. **50 Suppl**: p. S91-6.

Becker, K.A., et al., *Acid sphingomyelinase inhibitors normalize pulmonary ceramide and inflammation in cystic fibrosis.* Am J Respir Cell Mol Biol. **42**(6): p. 716-24.

Becker, K.A., et al., *The role of sphingolipids and ceramide in pulmonary inflammation in cystic fibrosis.* Open Respir Med J, 2010. **4**: p. 39-47.

Becker, K.A., et al., *Accumulation of ceramide in the trachea and intestine of cystic fibrosis mice causes inflammation and cell death.* Biochem Biophys Res Commun, 2010. **403**(3-4): p. 368-74.

Bezzerri, V., et al., *Transcription factor oligodeoxynucleotides to NF-kappaB inhibit transcription of IL-8 in bronchial cells.* Am J Respir Cell Mol Biol, 2008. **39**(1): p. 86-96.

Boot, R.G., et al., *Identification of the non-lysosomal glucosylceramidase as beta-glucosidase 2.* J Biol Chem, 2007. **282**(2): p. 1305-12.

Borowitz, D., *CFTR, bicarbonate, and the pathophysiology of cystic fibrosis.* Pediatr Pulmonol, 2015. **50 Suppl 40**: p. S24-S30.

Borthwick, L.A., et al., *Is CFTR-delF508 really absent from the apical membrane of the airway epithelium?* PLoS One, 2011. **6**(8): p. e23226.

Boucher, R.C., *Airway surface dehydration in cystic fibrosis: pathogenesis and therapy.* Annu Rev Med, 2007. **58**: p. 157-70.

Boucher, R.C., *An overview of the pathogenesis of cystic fibrosis lung disease.* Adv Drug Deliv Rev, 2002. **54**(11): p. 1359-71.

Brodlie, M., et al., *Ceramide is increased in the lower airway epithelium of people with advanced cystic fibrosis lung disease.* Am J Respir Crit Care Med, 2010. **182**(3): p. 369-75.

Cant, N., N. Pollock, and R.C. Ford, *CFTR structure and cystic fibrosis.* Int J Biochem Cell Biol, 2014. **52**: p. 15-25.

Cantin, A.M., et al., *Inflammation in cystic fibrosis lung disease: Pathogenesis and therapy.* J Cyst Fibros, 2015. **14**(4): p. 419-30.

Caretti, A., et al., *Anti-inflammatory action of lipid nanocarrier-delivered myriocin: therapeutic potential in cystic fibrosis.* Biochim Biophys Acta, 2013. **1840**(1): p. 586-94.

Carter, H.E., et al., *Biochemisrty of sphingolipides. III. Structure of sphingosine.* J. Biol. Chem., 1947. **170**: p. 285-294.

Carter, H.E., et al., *Biochemistry of the sphingolipids. XIII. Determination of the structure of cerebrosides from wheat flour.* J Biol Chem, 1961. **236**: p. 1912-6.

Castellani, C., et al., *Consensus on the use and interpretation of cystic fibrosis mutation analysis in clinical practice.* J Cyst Fibros, 2008. **7**(3): p. 179-96.

Chigorno, V., et al., *Formation of a cytosolic ganglioside-protein complex following administration of photoreactive ganglioside GM1 to human fibroblasts in culture.* FEBS Lett, 1990. **263**(2): p. 329-31.

Chmiel, J.F., M. Berger, and M.W. Konstan, *The role of inflammation in the pathophysiology of CF lung disease.* Clin Rev Allergy Immunol, 2002. **23**(1): p. 5-27.

Chmiel, J.F. and P.B. Davis, *State of the art: why do the lungs of patients with cystic fibrosis become infected and why can't they clear the infection?* Respir Res, 2003. **4**: p. 8.

Coakley, R.D., et al., *Abnormal surface liquid pH regulation by cultured cystic fibrosis bronchial epithelium.* Proc Natl Acad Sci U S A, 2003. **100**(26): p. 16083-8.

Couet, J., et al., *Identification of peptide and protein ligands for the caveolin-scaffolding domain. Implications for the interaction of caveolin with caveolae-associated proteins.* J Biol Chem, 1997. **272**(10): p. 6525-33.

De Lisle, R.C., *Pass the bicarb: the importance of HCO3- for mucin release.* J Clin Invest, 2009. **119**(9): p. 2535-7.

Dechecchi, M.C., et al., *Modulators of sphingolipid metabolism reduce lung inflammation.* Am J Respir Cell Mol Biol, 2011. **45**(4): p. 825-33.

Dechecchi, M.C., et al., *Anti-inflammatory effect of miglustat in bronchial epithelial cells.* J Cyst Fibros, 2008. **7**(6): p. 555-65.

Degroote, S., J. Wolthoorn, and G. van Meer, *The cell biology of glycosphingolipids.* Semin Cell Dev Biol, 2004. **15**(4): p. 375-87.

Elborn, J.S., *Cystic fibrosis.* Lancet, 2016. **388**(10059): p. 2519-2531.

Ellsworth, R.E., et al., *Comparative genomic sequence analysis of the human and mouse cystic fibrosis transmembrane conductance regulator genes.* Proc Natl Acad Sci U S A, 2000. **97**(3): p. 1172-7.

Engelhardt, J.F., et al., *Expression of the cystic fibrosis gene in adult human lung.* J Clin Invest, 1994. **93**(2): p. 737-49.

Evans, D.J., et al., *Pseudomonas aeruginosa invasion and cytotoxicity are independent events, both of which involve protein tyrosine kinase activity.* Infect Immun, 1998. **66**(4): p. 1453-9.

Fanen, P., A. Wohlhuter-Haddad, and A. Hinzpeter, *Genetics of cystic fibrosis: CFTR mutation classifications toward genotype-based CF therapies.* Int J Biochem Cell Biol, 2014. **52**: p. 94-102.

Farinha, C.M. and P. Matos, *Repairing the basic defect in cystic fibrosis - one approach is not enough.* FEBS J, 2016. **283**(2): p. 246-64.

Fingerhut, R., et al., *Degradation of gangliosides by the lysosomal sialidase requires an activator protein.* Eur J Biochem, 1992. **208**(3): p. 623-9.

Fleiszig, S.M., et al., *Relationship between cytotoxicity and corneal epithelial cell invasion by clinical isolates of Pseudomonas aeruginosa.* Infect Immun, 1996. **64**(6): p. 2288-94.

Futerman, A.H. and Y.A. Hannun, *The complex life of simple sphingolipids.* EMBO Rep, 2004. **5**(8): p. 777-82.

Gatti, R., et al., *Comparative study of 15 lysosomal enzymes in chorionic villi and cultured amniotic fluid cells. Early prenatal diagnosis in seven pregnancies at risk for lysosomal storage diseases.* Prenat Diagn, 1985. **5**(5): p. 329-36.

Gault, C.R., L.M. Obeid, and Y.A. Hannun, *An overview of sphingolipid metabolism: from synthesis to breakdown.* Adv Exp Med Biol, 2010. **688**: p. 1-23.

Giussani, P., et al., *Sphingolipids: key regulators of apoptosis and pivotal players in cancer drug resistance.* Int J Mol Sci, 2014. **15**(3): p. 4356-92.

Gobbi, M., et al., *Lipid-based nanoparticles with high binding affinity for amyloid-beta1-42 peptide.* Biomaterials, 2010. **31**(25): p. 6519-29.

Grassme, H., et al., *CFTR-dependent susceptibility of the cystic fibrosis-host to Pseudomonas aeruginosa.* Int J Med Microbiol. **300**(8): p. 578-83.

Grassmé, H., et al., *CD95 signaling via ceramide-rich membrane rafts.* J Biol Chem, 2001. **276**(23): p. 20589-96.

Grassme, H., et al., *Host defense against Pseudomonas aeruginosa requires ceramide-rich membrane rafts.* Nat Med, 2003. **9**(3): p. 322-30.

Guilbault, C., et al., *Fenretinide corrects newly found ceramide deficiency in cystic fibrosis.* Am J Respir Cell Mol Biol, 2008. **38**(1): p. 47-56.

Guilbault, C., et al., *Cystic fibrosis fatty acid imbalance is linked to ceramide deficiency and corrected by fenretinide.* Am J Respir Cell Mol Biol, 2009. **41**(1): p. 100-6.

Gustavsson, J., et al., *Localization of the insulin receptor in caveolae of adipocyte plasma membrane.* FASEB J, 1999. **13**(14): p. 1961-71.

Hakomori, S., *Bifunctional role of glycosphingolipids. Modulators for transmembrane signaling and mediators for cellular interactions.* J Biol Chem, 1990. **265**(31): p. 18713-6.

Hamai, H., et al., *Defective CFTR increases synthesis and mass of sphingolipids that modulate membrane composition and lipid signaling.* J Lipid Res, 2009. **50**(6): p. 1101-8.

Hannun, Y.A. and L.M. Obeid, *Principles of bioactive lipid signalling: lessons from sphingolipids.* Nat Rev Mol Cell Biol, 2008. **9**(2): p. 139-50.

Hoegger, M.J., et al., *Impaired mucus detachment disrupts mucociliary transport in a piglet model of cystic fibrosis.* Science, 2014. **345**(6198): p. 818-22.

Hoffman, L.R. and B.W. Ramsey, *Cystic fibrosis therapeutics: the road ahead.* Chest. **143**(1): p. 207-13.

Huwiler, A., et al., *Physiology and pathophysiology of sphingolipid metabolism and signaling.* Biochim Biophys Acta, 2000. **1485**(2-3): p. 63-99.

Ichikawa, S. and Y. Hirabayashi, *Glucosylceramide synthase and glycosphingolipid synthesis.* Trends Cell Biol, 1998. **8**(5): p. 198-202.

Itokazu, Y., et al., *Reduced GM1 ganglioside in CFTR-deficient human airway cells results in decreased beta1-integrin signaling and delayed wound repair.* Am J Physiol Cell Physiol, 2014. **306**(9): p. C819-30.

Jeckel, D., et al., *Glucosylceramide is synthesized at the cytosolic surface of various Golgi subfractions.* J Cell Biol, 1992. **117**(2): p. 259-67.

Kabayama, K., et al., *TNFalpha-induced insulin resistance in adipocytes as a membrane microdomain disorder: involvement of ganglioside GM3.* Glycobiology, 2005. **15**(1): p. 21-9.

Kabayama, K., et al., *Dissociation of the insulin receptor and caveolin-1 complex by ganglioside GM3 in the state of insulin resistance.* Proc Natl Acad Sci U S A, 2007. **104**(34): p. 13678-83.

Kerem, B., et al., *Identification of the cystic fibrosis gene: genetic analysis.* Science, 1989. **245**(4922): p. 1073-80.

Kolter, T., R.L. Proia, and K. Sandhoff, *Combinatorial ganglioside biosynthesis.* J Biol Chem, 2002. **277**(29): p. 25859-62.

Konstan, M.W., et al., *Clinical use of Ibuprofen is associated with slower FEV1 decline in children with cystic fibrosis.* Am J Respir Crit Care Med, 2007. **176**(11): p. 1084-9.

Kytzia, H.J. and K. Sandhoff, *Evidence for two different active sites on human beta-hexosaminidase A. Interaction of GM2 activator protein with beta-hexosaminidase A.* J Biol Chem, 1985. **260**(12): p. 7568-72.

Lahiri, S. and A.H. Futerman, *The metabolism and function of sphingolipids and glycosphingolipids.* Cell Mol Life Sci, 2007. **64**(17): p. 2270-84.

Levy, M. and A.H. Futerman, *Mammalian ceramide synthases.* IUBMB Life, 2010. **62**(5): p. 347-56.

Loberto, N., et al., *The membrane environment of endogenous cellular prion protein in primary rat cerebellar neurons.* J Neurochem, 2005. **95**(3): p. 771-83.

Loberto, N., et al., *GBA2-encoded beta-glucosidase activity is involved in the inflammatory response to Pseudomonas aeruginosa.* PLoS One, 2014. **9**(8): p. e104763.

Mansson, J.E., et al., *Trisialosyllactosylceramide (GT3) is a ganglioside of human lung.* FEBS Lett, 1986. **196**(2): p. 259-62.

Martin, E., et al., *Loss of function of glucocerebrosidase GBA2 is responsible for motor neuron defects in hereditary spastic paraplegia.* Am J Hum Genet, 2013. **92**(2): p. 238-44.

McCarthy, V.A. and A. Harris, *The CFTR gene and regulation of its expression.* Pediatr Pulmonol, 2005. **40**(1): p. 1-8.

Merrill, A.H., Jr., *De novo sphingolipid biosynthesis: a necessary, but dangerous, pathway.* J Biol Chem, 2002. **277**(29): p. 25843-6.

Merrill, A.H., Jr., *Sphingolipid and glycosphingolipid metabolic pathways in the era of sphingolipidomics.* Chem Rev, 2011. **111**(10): p. 6387-422.

Merrill, A.H., Jr. and D.D. Jones, *An update of the enzymology and regulation of sphingomyelin metabolism.* Biochim Biophys Acta, 1990. **1044**(1): p. 1-12.

Milla, C.E. and R.B. Moss, *Recent advances in cystic fibrosis.* Curr Opin Pediatr, 2015. **27**(3): p. 317-24.

Moran, O., *On the structural organization of the intracellular domains of CFTR.* Int J Biochem Cell Biol, 2014. **52**: p. 7-14.

Nahrlich, L., et al., *Therapy of CF-patients with amitriptyline and placebo--a randomised, double-blind, placebo-controlled phase IIb multicenter, cohort-study.* Cell Physiol Biochem, 2013. **31**(4-5): p. 505-12.

Nichols, D.P. and J.F. Chmiel, *Inflammation and its genesis in cystic fibrosis.* Pediatr Pulmonol, 2015. **50 Suppl 40**: p. S39-56.

O'Sullivan, B.P. and S.D. Freedman, *Cystic fibrosis.* Lancet, 2009. **373**(9678): p. 1891-904.

Ohanian, J. and V. Ohanian, *Sphingolipids in mammalian cell signalling.* Cell Mol Life Sci, 2001. **58**(14): p. 2053-68.

Overkleeft, H.S., et al., *Generation of specific deoxynojirimycin-type inhibitors of the non-lysosomal glucosylceramidase.* J Biol Chem, 1998. **273**(41): p. 26522-7.

Perez-Vilar, J. and R.C. Boucher, *Reevaluating gel-forming mucins' roles in cystic fibrosis lung disease.* Free Radic Biol Med, 2004. **37**(10): p. 1564-77.

Pezzulo, A.A., et al., *Reduced airway surface pH impairs bacterial killing in the porcine cystic fibrosis lung.* Nature, 2012. **487**(7405): p. 109-13.

Pier, G.B., et al., *Role of mutant CFTR in hypersusceptibility of cystic fibrosis patients to lung infections.* Science, 1996. **271**(5245): p. 64-7.

Plotkowski, M.C., et al., *Pseudomonas aeruginosa internalization by human epithelial respiratory cells depends on cell differentiation, polarity, and junctional complex integrity.* Am J Respir Cell Mol Biol, 1999. **20**(5): p. 880-90.

Poulsen, J.H., et al., *Bicarbonate conductance and pH regulatory capability of cystic fibrosis transmembrane conductance regulator.* Proc Natl Acad Sci U S A, 1994. **91**(12): p. 5340-4.

Prinetti, A., et al., *Glycosphingolipid behaviour in complex membranes.* Biochim Biophys Acta, 2009. **1788**(1): p. 184-93.

Ramu, Y., Y. Xu, and Z. Lu, *Inhibition of CFTR Cl- channel function caused by enzymatic hydrolysis of sphingomyelin.* Proc Natl Acad Sci U S A, 2007. **104**(15): p. 6448-53.

Riordan, J.R., et al., *Identification of the cystic fibrosis gene: cloning and characterization of complementary DNA.* Science, 1989. **245**(4922): p. 1066-73.

Rommens, J.M., et al., *Identification of the cystic fibrosis gene: chromosome walking and jumping.* Science, 1989. **245**(4922): p. 1059-65.

Rother, J., et al., *Biosynthesis of sphingolipids: dihydroceramide and not sphinganine is desaturated by cultured cells.* Biochem Biophys Res Commun, 1992. **189**(1): p. 14-20.

Scandroglio, F., et al., *Lipid content of brain, brain membrane lipid domains, and neurons from acid sphingomyelinase deficient mice.* J Neurochem, 2008. **107**(2): p. 329-38.

Schutze, S., V. Tchikov, and W. Schneider-Brachert, *Regulation of TNFR1 and CD95 signalling by receptor compartmentalization.* Nat Rev Mol Cell Biol, 2008. **9**(8): p. 655-62.

Seitz, A.P., et al., *Ceramide and sphingosine in pulmonary infections.* Biol Chem, 2015. **396**(6-7): p. 611-20.

Shimeno, H., et al., *Partial purification and characterization of sphingosine N-acyltransferase (ceramide synthase) from bovine liver mitochondrion-rich fraction.* Lipids, 1998. **33**(6): p. 601-5.

Simons, K. and J.L. Sampaio, *Membrane organization and lipid rafts.* Cold Spring Harb Perspect Biol, 2011. **3**(10): p. a004697.

Sonnino, S. and A. Prinetti, *Gangliosides as regulators of cell membrane organization and functions.* Adv Exp Med Biol, 2010. **688**: p. 165-84.

Sonnino, S. and A. Prinetti, *Membrane domains and the "lipid raft" concept.* Curr Med Chem, 2013. **20**(1): p. 4-21.

Sorli, S.C., et al., *The nonlysosomal beta-glucosidase GBA2 promotes endoplasmic reticulum stress and impairs tumorigenicity of human melanoma cells.* FASEB J, 2013. **27**(2): p. 489-98.

Spence, M.W., *Sphingomyelinases.* Adv Lipid Res, 1993. **26**: p. 3-23.

Stoltz, D.A., D.K. Meyerholz, and M.J. Welsh, *Origins of cystic fibrosis lung disease.* N Engl J Med, 2015. **372**(4): p. 351-62.

Stonehouse, M.J., et al., *A novel class of microbial phosphocholine-specific phospholipases C.* Mol Microbiol, 2002. **46**(3): p. 661-76.

Tagami, S., et al., *Ganglioside GM3 participates in the pathological conditions of insulin resistance.* J Biol Chem, 2002. **277**(5): p. 3085-92.

Teichgraber, V., et al., *Ceramide accumulation mediates inflammation, cell death and infection susceptibility in cystic fibrosis.* Nat Med, 2008. **14**(4): p. 382-91.

Tizzano, E.F. and M. Buchwald, *CFTR expression and organ damage in cystic fibrosis.* Ann Intern Med, 1995. **123**(4): p. 305-8.

Trezise, A.E., et al., *Expression of the cystic fibrosis gene in human foetal tissues*. Hum Mol Genet, 1993. **2**(3): p. 213-8.

Tsui, L.C. and R. Dorfman, *The cystic fibrosis gene: a molecular genetic perspective.* Cold Spring Harb Perspect Med, 2013. **3**(2): p. a009472.

Uhlig, S. and E. Gulbins, *Sphingolipids in the lungs.* Am J Respir Crit Care Med, 2008. **178**(11): p. 1100-14.

van Meer, G. and Q. Lisman, *Sphingolipid transport: rafts and translocators.* J Biol Chem, 2002. **277**(29): p. 25855-8.

van Meer, G. and W.L. Vaz, *Membrane curvature sorts lipids. Stabilized lipid rafts in membrane transport.* EMBO Rep, 2005. **6**(5): p. 418-9.

van Meer, G., D.R. Voelker, and G.W. Feigenson, *Membrane lipids: where they are and how they behave.* Nat Rev Mol Cell Biol, 2008. **9**(2): p. 112-24.

Vilela, R.M., et al., *Inhibition of IL-8 release from CFTR-deficient lung epithelial cells following pre-treatment with fenretinide.* Int Immunopharmacol, 2006. **6**(11): p. 1651-64.

Weiser, N., et al., *Paracellular permeability of bronchial epithelium is controlled by CFTR.* Cell Physiol Biochem, 2011. **28**(2): p. 289-96.

Yamaji, T. and K. Hanada, *Sphingolipid metabolism and interorganellar transport: localization of sphingolipid enzymes and lipid transfer proteins.* Traffic, 2015. **16**(2): p. 101-22.

Yang, Y. and S. Uhlig, *The role of sphingolipids in respiratory disease.* Ther Adv Respir Dis, 2011. **5**(5): p. 325-44.

Zabner, J., et al., *Development of cystic fibrosis and noncystic fibrosis airway cell lines.* Am J Physiol Lung Cell Mol Physiol, 2003. **284**(5): p. L844-54.

Zhang, Y., et al., *DC-Chol/DOPE cationic liposomes: a comparative study of the influence factors on plasmid pDNA and siRNA gene delivery.* Int J Pharm, 2010. **390**(2): p. 198-207.

Zschoche, A., et al., *Hydrolysis of lactosylceramide by human galactosylceramidase and GM1-beta-galactosidase in a detergent-free system and its stimulation by sphingolipid activator proteins, sap-B and sap-C. Activator proteins stimulate lactosylceramide hydrolysis.* Eur J Biochem, 1994. **222**(1): p. 83-90.